A SIMPLE SEISMIC PERFORMANCE ASSESSMENT TECHNIQUE FOR UNREINFORCED BRICK MASONRY STRUCTURES

A THESIS SUBMITTED TO
THE GRADUATE SCHOOL OF NATURAL AND APPLIED SCIENCES
OF
MIDDLE EAST TECHNICAL UNIVERSITY

BY

ALPER ALDEMIR

IN PARTIAL FULFILLMENT OF THE REQUIREMENTS
FOR
THE DEGREE OF MASTER OF SCIENCE
IN
CIVIL ENGINEERING

SEPTEMBER 2010

Approval of the thesis:

A SIMPLE SEISMIC PERFORMANCE ASSESSMENT TECHNIQUE FOR UNREINFORCED BRICK MASONRY STRUCTURES

Submitted by **ALPER ALDEMIR** in partial fulfillment of the requirements for the degree of **Master of Science in Civil Engineering Department, Middle East Technical University** by,

Prof. Dr. Canan Özgen ____________________
Dean, Graduate School of **Natural and Applied Sciences**

Prof. Dr. Güney Özcebe ____________________
Head of Department, **Civil Engineering**

Assoc. Prof. Dr. Murat Altuğ Erberik ____________________
Supervisor, **Civil Engineering Dept., METU**

Examining Committee Members:

Prof. Dr. Haluk Sucuoğlu ____________________
Civil Engineering Dept., METU

Assoc. Prof. Dr. Murat Altuğ Erberik ____________________
Civil Engineering Dept., METU

Assoc. Prof. Dr. Barış Binici ____________________
Civil Engineering Dept., METU

Assoc. Prof. Dr. Ahmet Türer ____________________
Civil Engineering Dept., METU

Assoc. Prof. Dr. Hasan Hüsnü Korkmaz ____________________
Civil Engineering Dept., Selçuk University

Date: Sep 16, 2010

I hereby declare that all information in this document has been obtained and presented in accordance with academic rules and ethical conduct. I also declare that, as required by these rules and conduct, I have fully cited and referenced all material and results that are not original to this work.

Name, Last name: Alper ALDEMIR

Signature

ABSTRACT

A SIMPLE SEISMIC PERFORMANCE ASSESSMENT TECHNIQUE FOR UNREINFORCED BRICK MASONRY STRUCTURES

Aldemir, Alper
M.Sc., Department of Civil Engineering
Supervisor: Assoc. Prof. Dr. Murat Altuğ Erberik

September 2010, 142 pages

There are many advantages of masonry construction like widespread geographic availability in many forms, colors and textures, comparative cheapness, fire resistance, thermal and sound insulation, durability, etc. For such reasons, it is still a commonly used type of residential construction in rural and even in urban regions. Unfortunately, its behavior especially under the effect of earthquake ground motions has not been identified clearly because of its complex material nature. Hence, the masonry buildings with structural deficiencies belong to the most vulnerable class of structures which have experienced heavy damage or even total collapse in previous earthquakes, especially in developing countries like Turkey. This necessitates new contemporary methods for designing safer masonry structures or assessing their performance. Considering all these facts, this study aims at the generation of a new performance-based technique for unreinforced brick masonry structures. First, simplified formulations are recommended to estimate idealized capacity curve parameters of masonry components (piers) by using the finite element analysis results of ANSYS and regression analysis through SPSS software. Local limit states for individual masonry piers are also obtained. Then, by combining the component behavior, lateral capacity curve of the masonry building is constructed together with the global limit states. The final step is to define seismic demand of the design earthquake from the building through TEC2007 method. By using this simple technique, a large population of masonry buildings can be examined in a relatively short period of time noting that the performance estimations are quite reliable since they are based on sophisticated finite element analysis results.

Keywords: Unreinforced Masonry Buildings, Masonry Pier, Seismic Performance, Capacity Curve, In-plane Behavior

ÖZ

TUĞLA YIĞMA YAPILAR İÇİN BASİT BİR DEPREM PERFORMANSI DEĞERLENDİRME YÖNTEMİ

Aldemir, Alper
Yüksek Lisans, İnşaat Mühendisliği Bölümü
Tez Yöneticisi: Doç.Dr. Murat Altuğ Erberik

Eylül 2010, 142 sayfa

Yığma yapıların, ısı ve ses izolasyonuna sahip olması, göreceli olarak ekonomik olması, yangına karşı dayanıklılığı, her türlü form, şekil ve renkte üretilebilmesi gibi pek çok avantajı bulunmaktadır. Bundan dolayı bu yapılar hem kırsal hem de kentsel alanlarda hala çokça tercih edilmektedirler. Maalesef bu tip yapıların deprem yer hareketi etkisi altındaki davranışları karmaşık malzeme özelliklerinden dolayı tam olarak açıklanamamıştır. Bundan ötürü yapısal olarak eksiklikleri bulunan yığma yapılar, depremler sonrası en çok hasar gören yapı tipleridir. Yatay yükler altında zayıf davranış gösteren bu yapıların daha iyi tasarlanması ya da daha önceden belirlenmiş yük etkilerinin altında nasıl davranacağının değerlendirilmesi için güncel metotların geliştirilmesi gerekmektedir. Tüm bu yukarıdaki eksiklikleri göz önüne alarak bu araştırmada tuğla yığma yapıların değerlendirilmesine olanak sağlayan performansa dayalı yeni bir metot geliştirilmesi hedef olarak seçilmiştir. Öncelikle ANSYS'te yapılan sonlu eleman analizlerini ve elde edilen sonuçların SPSS'teki regresyon analizlerini kullanarak yığma yapılarda bulunan dikey elemanların

kapasite eğrilerini belirlemek için basitleştirilmiş bir yöntem geliştirilmiştir. Aynı zamanda herbir dikey elemanın performans limitleri de elde edilmiştir. Tüm elemanların etkileri birleştirilerek binanın performans noktaları ve kapasite eğrisi oluşturulmuştur. Son aşamada ise binanın olası bir deprem altındaki performansı TEC2007'deki metotlar kullanılarak belirlenmiştir. Bu basit metotla amaçlanan birçok yığma yapının çok kısa bir zaman içinde incelenebilmesidir. Ayrıca bu değerlendirme komplike sonlu eleman analiz sonuçlarına dayandığı için oldukça güvenilirdir.

Anahtar Kelimeler: Yığma Yapılar, Yığma Duvar, Sismik Performans, Kapasite Eğrisi, Düzlemsel Davranış

To My Family

ACKNOWLEDGMENT

The author wishes to express his deepest gratitude to his supervisor Assoc.Prof.Dr. Murat Altuğ Erberik for his guidance, careful supervision, criticisms, patience and insight throughout the research.

The author would also like to thank Prof.Dr. Haluk Sucuoğlu for his willingness to help, and comments.

The assistance of İlker Kazaz when solving the problems related to the finite element program utilized throughout this study is gratefully acknowledged.

My special thanks go to Taylan Solmaz, İsmail Ozan Demirel, Andaç Lüleç, Emre Özkök, Efe Gökçe Kurt, Emrah Erşan Erdoğan and Uğur Akpınar. I will always remember with pleasure the inspiring discussions and activities we had.

My deepest gratitude goes to my family for their constant support and encouragement. This dissertation would not have been possible without them.

The author wishes to thank in particular all those people whose friendly assistance and wise guidance supported him throughout the duration of this research.

TABLE OF CONTENTS

LIST OF TABLES

TABLES

LIST OF FIGURES

FIGURES

LIST OF SYMBOLS / ABBREVATIONS

a	Length of Compression Block
A	Gross Floor Area
AAC	Autoclave Aerated Concrete
ACI	American Concrete Institute
a_g	Design Ground Acceleration
a_i	Undetermined Coefficients
ASCE	American Society of Civil Engineers
A_w	Cross-sectional Area of a Wall
b	Shear Stress Distribution Factor
b_i	Undetermined Coefficients
CEN	European Committee for Standardization
C_i	Undetermined Coefficients in the Regression Analysis
E	Young's Modulus
E_m	Young's Modulus of Masonry Wall
F	A Function of the Principal Stress States (σ_{xp}, σ_{yp}, σ_{zp})
f'_{dt}	Lower Bound of Masonry Diagonal Tension Strength
f'_m	Lower Bound of Masonry Compressive Strength
f_1	Compressive Strength for a State of Biaxial Compression superimposed on Hydrostatic Stress State
f_2	Compressive Strength for a State of Uniaxial Compression superimposed on hydrostatic stress state
f_a	Lower Bound of Vertical Axial Compressive Stress
f_b	Compressive Strength of a Brick Element
f_c	Uniaxial Crushing Strength of a Material
f_{cb}	Biaxial Compressive Strength of a Material
F_e	Elastic Force Demand
F_L	Loads acting on a Cross-section
f_m	Compressive Strength of a Masonry Wall

f_{mt}	Tensile Strength of a Masonry Wall
F_R	Resistance or Capacity of a Cross-section
F_{R1}	Reduced Inelastic Force Demand
f_t	Uniaxial Tensile Strength of a Material
F_u	Ultimate Lateral Load Capacity of a Masonry Wall
F_y	Yield Lateral Load Capacity of a Masonry Wall
g	Gravitational Acceleration
G	Shear Modulus
h	Height of a Wall
h_{eff}	Effective Height of a Wall
H_o	Height to the Inflection Point
I	Building Importance Factor
IBC	International Building Code
ICC	International Code Council
IDA	Incremental Dynamic Analysis
L	Length of a Member
L'	Effective Uncracked Section Length
l_b	Void Length
L_d	Minimum Total Length of Load-bearing Walls in any orthogonal Direction
LDP	Linear Dynamic Procedure
l_n	Unsupported Wall Length
LS	Limit State
LSP	Linear Static Procedure
l_w	Length of a Wall
MSJC	Masonry Standards Joint Committee
M_u	Flexural Strength of a Section
NDP	Nonlinear Dynamic Procedure
NSP	Nonlinear Static Procedure
N_{totali}	Total Force on a Pier at the ith Storey
p	Axial Pressure on a Cross-section
P	Axial Force on a Cross-section

P_{lb}	Lower Bound of Vertical Compressive Stress
Q4	Four-node Plane Element
Q6	Six-node Plane Element
R_1	Reduction Factor
R^2	Coefficient of Determination
R_{dt}	Lateral Capacity of a Masonry Wall due to Diagonal Tension Failure
R_f	Lateral Capacity of a Masonry Wall due to Flexural Failure
R_{ss}	Lateral Capacity of a Masonry Wall due to Sliding Shear Failure
S	Failure Surface expressed in terms of Principal Stresses
t	Thickness of a Wall
T	First Natural Vibration Period of a Structure
T_A	The short Characteristic Period of a Spectrum
t_{eff}	Effective Thickness of a Wall
TMS	The Masonry Society
u_u	Ultimate Displacement Capacity of a Masonry Wall
u_y	Yield Displacement Capacity of a Masonry Wall
URM	Unreinforced Masonry
V_{bo}	Shear Bond Strength at zero Compression
V_{dt}	Lateral Strength limited by Diagonal Tension Stress
V_{fl}	Ultimate Shear Capacity of a Section
V_{tc}	Lateral Strength limited by Toe Compressive Stress
V_y	Yield Lateral Force
$\hat{y}$	Dependent Variable in Regression Analysis
α	Effective Height Determination Factor
β_c	Shear Transfer Coefficient for closed Crack
β_t	Shear Transfer Coefficient for open Crack
η	Angle of Similarity
λ	Aspect Ratio of a Wall
μ	Coefficient of Friction

ν	Poisson's Ratio
σ_h	Hydrostatic Stress State
σ_{xp}	Principal Stresses in the direction x
σ_y	Axial Pressure
σ_{yp}	Principal Stresses in the direction y
σ_{zp}	Principal Stresses in the direction z

CHAPTER 1

INTRODUCTION

1.1. Non-engineered Construction in general

The non-engineered construction includes informally constructed buildings erected by using traditional methods without involvement of engineers or architects in the design and construction process. Any structural material, i.e. masonry, wood, reinforced concrete, etc. could be utilized in the non-engineered buildings.

As the main subject of this study is non-engineered masonry construction, the rest of this chapter deals with the more detailed information on masonry construction practice.

Traditionally, masonry structures are constructed by using both lime and cement as binding material and locally available constructional materials are tried to be selected for economical purposes. For instance, in rocky regions, there exists hegemony of stone buildings whereas lots of earthen buildings (adobe) are raised in districts lacking of underground wealth.

Sometimes, reinforced concrete elements may also be seen in non-engineered buildings. These include reinforced concrete slabs, lintels, bond beams, and tie columns. However, these members are constructed in a traditional manner. In other words, the lateral stabilization of these structures is not taken into consideration. Besides, the detailing of them does not depend on any theoretical rules.

Most of the building stock all over the world, especially in developing countries, is constituted by masonry structures. As it has been stated by The Masonry Society, masonry makes up approximately 70% of the existing building inventory in the United States. Although this percentage may have been slightly changed now, there is no doubt that the share of masonry structures in total building stock of the United States is still huge. Masonry construction is also very common in Mediterranean and Central European countries with numerous historical stone and brick masonry buildings. (Erberik *et al.*, 2008) Most importantly, a high proportion of this masonry stock is built without intervention by qualified technical people in design. (Arya *et al.*, 1986)

The importance of these non-engineered structures is also summarized by Arya *et al.* (1986) :

"The safety of the non-engineered buildings from the fury of earthquakes is a subject of highest priority in view of the fact that in the moderate to severe seismic zones of the world more than 90% of the population is still living and working in such buildings and that most losses of lives during earthquakes have occurred due to their collapse. The risk to life is further increasing due to rising population particularly in the developing countries, poverty of the people, scarcity of modern building materials, viz. cement and steel, lack of awareness and necessary skills."

Therefore, it is very vital to improve the traditional design concepts of these buildings and some condition evaluation techniques to assess the readily available individual structures or a stock of structures ought to be developed.

1.2. Performance-based Design and Assessment Techniques in general

Performance-based techniques generally aim at designing structures for the intended level of damage or at evaluating the existing structures' performance under the effect of anticipated loading conditions. Therefore, they all have three common stages.

1) Formation of limit state

2) Capacity estimation
3) Demand calculation

The first stage is to identify the design limits. Both the design engineer and the client take part in this step. In other words, the tolerable damage level is stated by the employer and the design engineer could come up with a structure just satisfying the needs.

As the above steps summarize, the capacity and the demand should be determined next. Therefore, the codes and standards recommend some methods for both the analysis and the capacity calculations by collecting the experience gained after some devastating earthquakes, lots of laboratory tests and traditional methods (common practices).

Performance-based techniques are becoming more popular among the civil engineers. This is because; unlike force-based techniques, it gives the opportunity to design a structure for different damage states after the extreme events like earthquakes. In other words, the most powerful aspect of this aproach is that it gives the possibility to predict the damages. To do this, a physical parameter like displacements, drift ratios, plastic rotations, etc. is, firstly, selected to determine the damage levels of any members. Of course, the parameter should possess two features.

1) It should have the largest confidence from the analysis, i.e. the parameter has to be estimated with an acceptable error.
2) It ought to describe the damage level well.

Today, some provisions select the plastic rotations for the damage parameter but the studies show that the commonly used analysis technique (nonlinear static analysis) is not good at determining the plastic rotations. Thus, Chopra and Goel (2002) state that it is preferable to use the drift ratios for the damage parameter since they are better estimated by pushover analysis and are good indicators of damage.

Therefore, the weaknesses in the methods for analysis and demand calculations are investigated and have been tried to be improved recently.

1.3. Objective and Scope

Performance-based approaches have become very popular in earthquake engineering in both design and evaluation stages. Since performance-based approaches depend on quantification of damage, and in turn, quantification of damage is realistically achieved after obtaining the displacement demand of a structure, these techniques have been successfully employed for reinforced concrete and steel frame structures. However, masonry structures are different in the sense that they are relatively more rigid with rather limited displacement capacity and can be regarded as non-ductile structures, which cannot undergo significant inelastic deformations. In addition to this, and as mentioned before, masonry structures are generally constructed without engineering touch, so it becomes very difficult to predict the actual seismic behavior of these structures since they involve many uncertainties. Hence implementation of performance-based techniques to masonry structures is not straightforward as in the case of frame structures.

Considering the above discussion, this study is an attempt to develop a performance-based technique for unreinforced brick masonry structures. If properly adopted, it can also be used as a design approach in the future. The technique involves the capacity evaluation of masonry piers based on the assumption that the piers are weaker than spandrels and the damage is accumulated in piers. In-plane behavior is obtained by detailed finite element analysis of individual piers with different compressive strength values, aspect ratios and vertical stress levels. Then, the in-plane capacity curves are idealized in a bilinear fashion with four structural parameters in terms of force and displacement. Local limit states of individual piers are also attained. The next step is to obtain simple empirical relationships for the structural parameters in terms of easily obtainable geometrical (length, thickness and aspect ratio) and mechanical (compressive strength and vertical stress level) properties through regression analyses. As the final step, the capacity curve of the building is constructed by the contribution of in-plane capacity curves of individual piers together with global limit states. Hence, it becomes possible to estimate the capacity of a population of masonry buildings without performing detailed and time consuming finite element analysis but by implicitly using the results of such an elaborate method of analysis.

The proposed method is applied to an actual unreinforced brick masonry building in Istanbul and the obtained results from both complicated ANSYS analysis and the simplified method are in an acceptable range although the method contains major assumptions for the sake of simplicity.

This study is mainly focused on the capacity evaluation of brick masonry buildings and quantification of seismic demand is treated in another on-going study, but for the sake of completeness of performance-based evaluation, at the end of the case study section, there is a short discussion about how to handle seismic demand and capacity together and what the output is.

The study is composed of six chapters. First chapter gives a general overview about non-engineered construction, and in particular unreinforced masonry construction and a brief background for performance-based design and assessment techniques.

Chapter 2 deals with codes and standards for design of masonry structures, mainly focusing on the comparison of masonry-related documentation of the current Turkish Earthquake Code with the international codes. At the end of the chapter, there exists a critique about the state of masonry design in Turkey. This chapter is important to visualize what is currently being done in Turkey for the design and evaluation of unreinforced masonry buildings, since these two concepts cannot be clearly separated from each other in the case of masonry buildings as they both use similar force-based calculation procedures.

New concepts for design and analysis of masonry structures is discussed in Chapter 3, introducing displacement-based design as opposed to force-based design, which is currently being used for masonry structures. All analysis tools (linear static procedure, linear dynamic procedure, nonlinear static procedure, nonlinear dynamic procedure and incremental dynamic analysis) used in these design approaches are briefly explained. Then, in-plane behavior and failure modes of masonry piers are presented together with the studies carried out for the attainment of performance limit states of masonry piers. The final part of this chapter is devoted to modeling strategies used for masonry structures.

Chapter 4 presents finite element modeling of in-plane behavior of masonry wall elements. This chapter begins with a discussion about the finite element modeling techniques for masonry wall elements. Then, the element type (Solid 65) used in the finite element program (ANSYS) is described with all its features and limitations. The final part of this chapter includes the verification of the finite element model used in this study through experimental data.

Chapter 5 explains the development of the performance-based technique for unreinforced brick masonry buildings in Turkey. The first part of this chapter contains information about material characteristics of brick masonry units in Turkey. Then, the capacity curve generation of masonry piers with different geometrical and mechanical properties is conducted using finite element analysis. The next step is to idealize analytically obtained capacity curves by using four parameters and obtain simple empirical relationships for these structural parameters through regression analysis. The remaining part of this chapter is devoted to the implementation of the procedure to an existing masonry building in Istanbul.

Chapter 6 contains a brief summary of the research work and conclusions obtained from this study.

CHAPTER 2

CODES AND STANDARDS FOR DESIGN OF MASONRY STRUCTURES

2.1. Introduction

Codes, standards and specifications are documents that represent “state-of-the-art” and translate the accumulated professional and technical knowledge, and complex research developments into simple procedures suitable for routine design process. Hence, codes and standards are authoritative sources of information for designers and they represent a unifying order of engineering practice. (Taly, 2000)

Design and construction of masonry requires consideration of properties and parameters that affect the structural behavior. Increasing awareness of the seismic risk, new geological and seismological evidences, as well as technological developments in materials results in a design assisted by building material properties, dynamic characteristics of the building and load deflection characteristics of building components. Consequently, some requirements about number of stories, story heights, strength of masonry units, minimum thickness of load-bearing walls, minimum total length of load-bearing walls, openings in load-bearing walls etc. are embedded into the codes empirically or analytically. (Erberik *et al.*, 2008)

This part of the study provides a comparison of the codes and standards for unreinforced masonry design. Since, earthquake resistant masonry design practice in Turkey is still characterized by a rather high level of empirical requirements only for unreinforced masonry; this part of the study is devoted to compare some basic geometrical and mechanical requirements on masonry structures by utilizing various codes and standards. (Erberik *et al.*, 2008)

At the beginning of this chapter, the definition of simple buildings is introduced in order to clarify the building types that will be considered in the rest of the chapter.

Afterwards, widely used codes and standards for masonry design are presented briefly in two parts as ***international codes and standards*** and ***national codes and standards***.

Next, comparative information is given about various design requirements for masonry structures present in different standards that are listed as follows: Turkish Earthquake Code 1975 (TEC1975), 1998 (TEC1998) and 2007 (TEC2007), Masonry Standards Joint Committee 2005 (MSJC2005), International Code Council 2006 (IBC2006) and European Committee for Standardization 2003a (Eurocode 6) and 2003b (Eurocode 8).

Final part of this chapter is devoted to a brief criticism about the state of masonry design in Turkey.

2.2. International Codes and Standards

One of the most recognized design provisions in the United States is the International Building Code (IBC) that has been developed by the International Code Council (ICC). It references consensus design provisions and specifications. The first edition of IBC was published in 2000 whereas the version investigated in this study has been published in 2006. One chapter of IBC is devoted to masonry structures with the requirements and definitions in terms of materials, construction, quality assurance, seismic design, working stress design, strength design, empirical design, and non-structural masonry.

Another important code that is widely used in the United States is the "Building Code Requirements for Masonry Structures" that has been developed by Masonry Standards Joint Committee (MSJC). This committee has been established by three sponsoring societies: American Concrete Institute (ACI), American Society of Civil

Engineers (ASCE) and The Masonry Society (TMS). The studied version of the MSJC code (2005) covers general building code requirements and specifications of masonry structures, including allowable stress design, strength design, empirical design and prestressed design of masonry. In addition to this, one chapter is devoted to veneer and glass unit masonry. (Erberik *et al.*, 2008)

The design of masonry structures in Mediterranean and Central European countries is covered by the Eurocode, which is an assembly of standards for structural design developed by the European Committee for Standardization (CEN). Eurocode 6 specially deals with masonry structures in three parts. First part consists of common rules for reinforced and unreinforced masonry structures, whereas the second part consists of design, selection of materials and execution of masonry. Final part contains simplified calculation methods for unreinforced masonry structures (European Committee for Standardization 2003a). Besides Eurocode 6, in Eurocode 8, there is a chapter that states specific rules for masonry buildings, including materials and bonding patterns, types of construction and behavior factors, structural analysis, design criteria and construction rules, safety verification, rules for simple masonry buildings (European Committee for Standardization 2003b). (Erberik *et al.*, 2008)

2.3. National Codes and Standards

In Turkey, the first earthquake design code was published in 1940, after the devastating Erzincan Earthquake in 1939. Although there had been some efforts to update this immature code in 1942, 1947, 1953, 1961 and 1968, these were not adequate to ensure the seismic safety of building structures until the release of “The Specifications for Structures to be Built in Disaster Areas” (TEC1975) by the Turkish Ministry of Public Works and Settlement in 1975. However, economical and physical losses continued to increase with the occurrence of each earthquake even afterwards. Hence, the next seismic design code (TEC1998) was published in 1998. This code included major revisions when compared to the previous specifications and it was more compatible with the well-recognized international codes.

Nevertheless, earthquake codes should be periodically updated according to the needs of the construction industry and lessons learned during the use of the code. Consequently, TEC1998 has also been replaced by the current code (TEC2007) in 2007. The new version of the code also includes chapters related with repair and strengthening of existing buildings damaged by earthquakes or prone to be affected by disasters. (Erberik *et al.*, 2008)

In TEC1975, there was a section about the design of masonry structures with very general terms including the number of stories, materials to be used in masonry walls, required wall thickness, stability of walls and openings in walls. In TEC1998, the section was edited and put into a more readable format with clear figures and there were some additions like the calculation of minimum total length of load-bearing walls in the direction of earthquake, recommendations for the values of the parameters to be used in the calculation of the equivalent elastic seismic load that is assumed to be acting on the structure and design of vertical bond beams. Finally, in TEC2007, the most significant improvement related to the design of masonry structures is the addition of simple procedures for the calculation of vertical and shear stresses in masonry walls. Furthermore, the existing clauses are refined according to the current state of practice. (Erberik *et al.*, 2008)

2.4. Comparison of Codes and Standards for Design of Masonry Structures

This section includes a comparison of international and national codes and standards about design of masonry structures. The comparison is based on some basic design parameters for masonry structures: number of stories, storey height, strength requirements for masonry units, minimum thickness of load bearing walls, minimum required length of load-bearing walls, openings and maximum unsupported length of load bearing walls.

2.4.1. Number of Stories

It has been observed that one of the important structural parameters that is related to seismic damage of masonry buildings is the number of stories, in accordance with the observations from previous major earthquakes in Turkey. The buildings with three or more stories suffered severe damage whereas the buildings with one or two stories generally exhibited adequate resistance under seismic action. In the Turkish Earthquake Code, maximum number of stories permitted for masonry buildings (excluding a single basement) depends on the seismic zone (Table 2.1). The requirements for the maximum number of stories did not change from version to version as far as Turkish Earthquake Code is concerned. In addition, the code allows a penthouse with gross area not exceeding 25% of the building area at foundation level. Adobe buildings are allowed with a single story excluding the basement in all seismic zones.

Table 2.1. Maximum Permitted Number of Stories for Unreinforced Masonry Buildings According to Different Earthquake Codes. (Seismic zones are defined according to TEC2007 and NL means there is no limitation.)

	Seismic zones in terms of design ground acceleration (a_g)			
	Zone 1 ***($a_g \geq 0.4g$)***	***Zone 2*** ***($0.3g \leq a_g < 0.4g$)***	***Zone 3*** ***($0.2g \leq a_g < 0.3g$)***	***Zone 4*** ***($0.1g \leq a_g < 0.2g$)***
TEC1975	2	3	3	4
TEC1998	2	3	3	4
TEC2007	2	3	3	4
Eurocode 6	2	2	NL	NL
Eurocode 8	1	1	2	3

According to Tomazevic (1999), in European state-of-practice, limitations regarding number of stories have been relaxed based on the results of recent experimental and theoretical investigations and on improvements in technology and methods of design. Except for unreinforced masonry located in seismic zones with design ground acceleration (a_g) equal to or greater than 0.3g (g is the gravitational acceleration), which is not allowed for earthquake resistant walls in buildings higher than two storeys, no limitations regarding height of masonry buildings are specified in Eurocode 6. However, in Eurocode 8, some limitations for maximum number of stories are given for a special class of masonry structures called as “simple buildings”. (Table 2.1) By definition, simple buildings are structures with an approximately regular plan and elevation, where the ratio between the length of the long and short side is not more than 4, and the projections or recesses from the rectangular shape are not greater than 15% of the length of side parallel to the direction of projection. Simple buildings comply with the provisions regarding the quality of masonry materials and construction rules specified in Eurocode and for these buildings, explicit and detailed safety verifications are not mandatory. At this point, it is important to note that simple buildings are very much alike the masonry buildings designed according to the empirical rules of TEC2007. All comparisons are for unreinforced masonry buildings since reinforced masonry design is not explicitly reflected in Turkish earthquake code and also reinforced masonry construction is not very applicable in Turkey.

In IBC2006, there are provisions about the allowable building height, which depends on the wind velocity and are summarized in Table 2.2. Finally, in MSJC2005, it has been stated that buildings relying on masonry walls as part of their lateral load resisting system shall not exceed 10.67 m in height. Depending on the story height of the building, this crudely means that the maximum permitted number of stories regardless of any level of seismic action is 3 or 4.

Table 2.2. Maximum Permitted Building Heights for Unreinforced Masonry Buildings According to IBC 2006

	Wind Velocity			
	<40	***>40***	***>45***	***>49***
Building Height	55.1 m	18.4 m	10.7 m	-

2.4.2. Storey Height

According to all the last three versions of Turkish earthquake code, story height of masonry buildings is limited to 3 m from one floor top level to the other. Height of the single storey adobe building cannot be more than 2.7 m from ground to the rooftop. In the case where a basement is made, height of the adobe building is limited to 2.4 m.

The maximum storey height is 3.5 m in Eurocode 6 and Eurocode 8. However, there are no storey height limitations in IBC2006 and MSJC2005.

2.4.3. Strength Requirements for Masonry Units

There are similar considerations about the strength requirements for masonry units in the last three versions of Turkish earthquake code. In TEC1975, the minimum compressive strength of structural masonry materials was limited to 5 MPa for artificial blocks and 35 MPa for natural stones. Compressive strength of natural stones to be used in basements was limited to 10 MPa. It was not allowed to use a compressive strength value less than 7.5 MPa for artificial masonry materials that are used in basements. According to TEC1998, masonry materials to be used in the construction of load-bearing walls were natural stone, solid brick, bricks with vertical holes satisfying the maximum void ratios defined in the relevant Turkish standards (TS2510 and TS705), solid concrete blocks and other similar blocks. The minimum compressive strength of structural masonry materials was limited to 5 MPa on the basis gross compression area parallel to the direction of holes. Similarly, compressive strength of natural stones to be used in basements was limited to 10 MPa. Finally, in TEC2007, masonry materials to be used in the construction of load-bearing walls are defined in the same manner as it was in TEC1998 with one exception: Turkish standard TS705 has been replaced by TS EN 771-1. The same values have been considered for the minimum compressive strength of structural masonry materials and compressive strength of natural stones to be used in basements. But, in addition to the minimum compressive strength of masonry structural materials, there are requirements about allowable normal strength of masonry walls in TEC2007, which may be obtained from compressive strength of masonry units. It is worth to mention that, this part is absent in two previous versions, TEC1975 and TEC1998. (Erberik *et al.*, 2008)

Table 2.3. Allowable Compressive Strength of Masonry Walls According to TEC2007

Average Compressive Strength of Units (MPa)	***Mortar Class (MPa)***				
	A (15)	***B (11)***	***C (5)***	***D (2)***	***E (0.5)***
25	*1.8*	*1.4*	*1.2*	*1.0*	*0.8*
16	*1.4*	*1.2*	*1.0*	*0.8*	*0.7*
11	*1.0*	*0.9*	*0.8*	*0.7*	*0.6*
7	*0.8*	*0.7*	*0.7*	*0.6*	*0.5*
5	*0.6*	*0.5*	*0.5*	*0.4*	*0.4*

The allowable compressive strength values can be calculated by three methods :

- Walls that are constructed by using the same units and same mortar as the designed ones are tested (Wallette Test) and the quarter of their average strength is the allowable compressive strength of masonry wall.
- If prism tests are available for the intended units and mortar, the allowable compressive strength is the average value of prism tests divided by 8.
- If neither wallette tests nor prism tests are available, the allowable compressive strength can be taken from Table 5.2 of TEC2007. (See Table 2.3)
- If no tests are performed, the allowable compressive strength can be taken from Table 5.3 of TEC 2007. (See Table 2.4)

Table 2.4. Allowable Compressive Strength of Masonry Walls According to TEC2007

Unit and Mortar Type	***Allowable Strength (MPa)***
Factory Bricks with Vertical holes (Void ratio less than 35%)	1.0
Factory Bricks with Vertical holes (Void ratio between 35% and 45%)	0.8
Factory Bricks with Vertical holes (Void ratio greater than 45%)	0.5
Solid factory or Local Brick	0.8
Stone	0.3
Autoclave Aerated Concrete	0.6
Solid Concrete Block	0.8

According to Eurocode 6 and Eurocode 8, the use of fired clay units, calcium silicate units, concrete units, autoclave aerated concrete units, manufactured stone units and dimensioned natural stone units are allowed for the construction of masonry buildings in seismic zones. In all cases, the strength of masonry units should comply with the requirements of relevant European Standards (EN 771-1 to EN 771-6). Relatively low minimum mean values of compressive strength of masonry units to be used for the construction of structural walls are specified in the relevant standards. Accordingly, the normalized compressive strength values of masonry units are 2.5 MPa for clay units, 5.0 MPa for calcium silicate units, 1.8 MPa for concrete aggregate and autoclave aerated concrete units and 15 MPa for manufactured stone units. The term “normalized compressive strength” is defined as the mean value of a reference strength determined by testing at least ten equivalent, air-dried, 100mm×100mm specimens cut from the related unit. Shape factors are also introduced in Eurocode 6 in order to convert normalized compressive strength to the compressive strength of a unit with actual dimensions.

Table 2.5. Compressive Strength of Clay Masonry According to IBC2006

NET AREA COMPRESSIVE STRENGTH OF CLAY MASONRY UNITS (psi) [MPa]		***NET AREA COMPRESSIVE STRENGTH OF MASONRY (psi) [MPa]***
Type M or S mortar	***Type N mortar***	
1,700 [11.71]	2,100 [14.47]	1,000 [6.89]
3,350 [23.08]	4,150 [28.59]	1,500 [10.34]
4,950 [34.11]	6,200 [42.72]	2,000 [13.78]
6,600 [45.47]	8,250 [56.84]	2,500 [17.23]
8,250 [56.84]	10,300 [70.97]	3,000 [20.67]
9,900 [68.21]	-	3,500 [24.12]
13,200 [90.95]	-	4,000 [27.56]

In IBC2006, the strength requirements of masonry units are determined by making references to related specifications of the American Standards (ASTM C 62, ASTM C 216 or ASTM C 652). However, the masonry wall strengths can be determined by using tables in IBC 2006, which are based on the strength of masonry units and the type of mortar. (See Table 2.5 and Table 2.6) In MSJC2005, for the strength design of masonry, it is required that, except for architectural components of masonry, the specified compressive strength of masonry should be equal to or more than 10.3 MPa.

Table 2.6. Compressive Strength of Concrete Masonry According to IBC2006

NET AREA COMPRESSIVE STRENGTH OF CONCRETE MASONRY UNITS (psi) [MPa]		***NET AREA COMPRESSIVE STRENGTH OF MASONRY (psi) [MPa]***
Type M or S mortar	***Type N mortar***	
1,250 [8.62]	1,300 [8.96]	1,000 [6.89]
1,900 [13.1]	2,150 [14.8]	1,500 [10.34]
2,800 [19.3]	3,050 [21]	2,000 [13.78]
3,750 [25.9]	4,050 [27.9]	2,500 [17.23]
4,800 [33.1]	5,250 [36.2]	3,000 [20.67]

Moreover, for the empirical design of masonry walls, the masonry wall strength can be determined as a function of the compressive strength of the masonry unit and the type of mortar, as in the case of IBC2006. (Table 2.7)

Table 2.7. Allowable Compressive Stresses for Empirical Design of Masonry According to MSJC2005

Construction; Compressive Strength of masonry Unit, Gross Area, psi (MPa)	**Allowable compressive stress[1] based on gross cross-sectional area, psi (MPa)**	
	Type M or S mortar	***Type N mortar***
Solid masonry of brick and other solid units of clay or shale; sand-lime or concrete brick:		
8000 (55.16) or greater	350 (2.41)	300 (2.07)
4500 (31.03)	225 (1.55)	200 (1.38)
2500 (17.23)	160 (1.10)	140 (0.97)
1500 (10.34)	115 (0.79)	100 (0.69)
Grouted masonry of clay or shale; sand-lime or concrete brick:		
4500 (31.03) or greater	225 (1.55)	200 (1.38)
2500 (17.23)	160 (1.10)	140 (0.97)
1500 (10.34)	115 (0.79)	100 (0.69)
Solid masonry of solid concrete masonry units:		
3000 (20.69)	225 (1.55)	200 (1.38)
2000 (13.79)	160 (1.10)	140 (0.97)
1200 (8.27)	115 (0.79)	100 (0.69)
Masonry of hollow load bearing units:		
2000 (13.79) or greater	140 (0.97)	120 (0.83)
1500 (10.34)	115 (0.79)	100 (0.69)
1000 (6.90)	75 (0.52)	70 (0.48)
700 (7.83)	60 (0.41)	55 (0.38)
Hollow walls (noncomposite masonry bonded[2]):		
Solid Units		
2500 (17.23) or greater	160 (1.10)	140 (0.97)
1500 (10.34)	115 (0.79)	100 (0.69)
Hollow Units	75 (0.52)	70 (0.48)
Stone ashlar masonry:		
Granite	720 (4.96)	640 (4.41)
Limestone or marble	450 (3.10)	400 (2.76)
Sandstone or cast stone	360 (2.48)	320 (2.21)
Rubble stone masonry:		
Coursed, rough or random	120 (0.83)	100 (0.69)

[1] Linear interpolation shall be permitted for determining allowable stresses for masonry units having compressive strengths which are intermediate between those given in the table.

[2] Where floor and roof loads are carried upon one wythe, the gross cross-sectional area is that of the wythe under load, if both withes are loaded, the gross cross-sectional area is that of the wall minus the area of the cavity between the wythes. Walls bonded with met al. ties shall be considered as noncomposite walls, unless collar joints are filled with mortar or grout.

2.4.4. Minimum Thickness of Load-Bearing Walls

The minimum wall thicknesses required to be applied to load-bearing walls in accordance with TEC2007, excluding plaster thicknesses, are summarized in Table 2.8 depending on the number of stories. It has been stated that in the basement and ground floor walls of the building, natural stone or concrete would only be used as the load-bearing wall material in all earthquake zones. In addition to this, when there is no basement, minimum wall thicknesses given in Table 2.8 for ground story and for upper stories should be applied. If penthouses permitted by the code, wall thickness specified for each of the storey in Table 2.8 shall also be applied for penthouse. As seen from Table 2.8, the required minimum wall thicknesses in TEC2007 are almost half of the minimum wall thicknesses required in TEC1975. (Note that the values in brackets are taken from TEC1975; others are taken from TEC1998 and TEC2007.)

Table 2.8. Minimum Thicknesses of Load-bearing Walls According to TEC1975, TEC1998 and TEC2007

Seismic Zone	**Stories Permitted**	**Natural Stone (mm)**	**Concrete (mm)**	**Brick (thickness)**	**Others (mm)**
1, 2, 3, 4	Basement	500	250	1 (1.5)	200 (400)
	Ground story	500	-	1	200 (300)
1, 2, 3, 4	Basement	500	250	1.5	300 (400)
	Ground story	500	-	1	200 (300)
	First story	-	-	1	200 (300)
2, 3, 4	Basement	500	250	1.5	300 (400)
	Ground story	500	-	1.5	300 (400)
	First story	-	-	1	200 (300)
	Second story	-	-	1	200 (300)
4	Basement	500	250	1.5	300 (400)
	Ground story	500	-	1.5	300 (400)
	First story	-	-	1.5	300 (400)
	Second story	-	-	1	200 (300)
	Third story	-	-	1	200 (300)

According to Eurocode 6, the recommended minimum thickness of load bearing walls is only 100 mm. In Eurocode 8, the minimum effective wall thicknesses of buildings in seismic zones are given as well as the maximum value of the ratio of the effective wall height to its effective thickness. According to Eurocode 8, required minimum effective wall thicknesses and maximum value of the ratio h_{eff} /t_{eff} are given in Table 2.9. Parameters h_{eff} and t_{eff} stand for the effective height of the wall and the thickness of the wall, respectively.

Table 2.9. Recommended Geometric Requirements for Shearwalls According to Eurocode 8

Masonry type	$t_{eff,min}$ ***(mm)***	$(h_{eff}/t_{eff})_{max}$
Unreinforced, with natural stone units	350	9
Unreinforced, with any other type of units	240	12
Unreinforced, with any other type of units, in cases of low seismicity	170	15
Confined masonry	240	15
Reinforced masonry	240	15

According to IBC2006, the minimum thickness of masonry bearing walls should satisfy the following rules.

- For bearing walls: The minimum thickness of masonry bearing walls more than one story high shall be 203 mm. Bearing walls of one-story buildings shall not be less than 152 mm thick.
- Rubble stone walls: The minimum thickness of rough, random or coursed rubble stone walls shall be 406 mm.
- Shearwalls (They are defined as masonry walls upon which the structure depends for lateral stability.): The minimum thickness of masonry shearwalls shall be 203mm.

The minimum thickness requirements for MSJC2005 are exactly the same as the IBC2006.

2.4.5. Minimum Required Length of Load-Bearing Walls

In TEC2007, the ratio of the minimum total length of masonry load-bearing walls in any of the orthogonal directions in plan (excluding window and door openings) to gross floor area (excluding cantilever floors) is calculated by considering the following criterion

$$L_d /A \geq 0.20\ I\ (m/m^2) \tag{2.1}$$

In the above equation, L_d denotes minimum total length of load-bearing walls in any orthogonal direction, A stands for the gross floor area and I represents building importance factor which is equal to unity for residential buildings. (See Figure 2.1) Hence, Equation (2.1) indicates that for a residential building with a plan area of 100 m^2, total length of load-bearing walls should be at least 20 m in both orthogonal directions. This criterion was slightly different in the previous version of the code, TEC1998, where the constant term was 0.25 instead of 0.20. Thus, this means a reduction of 5 m in the total length of the walls in one direction for a building with a plan area of 100 m^2. Finally, it should also be noted that there was no such a criterion in TEC1975.

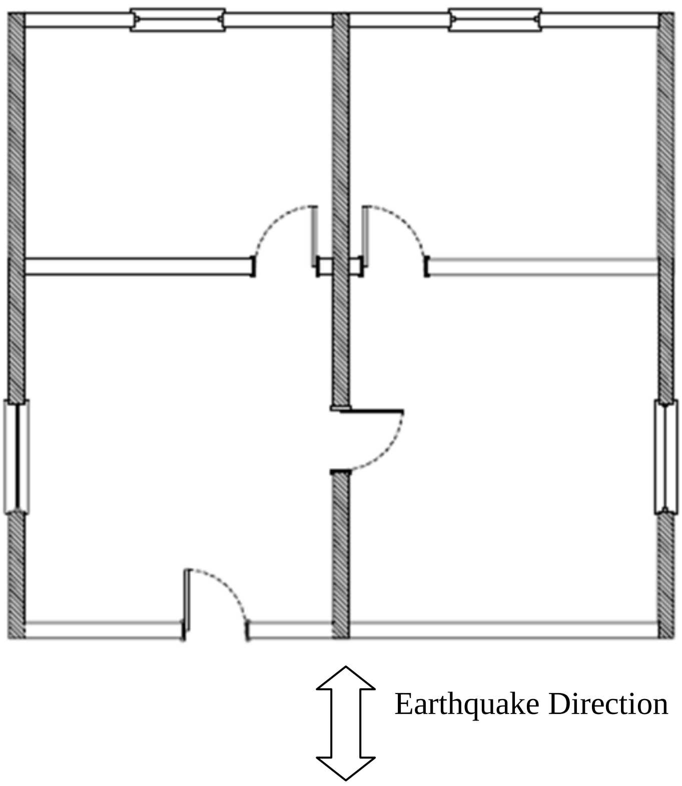

Figure 2.1. Minimum Total Length of Load Bearing Walls [TEC2007]

In Eurocode 8, minimum sum of cross sectional areas of horizontal shear walls in each direction as percentage of the total floor area per storey is given instead of minimum total length of load bearing walls in each orthogonal direction. The requirements for unreinforced masonry buildings are given in Table 2.10. In this table, the parameter S is the soil factor that depends on the site class and ranges between 1.0-1.8. The parameter k is a correction factor that is used in cases where at least 70% of the shear walls under consideration are longer than 2 m, otherwise equal to unity. For the sake of comparison, the last two rows of Table 2.10 are devoted to typical values obtained by Equation (2.1) taken from Turkish codes, assuming constant thicknesses of 200 mm and 300 mm for all load-bearing walls in a typical story and I=1 (residential building). As it is observed in Table 2.10, TEC2007 yields safer values than Eurocode 8 in most of the cases.

Table 2.10. Comparison of Minimum Total Cross-sectional Area of Load-bearing Walls as Percentage of Total Floor Area According to Eurocode 8 and TEC2007. (The abbreviation N/A means "not acceptable".)

<table>
<tr><th colspan="2">Acceleration at site a_gS (in g)</th><th>≤ 0.07k</th><th>≤ 0.10k</th><th>≤ 0.15k</th><th>≤ 0.20k</th></tr>
<tr><td>Earthquake Code</td><td>No. of stories</td><td colspan="4">Minimum total cross-sectional area of load-bearing walls as percentage of total floor area</td></tr>
<tr><td rowspan="4">Eurocode 8</td><td>1</td><td>2.0 %</td><td>2.0 %</td><td>3.5 %</td><td>N/A</td></tr>
<tr><td>2</td><td>2.0 %</td><td>2.5 %</td><td>5.0 %</td><td>N/A</td></tr>
<tr><td>3</td><td>3.0 %</td><td>5.0 %</td><td>N/A</td><td>N/A</td></tr>
<tr><td>4</td><td>5.0 %</td><td>N/A</td><td>N/A</td><td>N/A</td></tr>
<tr><td>TEC2007 (t=200mm)</td><td colspan="5">4.0 %</td></tr>
<tr><td>TEC2007 (t=300mm)</td><td colspan="5">6.0 %</td></tr>
</table>

In IBC2006, the minimum cumulative length of masonry shear walls provided in each orthogonal direction should be 0.4 times the long dimension of the building. Cumulative length of shear walls is calculated without including the openings. According to MSJC2005, the minimum cumulative length requirement is similar to the requirement in IBC2006.

2.4.6. Openings and Maximum Unsupported Length of Load Bearing Walls

According to TEC2007, unsupported length of a load-bearing wall between the connecting wall axes in the perpendicular direction shall not exceed 5.5 m in the first seismic zone and 7.5 m in other seismic zones. (See Figure 2.2) In contrast, the unsupported length should be less than 5.5 m in the first seismic zone and less than 7 m in all other seismic zones according to TEC1975 and TEC1998. In adobe buildings, unsupported wall length should be less than 4.5 m in accordance with TEC1975, TEC1998 and TEC2007.

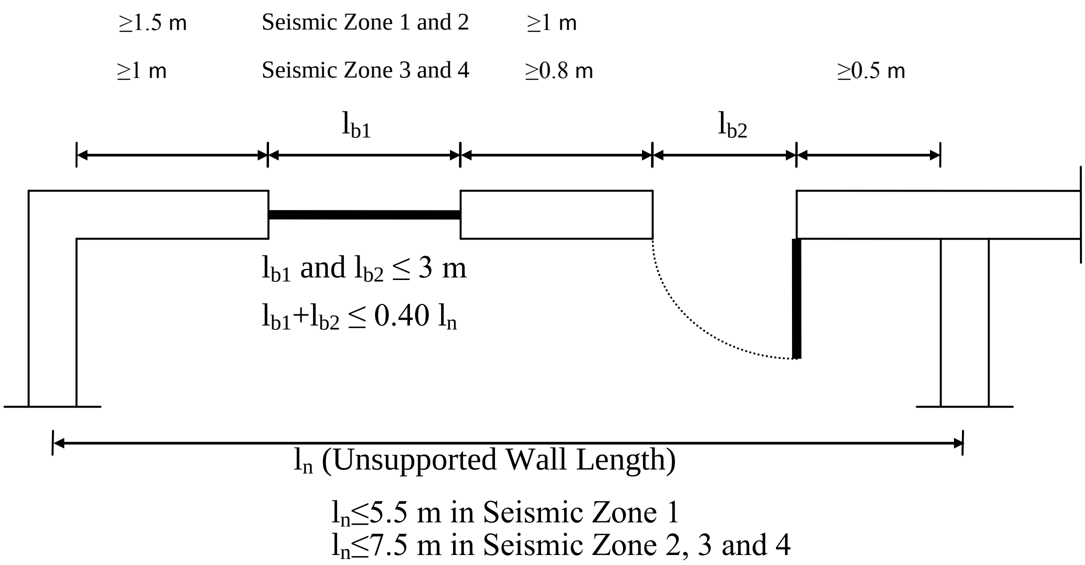

Figure 2.2. The Wall and Void Length Rules According to TEC2007

The distance between the corner of the building and the nearest opening should be less than 1.50 m in seismic zone 1 and 2 and 1.0 m in the seismic zone 3 and 4 considering all versions of Turkish Earthquake Code. (See Figure 2.2) However, according to TEC1975, in the case where the building height is less than 7.5 m, the mentioned plan length may be reduced to 1.0 m in the first and second seismic zones whereas this width can be lowered to 0.80 m in the third and fourth seismic zones.

Excluding the corners of buildings, plan lengths of the load-bearing wall segments between the window or door openings shall be neither less than ¼ of the width of larger opening on either side nor less than 0.8 m in the first and second seismic zones and 0.6 m in the third and fourth seismic zones according to TEC1975. On the contrary, this limit is increased to 1.0 m in the first and second seismic zones and 0.8 m in the third and fourth seismic zones in TEC1998 and TEC2007. (See Figure 2.2) For adobe construction, this width is minimum 0.60 m according to TEC1975 whereas 1 m according to TEC1998 and TEC2007.

According to TEC2007, the distance between the door or window opening and the intersecting wall should be more than 0.5 m in any seismic zones as far as any versions of Turkish Earthquake is concerned. (See Figure 2.2)

In terms of adobe construction, only one door opening shall be permitted in any bearing wall between two consecutive intersections in accord with all versions of Turkish Earthquake Code. However, the size limits differ from version to version. According to TEC1975 and TEC1998, door openings shall not be more than 1.00 m in horizontal, not more than 2.10 m in vertical direction while according to TEC2007, door openings shall not be more than 1.00 m in horizontal, not more than 1.90 m in vertical direction. Similarly, window opening limitations show some discrepancy among different versions. According to TEC1975, window openings shall not be more than 0.90 m in horizontal, not more than 1.40 m in vertical direction. On the other hand, according to TEC1998 and TEC2007, window openings shall not be more than 0.90 m in horizontal, not more than 1.20 m in vertical direction.

Table 2.11. Recommended Geometric Requirements for Masonry Shearwalls According to Eurocode8

Masonry type	***(l/h)min***
Unreinforced, with natural stone units	0.5
Unreinforced, with any other type of units	0.4
Unreinforced, with any other type of units, in cases of low seismicity	0.35
Confined masonry	0.3
Reinforced masonry	No Restriction

In Eurocode 8, the ratio of the length of the wall, l, to the greater clear height, h, of the openings adjacent to the wall, should not be less than a minimum value, $(l/h)_{min}$. The values of $(l/h)_{min}$ are given in Table 2.11. Moreover, the maximum unsupported length of a load-bearing wall should be less than 7 m.

According to IBC2006, there are no obligations about the openings on the masonry walls but masonry walls shall be laterally supported in either the horizontal or the vertical direction at intervals not exceeding those given in Table 2.12. The maximum unsupported length of load – bearing wall requirement in MSJC2005 is exactly the same as the requirement in IBC2006.

Table 2.12. The ratio of maximum wall length to thickness or wall height to thickness

Construction	***Maximum Wall Length(l/t) to Thickness or Wall Height to Thickness (h/t)***
Bearing walls	
Solid units or fully grouted	20
All others	18
Nonbearing walls	
Exterior	18
Interior	36

2.5. Critique about the State of Masonry Design in Turkey

In Turkey, a considerable percentage of the existing building stock is composed of masonry construction. There are many masonry structures which were built in 60s and 70s, and they are still in use, including governmental buildings. Also, a significant number of well-preserved old masonry structures still exist, proving that masonry can successfully resist loads and environmental impacts. In rural regions, one or two story masonry buildings are still being constructed. However, in Turkey, masonry construction is no longer popular because of the following reasons: (Erberik *et al.*, 2008)

- High strength masonry units are not produced in Turkey. Therefore, it is difficult to construct seismically safe masonry buildings with large plan areas in earthquake prone regions.
- It is not economical to construct one or two story masonry housings while it is possible to construct multi-storey reinforced concrete frame buildings, instead.

This has also been reflected in the Turkish Earthquake Code. The section for the seismic design of masonry structures has not been significantly improved in previous versions of the code and it is still limited to some empirical provisions for unreinforced masonry construction. The masonry section of the code was very primitive in 1975 version with very conservative limits as it should be. Then, new clauses have been added to versions in 1998 and 2007. Therefore, some of the limitations have been relaxed due to the introduction of new rules. However, as it is observed in the above sections, the design rules are still strict and conservative when compared to other international codes. This is not surprising, though, since the masonry part of the code relies on empirical design provisions only.

There are no recommendations for reinforced, confined or prestressed masonry construction, in other words, these types of construction are not encouraged in Turkish state of practice. However, just the opposite is true for international codes. These codes have detailed design provisions including different approaches (allowable stress design, strength design and empirical design) and different construction types of masonry (unreinforced, reinforced, confined and prestressed masonry). Then, it becomes possible to construct robust masonry buildings with more than 5 stories as it is encountered in many cities of Europe and the United States. (Erberik *et al.*, 2008)

In Turkey, current unreinforced masonry construction is limited to low-rise small dwellings in rural parts or in suburbs of large cities. However, it is also possible to encounter confined masonry buildings, especially in outskirts of Istanbul, a city under high seismic risk. Confined masonry is a construction system where masonry structural walls are confined on all four sides with reinforced concrete vertical and horizontal confining elements, which are not intended to carry either vertical or horizontal loads, and are eventually not designed to behave like moment resisting frames. There are clauses in the current Turkish code for the placement of horizontal and vertical confining members around masonry walls but these are empirical rules that do not rely on any engineering background and they are not sufficient to ensure the seismic safety of this type of construction in regions of high seismic hazard. Therefore, such structures are very vulnerable to seismic damage, and in turn to physical losses after an earthquake, as many examples of this have been observed during the major earthquakes in Turkey in the last two decades.

In the light of above discussions, the following points should be addressed:

- The masonry design part of Turkish Earthquake Code depends on empirical rules for unreinforced masonry only. Therefore, the design rules are eventually more conservative and strict than the ones in international codes.
- According to the empirical design philosophy, the engineer is constrained since he/she cannot violate the strict rules regarding the structural system like number of stories, geometry in plan, arrangement of walls, or in dimensioning of masonry members with standard sizes of masonry units. However, since international codes encourage the construction of other masonry systems like reinforced, confined and prestressed masonry, they are more flexible and allow different approaches to be used in the design stage of masonry construction.
- Due to the encouragement of design of different masonry construction systems like reinforced or confined in the earthquake code, it would have been possible to design and construct earthquake resistant low-rise and mid-rise residential dwellings which may be an alternative for comparatively vulnerable reinforced concrete moment resisting frame systems. (Erberik *et al.*, 2008)

CHAPTER 3

NEW CONCEPTS FOR DESIGN AND ANALYSIS OF MASONRY STRUCTURES

3.1. Introduction

In first part of this chapter, various design concepts used in civil engineering are introduced together with their major drawbacks. Since the focus of this study is mainly on the performance-based procedures, the most common analysis types that are essential to determine the displacement demands are discussed.

Finally, the concept of performance based design for masonry structures is presented. This part deals principally with the commonly used and the recently developed techniques for determining the performance of masonry structures.

3.2. Force-based vs. Displacement-based Design Procedures

The design tools for any structural types are divided into two main categories; namely ***force-based design*** and ***displacement-based design***. Every method has its own subcategories and its specific analysis methods. However, more detailed explanations of analysis methods belonging to displacement-based design are discussed in the rest of this chapter as the main scope of this study is performance-based design of masonry structures.

3.2.1. Force-based Design

According to the traditional force-based design concept, the main concern for designing structures or their components is the comparison of the loads acting on the cross-section (F_L) with the resistance or capacity (F_R) of that cross-section. If the capacity is larger than the load effects, the design is said to be proper. (See Equation

3.1) At first glance, it seems that this commonly used procedure is suitable to design structures as well as it is simple enough to be used by the practitioner engineers. In fact, this argument is generally true for vertical load effects. However, this simple procedure has some deficiencies when there exist lateral load effects like earthquake loading. To explain the problem, the analysis procedures should be summarized.

$$F_R > F_L \tag{3.1}$$

This method of analysis is investigated by separating into two subcategories:

1) Linear Static Procedure (LSP)
2) Linear Dynamic Procedure (LDP)

The analysis tool that has been commonly used in force-based design is the equivalent lateral load analysis (LSP). This method is preferred over the more complicated methods like response spectrum and time history analysis when the structure in concern is regular in plan and elevation and its dynamic behavior is dominated by first mode of vibration. According to this method, the earthquake effect is simulated by a lateral force on the structure. (See Figure 3.1) The pattern of the lateral load can be the mirror image of the first natural mode shape. Therefore, many standards recommend the inverted triangular or uniform loading shapes depending on the type of the building. However, the lateral load that should be resisted by the building for devastating earthquakes may be up to total weight of the structure. This reality makes the design nearly impossible as the sections appear to be so large that it is impractical and infeasible to build the designed structure.

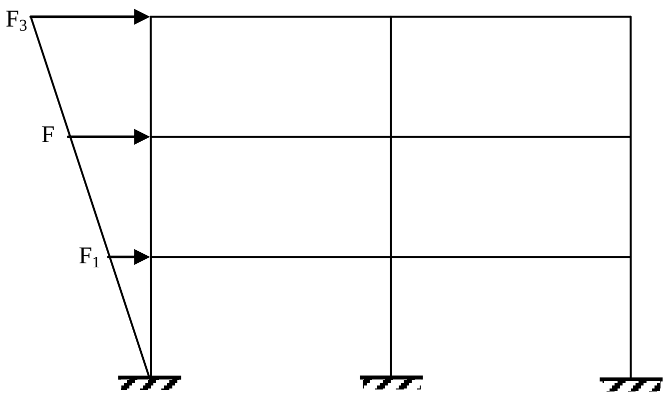

Figure 3.1. Equivalent Lateral Loading

Hopefully, many researchers come up with a new solution. This solution is to design the building inelastically, not elastically. In other words, some damage is allowed in the design stage but this damage should be repairable and no life loss is permitted. Consequently, the design force can be decreased by allowing inelastic deformations. In current codes, this decrease is done by using reduction factors (See Equation 3.2 and Figure 3.2).

$$F_{R1} = \frac{F_e}{R_1} \tag{3.2}$$

where F_e is the elastic force demand, R_1 is the reduction factor and F_{R1} is the reduced inelastic force demand.

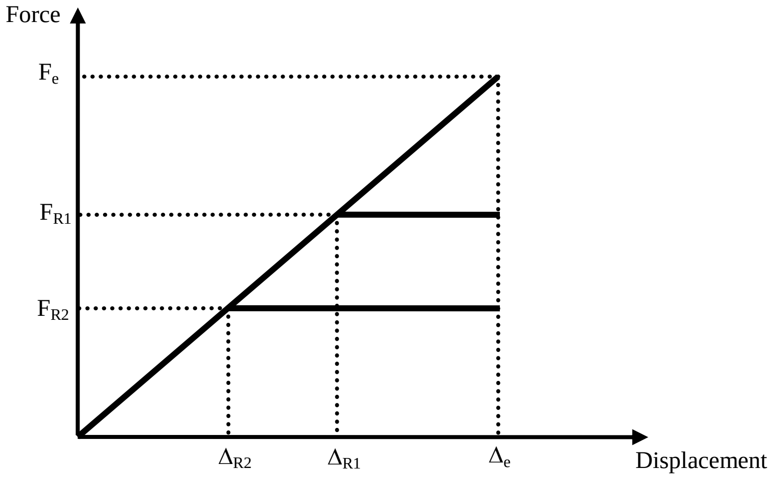

Figure 3.2. Force-Displacement Response of Elastic and Inelastic Systems: The Equal Displacement Approximation (Priestley *et al.*, 2007)

In Figure 3.2, the equal displacement assumption for elastic and inelastic systems is made. At first glance, this assumption seems wrong but the response statistics obtained from time history analysis (Priestley *et al.*, 2007; Chopra, 2001 and Atımtay, 2001) verify that the equal displacement principle holds for medium period structures. However, the equal energy principle should be used for the short period structures. This principle change is reflected in the reduction factors given in standards. For example, in TEC2007, the reduction factors are given in Equation 3.3.

$$R_a = 1.5 + (R - 1.5) * \frac{T}{T_A} \qquad for\ 0 \le T \le T_A \tag{3.3.a}$$

$$R_a = R \qquad for\ T > T_A \tag{3.3.b}$$

where R_a is the reduction factor, R is a variable depending on the structural type, T is the first natural vibration period and T_A is the short characteristic period of the spectrum.

Useful relationships can be obtained from Figure 3.2. Using similarity of triangles,

$$\frac{F_e - F_{R1}}{F_e} = \frac{\Delta_e - \Delta_{R1}}{\Delta_e} \Rightarrow \frac{\Delta_e}{\Delta_{R1}} = \frac{F_e}{F_{R1}} \Rightarrow \mu_1 = R_1 \qquad (3.4.a)$$

or

$$\frac{F_e - F_{R2}}{F_e} = \frac{\Delta_e - \Delta_{R2}}{\Delta_e} \Rightarrow \frac{\Delta_e}{\Delta_{R2}} = \frac{F_e}{F_{R2}} \Rightarrow \mu_2 = R_2 \qquad (3.4.b)$$

According to Equation 3.4, the design force reduction is allowed only if the displacement ductility can be satisfied. This means that the design should be based on another parameter; namely ductility. In contemporary codes, this is done by using some sort of special detailing of critical sections, which changes the behavior of the structural system and increase the ductility to the intended level. Therefore, the displacement capacity of the system is more important than the force capacity as far as the inelastic design is done. However, the force or displacement capacity is not different than each other in elastic systems. (Priestley *et al.*, 2007)

The above short explanation shows that the ductility capacity (displacement ductility or rotational ductility) of structural systems should be compared with the ductility demand of the earthquake in order to obtain a safe design. This comparison is not done in force based design, which is the major drawback of this design approach. Moreover, in force based design, all of the members are assumed to have the same ductility capacity, which is implied by using the same reduction factor for all of the members. (See Equation 3.4) This issue may result in unsafe situations for some structural members that are very vital for the stability of the whole system. (Priestley *et al.*, 2007)

3.2.2. Displacement-based Design

The need for determination of the displacement capacity of structures brings about new analysis methods. Of course, the technological innovations in the computer industry make these new methods feasible. For instance, *Nonlinear Static Procedure* (NSP), *Nonlinear Dynamic Procedure* (NDP) and *Incremental Dynamic Analysis* (IDA) have recently been used for this purpose.

3.2.2.1. Nonlinear Static Procedure (NSP)

This analysis tool known as pushover analysis is employed to determine the force displacement characteristics of structures. First of all, pushover analysis disregards the higher mode effects. In other words, it assumes that the structural behavior is dominated by the first natural vibration mode. Therefore, this method is only meaningful for first mode dominant structures. For example, according to TEC2007, this method is usable for structures that have at least 70% participating mass in the first mode of vibration. Hopefully, many of the frame structures obey this law and pushover analysis is one of the most popular analysis methods for displacement based design.

Pushover analysis is called as nonlinear because the system behaves nonlinear after the elastic capacity of any members is reached. Besides, it is a static analysis since the structure is analyzed in a stepwise manner, statically. More explicitly, there is no inertia effect or damping in pushover analysis. The structure is pushed laterally until any of its members enters their plastic region, till which the same stiffness matrix is used to obtain the displacements and forces.

The plasticity of the structure is defined by plastic hinges attained at both ends of each frame elements, i.e. beams, columns and shearwalls. These plastic hinges determine the behavior of the whole structural system. In other words, the hinge properties are reflected to the pushover curve of the structure.

Shortly, the outline of pushover analysis is given below.

1) The building is modeled as 2D or 3D.
2) Every member is attained two plastic hinges at its both ends. The hinge characteristics may be calculated by drawing interaction diagrams of members or the code-suggested hinges are used. In this stage, the plastic hinge length should be chosen. According to FEMA356, it may be chosen as half of height for beams and columns and as half of length but less than one storey height for shearwalls.

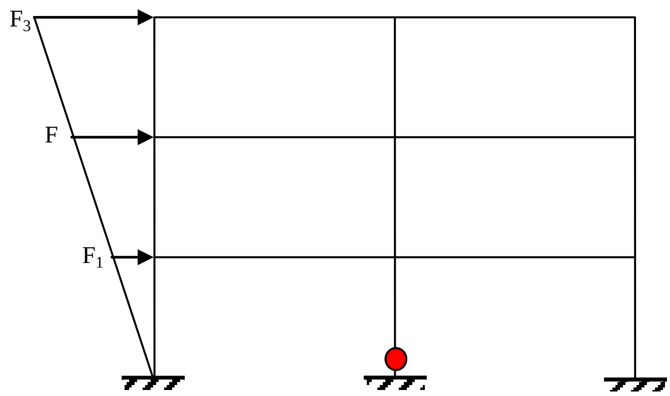

Figure 3.3. Lateral Loading Pattern in Pushover and the Formation of First Hinge

3) After the application of dead and live loads, the structure is analyzed under only these vertical loads.
4) Then, the structure is loaded laterally similar to its first mode shape until any of the members yield. (See Figure 3.3)
5) The stiffness matrix is updated following the yield of any members. The lateral load is increased a little bit till another yield occurs.
6) The structure is pushed until a mechanism occurs. (See Figure 3.4) Then, the base shear versus roof displacement is drawn, which is known as the capacity or pushover curve.

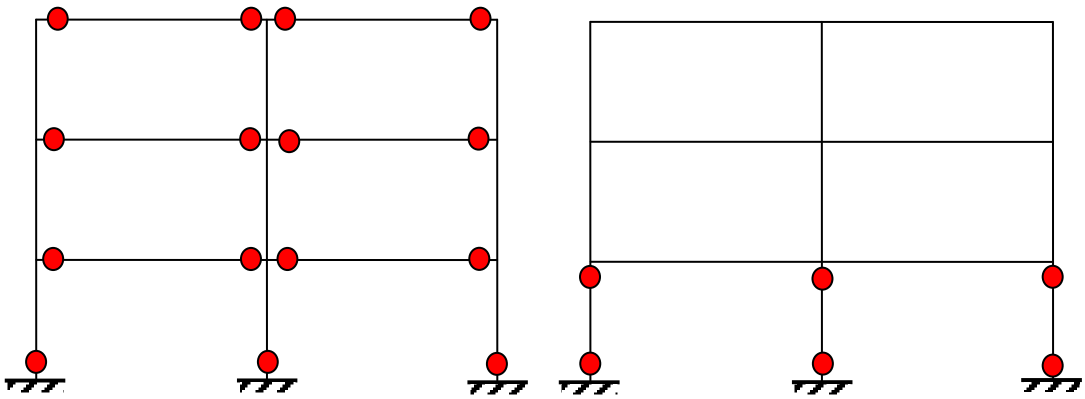

Figure 3.4. Failure Mechanisms

3.2.2.2. Nonlinear Dynamic Procedure (NDP)

Nonlinear dynamic procedure also known as nonlinear time history analysis is accepted as one of the best simulation of the dynamic response of structures. What makes the nonlinear time history analysis so powerful is that it considers the material nonlinearity by using some predefined force-deformation relationships. In literature, there are many hysteretic models for different structural components like reinforced concrete, steel, etc. Some of these models show very good agreement with the experimental data.

Nonlinear time history analysis also gives engineers the opportunity for analyzing the buildings for a given earthquake datum. More interestingly, earthquake data intended to be used in the analysis do not need to be site-recorded ones instead some artificially created data by using attenuation relations can also be utilized. This is because; the site conditions, the fault type, the distance to the fault, etc. affect the earthquake excitation and they change from site to site. Thus, these artificially created earthquake data may be preferred as they reflect these specific conditions of structures better. For example, the data recorded in 1999 Duzce earthquake is meaningful for the site that is close to the effect area of this devastating event like Duzce, Bolu, etc. but it may not be a significant test for a building erected in the USA or Japan.

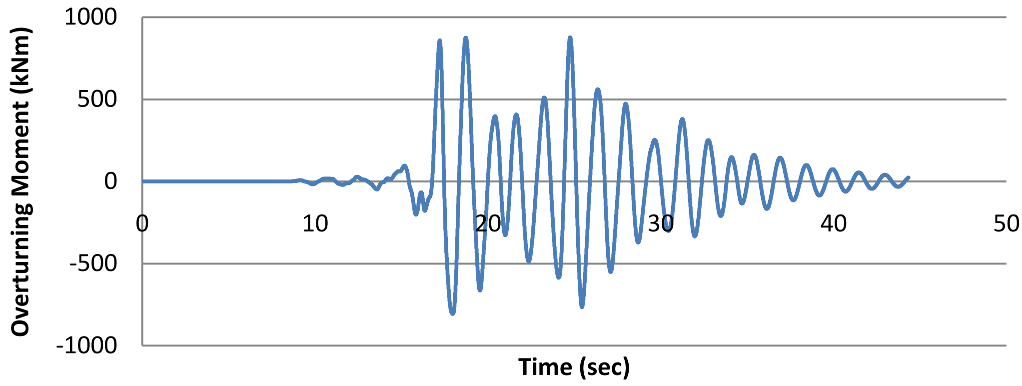

Figure 3.5. A sample overturning moment time history under Duzce 1999 Earthquake

Every member in a structure can be investigated by this analysis. The member forces and member end displacement changes may be determined for small time intervals up to milliseconds or less. (See Figures 3.5 and 3.6) Therefore, for a specified earthquake, the maximum displacement and maximum force demands could be obtained for design purposes. Moreover, since the displacement demands and capacities are known, the expected damage of the structural components is also obtained. However, it is not easy to interpret the nonlinear time history analysis results as there are millions of data for a medium scale structure. Besides, the computational effort for nonlinear time history analysis is very high, so, most of the time; it is not feasible to select this analysis type.

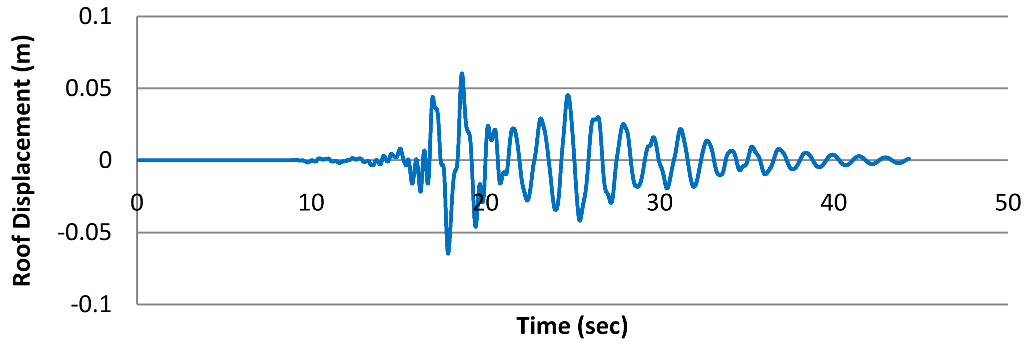

Figure 3.6. A sample roof displacement time history under Duzce 1999 Earthquake

3.2.2.3. Incremental Dynamic Analysis (IDA)

Most of the civil engineers suppose that the incremental dynamic analysis is one of the newest modeling techniques, becoming famous more and more nowadays. However, this technique appeared in 1977 by Bertero (1977). The starting point of this concept is summarized by Vamvatsikos (2002) as follows: “By analogy with passing from a single static analysis to the incremental static pushover, one arrives at the extension of a single time-history analysis into an incremental one, where the seismic 'loading' is scaled."

It can be said that this method is a contemporary time history analysis developed to determine the whole capacity curve of the structure not the capacity curve points for several different earthquakes. In other words, the time history analysis helps finding whether a specified earthquake exceeds the structural capacity or not. However, the incremental dynamic analysis shows the complete capacity curve. This is accomplished by using an incremental time history analysis. The term incremental states explicitly that the ground motion is scaled up in every step of analysis, which brings about the capacity curve formation.

The incremental dynamic analysis can be made linear or nonlinear. If the material properties of structural components are defined as linear elastic, the analysis is linear incremental dynamic analysis. As its name implies, the main property of linear analysis is that the IDA curve is also linear. (See Figure 3.7) Figure 3.7 is a sample IDA curve formed for a sample structure whose first period of vibration is 0.63 sec. In this sample analysis, Duzce (1999), Loma Prieta (1989) and Mexico City (1995) ground motions taken from Peer NGA Database are analyzed by using Nonlin v7.0. From Figure 3.7, it is apparent that IDA curves are dependent on the ground motions, meaning for the same acceleration the displacement demands show dispersion.

Figure 3.7. IDA curve for linear system (T_1=0.63sec and ξ=5%)

If the IDA analysis is done for a nonlinear structure with the same first period of vibration (0.63 sec) and a strain hardening of 5%, the IDA curves are completely different than their linear counterparts as expected. (See Figure 3.8)

Figure 3.8. IDA curve for nonlinear system (T_1=0.63sec, 5% strain hardening and ξ=5%)

From Figures 3.7 and 3.8, it can easily inferred that the demands of Loma Prieta (1989) earthquake is the most in linear analysis but Duzce (1999) earthquake demands the most in some parts of the nonlinear IDA curves. This shows that it is very difficult to guess the IDA curve shapes as only the material property difference causes thoroughly discrepant results.

The outline of the incremental dynamic analysis is given below.

1) The analytical model of building is created.
2) A suitable ground motion data for the building environment is selected.
3) With the selected ground motion, a nonlinear or linear time history analysis of analytical model is done. In this model, a damage measure like maximum interstory drift, maximum displacement, etc. is selected and that value is held in memory in order to use it in creating the incremental dynamic analysis curve.
4) After that, ground motion intensity measure like PGA, first mode spectral acceleration, etc. is determined and the selected ground motion is scaled up with respected to this intensity measure (IM). Then, another time history analysis is done with this scaled earthquake data.
5) Step 4 is repeated until a useful incremental dynamic analysis curve is decided to be reached.
6) Lastly, the selected intensity measure (IM) versus the selected damage measure (DM) is plotted, which is known as the incremental dynamic analysis curve.

3.3. In-plane Behavior of Masonry Walls in General

For displacement-based design, the nonlinear behavior of masonry components should be completely understood. The displacement-based performance limits are related to the behavior of masonry components under vertical and lateral forces. These load-bearing masonry components are named as piers, which are formed as masonry walls pierced by window and door openings. There are three different mechanisms of lateral force resistance for masonry components, which depend primarily on geometry, boundary conditions, magnitude of vertical loads and the characteristics of the brick unit, mortar and the interface between them. However, it should also be mentioned that, in practical cases, it is more possible to encounter mixed type of failure rather than observing only one mode of failure occurring in a masonry component.

3.3.1. Sliding Mechanism

This failure mode generally occurs in the cases that low levels of axial load and poor quality of mortar exist. As its name implies, the upper part of wall slides over the lower one. (See Figure 3.9.a) This action is generally due to the formation of horizontal tensile crack paths in the bed joints when the wall is subjected to reversed seismic action (Magenes and Calvi, 1997). This failure mode is brittle with a limited displacement capacity. However, if sliding mechanism occurs in the presence of high vertical compressive stresses or together with rocking failure mode, then it can be regarded as a desirable mechanism with a significant amount of nonlinear deformation and energy dissipation capacity (Abrams, 2001). In order to predict the shear strength associated with sliding, Mohr-Coulomb formulation is employed. Sliding shear resistance is directly related to shear strength of masonry (f_v)

$$R_{ss} = L * t * f_v \tag{3.5}$$

where

$$f_v = V_{bo} + \mu * \sigma_y \tag{3.6}$$

In the above equations, R_{ss} is the capacity due to sliding shear failure, L is the wall length, t is the wall thickness, V_{bo} is the shear bond strength at zero compression (in MPa), μ is the coefficient of friction, σ_y is the vertical stress (in MPa). Obviously, Equations 3.5 and 3.6 are based on the assumption that mean values of shear strength and vertical stress are used in the horizontal section of the wall where the actual stress distribution is non-uniform. In spite of being approximate, Equations 3.5 and 3.6 have been largely adopted in design and assessment of masonry structures, including the current Turkish Earthquake Code (2007).

If sliding behavior is accompanied by wall cracking due to flexural behavior, effective uncracked section length (L') should be used instead of the total horizontal length of the wall. This approach is adopted by the Eurocode 6 (2003). Parameter L' is calculated by ignoring the tensile strength of bed joints and assuming a simple variation of compressive stresses, generally constant or linear.

3.3.2. Diagonal Tension Mechanism

This failure mode is the most common one under seismic loads. The failure sign for this mechanism is the formation of diagonal cracks just before the attainment of lateral resistance (See Figure 3.9.b). According to Magenes and Calvi (1992), the diagonal cracking load generally lies between 85%-100% of the peak shear force. Most of the time, it manifests itself as x shaped cracks after earthquakes due to the reversible nature of seismic action. Inclined diagonal cracks generally follow the line of bed- and head-joints forming a zigzag path or they also go through bricks. The followed path depends on the relative strength of bricks, mortar and brick-mortar interface. In order to predict the shear strength associated with diagonal cracking, it is assumed that diagonal shear failure is attained when the principal stress at the center of the wall component attains a critical value, which is taken as the tensile strength of masonry (Turnsek and Cacovic, 1971).

$$R_{dt} = L * t * \frac{f_{mt}}{b} * \sqrt{\frac{\sigma_y}{f_{mt}} + 1} \qquad (3.7)$$

In the above equation, R_{dt} is the capacity due to diagonal tension failure, f_{mt} is the tensile strength of masonry (in MPa) and b is the shear stress distribution factor, which depends on the aspect ratio (H/L) of the masonry wall. Benedetti and Tomazevic (1984) suggest to use b=1.0 for H/L≤1, b=H/L for 1<H/L<1.5 and b=1.5 for H/L≥1.5. Although the above formulation is based on the assumption that masonry wall is an isotropic and homogeneous continuum, it has the advantage of being based on a single mechanical parameter, tensile strength of masonry, which can simply be obtained from experiments on masonry panels.

3.3.3. Rocking Mechanism

Rocking takes place when the aspect ratio of a wall is large enough to give rise to a high moment to shear ratio. Final failure is because of the overturning of the wall and simultaneous crushing of the compressed corner. (See Figure 3.9.c) Therefore, rocking is a flexural failure, which is a more ductile and so more desired mechanism. In the case of rocking mechanism, large displacements can be observed without a significant strength degradation, especially in the case where mean axial load is low in comparison with the compressive strength of masonry. The displacement capacity can be as high as 10% of the total wall height (Magenes and Calvi, 1997). Tests of unreinforced masonry pier components that experienced rocking mechanism were observed to exhibit nonlinear deformations more than ten times the apparent yield displacement (Erbay and Abrams, 2001). However, this limit is unusable since it does not govern the ultimate deformation capacity of the masonry component when compared to other brittle modes of failure, which generally take place before. In addition to this, behavior in rocking mechanism is largely nonlinear elastic, thus the energy dissipation capacity in a unit cycle is not high (Abrams, 2001).

The flexural resistance of a masonry wall depends on the crushing of the compressive part. Therefore, compressive strength of masonry is necessary for the quantification of the lateral strength in rocking mechanism. Considering the fact that behavior of masonry components under uniaxial compression is analogous to that of concrete, an equivalent rectangular compressive stress block can be employed in the calculation of flexural resistance of masonry wall section as

$$M_{Ru} = \frac{\sigma_y * t * L^2}{2}\left(1 - \frac{\sigma_y}{f_m}\right) \tag{3.8}$$

where M_{Ru} is the flexural capacity of the wall section and f_m is the compressive strength of masonry (in MPa). Hence, the maximum lateral strength can be computed from the following formulation

$$R_f = \frac{M_{Ru}}{\alpha * H} \tag{3.9}$$

where parameter α is a coefficient that defines the position of the moment inflection point along the height of the wall. Parameter α takes the value of 0.5 in the case of a fixed ended wall and 1.0 in the case of a cantilever wall.

Maximum strength of a masonry wall segment (R_U) can be regarded as the minimum value obtained from different modes of failure, i.e.

$$R_U = min\{R_{ss}, R_{dt}, R_f\} \tag{3.10}$$

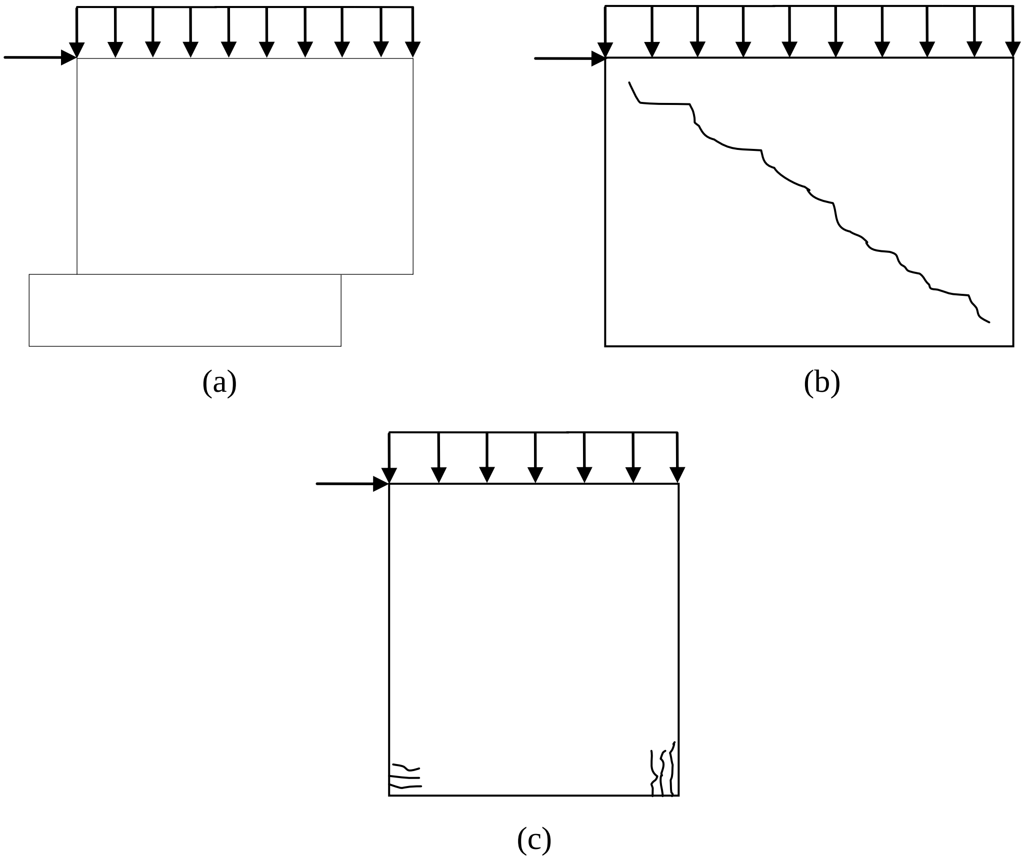

Figure 3.9. Different Failure Modes for Walls: (a) Sliding; (b) Diagonal-tension; (c) Rocking

3.4. Attainment of Performance Limit States for Masonry Walls

Different researchers studied on the performance limits of masonry components in terms of deformation capacities by considering also the aforementioned behavioral states. These are summarized in the following part of this chapter.

According to Priestley *et al.* (2007), the design drift for a damage control performance of rocking behavior can be obtained by limiting the masonry strain at the compressed toe of the wall (a reasonable value is given as 0.004) and assuming a linearly varying strain distribution in the lower section of the wall. If a maximum compression depth equal to 20% of the wall length is assumed, the design drift is obtained as 0.8%. Although larger values have been obtained from experimental results, this value is regarded as consistent with practical considerations, in relation with the drift levels of other failure modes. They also stated that design drifts for a damage control performance of shear behavior due to diagonal cracking are in the range of 0.4%-0.5%, hence smaller than the value recommended for flexural response.

Priestley *et al.* consider the sliding failure mode in a different manner defined by the following equation, where no contribution of cohesion is considered, assuming that the horizontal joint is already cracked in tension due to flexure

$$R_{ss} = L * t * (\mu * \sigma_y) \tag{3.11}$$

They also state that the sliding shear failure mode in this format is generally neglected in code approaches since it can be regarded as a part of a more general sliding shear behavior by Equation 3.5 and shear failure due to diagonal tension cracking is always more critical and brittle when compared to sliding shear failure. Hence they did not give any recommendations about design drift associated with sliding shear behavior.

Calvi (1999) presented a method that should be used for a global loss estimation of buildings and not for assessing the response of single building. Moreover, in this method, it is assumed that all masonry buildings are constructed by using traditional techniques and no seismic design provisions are utilized in the design process.

The average displacement and dissipation capacity of clay brick buildings and sub-assemblages are based on experimental and numerical data given in Magenes and Calvi (1997). Furthermore, only in-plane failure is taken into account, i.e. out-of-plane failure modes are ignored (The wall-to-slab connections are assumed to be proper).

In this method, the performance states, or limit states, for masonry structures are divided into three groups namely LS1, LS2 and LS3. The definitions given by Calvi are summarized below:

- *LS1:* It is associated with the minor structural damage and moderate non-structural damage. The building can immediately be in service after the earthquake without any need for significant strengthening and repair.
- *LS2:* In this limit state, significant structural damage and extensive non-structural damage exist. The building cannot be utilized after the earthquake without significant repair. Still, repair and strengthening are feasible.
- *LS3:* This performance level is related to the collapse. The repairing is neither possible nor economically reasonable. The structure will have to be demolished after the earthquake. Beyond this limiting state, global collapse with danger for human life has to be expected.

As this method is designed to investigate population of buildings, the limit states are not obtained through rigorous analyses and investigations. The following values (See Table 3.1) for each performance level that are valid for every structure are suggested by Calvi

Table 3.1. Limiting States for Brick Masonry Structures

Limiting State	***Drift Ratio (%)***
LS1	0.1
LS2	0.3
LS3	0.5

Calvi also states that a linear deformed shape should be assumed for masonry structures up to the performance level LS1 as no damage concentration occurs. In contrast, the soft storey mechanism in the first storey occurs in the performance levels LS2 and LS3 due to high levels of damage concentrations (Figure 3.10). Therefore, the comparison of drift ratio demands with the limiting values should be done for roof level in LS1 and for the first storey in LS2 and LS3.

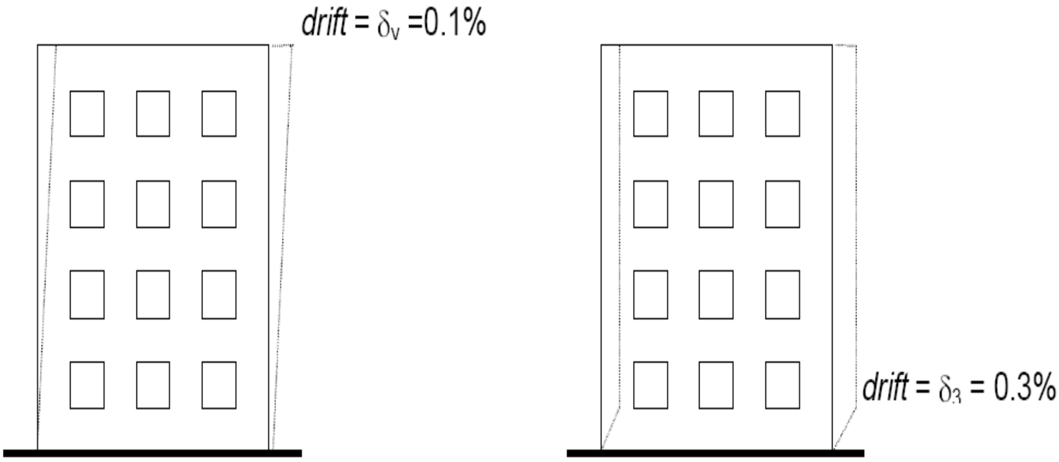

Figure 3.10. Assumed deformed shapes for a masonry building, considering limit states LS1 (left) and LS2 (right) (Calvi, 1999)

According to Tomazevic (2007), the resistance curves of unreinforced and confined masonry structures are adequately represented by the relation between the resistance (R) of the critical storey (most of the time, it is first storey) and the storey drift (d) of the same storey (Figure 3.11).

On the resistance curve, four limit states that determine the usability of buildings are defined as follows:

- *Crack (damage) Limit State:* This limit state (d_{cr}) is associated with the first crack occurrence that apparently affects the initial stiffness of the structural system. The serviceability limit can be decided by crack limit state.
- *Maximum Resistance:* As its name implies, it is the maximum force that can be tolerated by the structural system. (d_{Rmax})
- *Design Ultimate Limit State:* It is the limit of displacement after which the resistance curve is not dependable. As a common practice, the displacements up to the point where the actual force resistance degrades to 80% of the maximum force resistance are considered. After that point ($d_{0.8Rmax}$), the resistance curve cannot be utilized for design purposes. The residual resistance curve informs about the additional ductility and energy dissipation capacity of the structure.
- *Limit of Collapse:* This limit includes partial or total collapse of the building (d_{coll}).

The resistance curve is bilinearized in order to simplify the calculations. For this purpose, the equal energy principle is used (Figure 3.11).

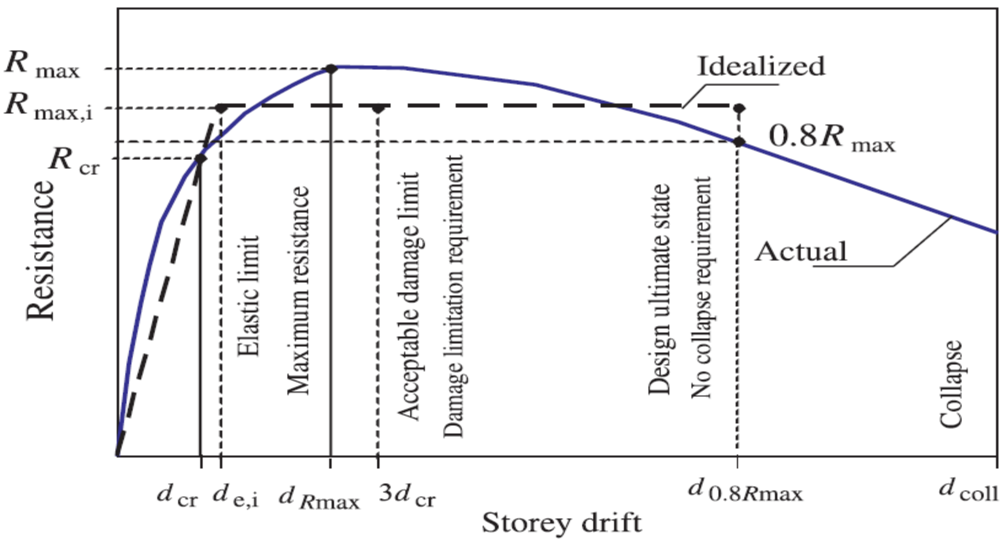

Figure 3.11. Idealization of Resistance Curve and Definition of Limit States

By using experimental data and the damage grades similar to European Macroseismic Scale (EMS-98) (Grünthal, 1998), the observed damage is related to the drift ratios (Figure 3.12). According to Tomazevic, the acceptable damages (repairable damages) are attained after the maximum force resistance is attained. More mathematically, this acceptable damage occurs at storey drifts that are approximately three times the storey drifts at the first crack formation in the walls.

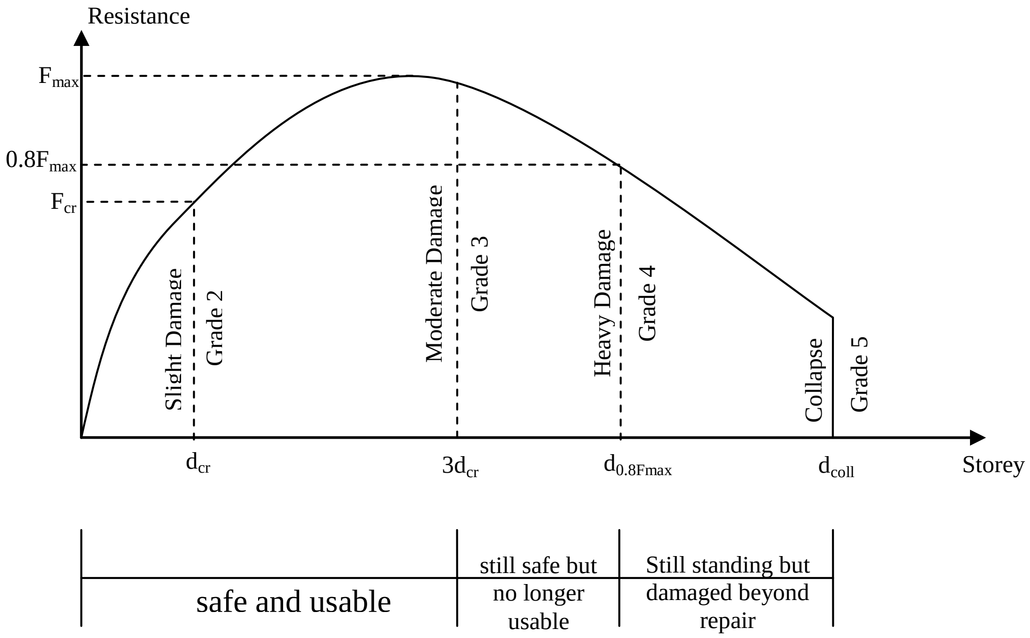

Figure 3.12. Drift Ratio and Damage State Relations found from Experiments

According to Abrams (2001), the main idea is that the masonry components that rocks or slides can be considered to possess significant ductility since the overall force-deflection curves for these failure modes are nonlinear. Moreover, Abrams states that rocking and sliding mechanisms are inherently displacement-controlled actions in which peak strengths can be resisted as large nonlinear deformations are imposed during seismic excitation, thus lend themselves well to performance-based approaches based on displacements. However, other modes of failures i.e. diagonal tension and toe crushing are more brittle, so the force-based design is more suitable for them.

As Abrams stated, after the mode of failure is determined the force-deflection curve and the acceptable performance limits of primary and secondary walls are taken from FEMA273 in terms of deformation capacities for each performance state (see Figure

3.13 and Table 3.2). Finally, the demands are compared with the aforementioned performance limits and the design is accepted when all of the members pass this check. At first glance, this seems too conservative but this method is intended to be used in rehabilitation procedure, so this procedure should be capable of identifying the most critical component that must be strengthened first.

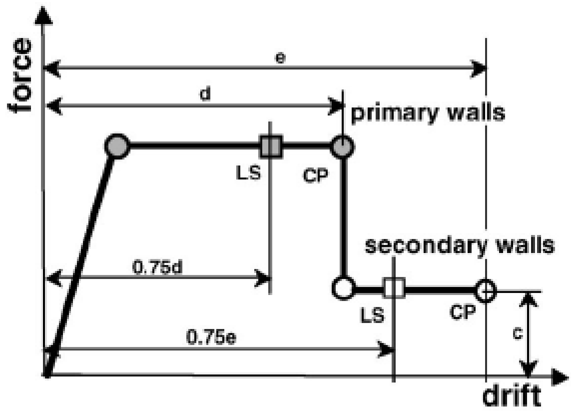

Figure 3.13. Idealized force-deflection curve for walls and piers

Table 3.2. Acceptable Performance Limits for URM Walls and Piers

				Acceptable Criteria				
				Primary Members			Secondary Members	
Behaviour Mode	***c (%)***	***d (%)***	***e (%)***	***IO (%)***	***LS (%)***	***CP (%)***	***LS (%)***	***CP (%)***
Bed-joint Sliding	0.6	0.4	0.8	0.1	0.3	0.4	0.6	0.8
Rocking	0.6	$0.4\frac{h_{eff}}{L}$	$0.8\frac{h_{eff}}{L}$	0.1	$0.3\frac{h_{eff}}{L}$	$0.4\frac{h_{eff}}{L}$	$0.6\frac{h_{eff}}{L}$	$0.8\frac{h_{eff}}{L}$

* IO stands for immediate occupancy, LS is life safety and CP is collapse prevention.

Alcocer *et al.* (2004) presented a method for performance-based design and evaluation of confined masonry construction. Their study aims at determining the earthquake performance of masonry houses in Mexico, where the confined masonry is the most widely preferred structural system. Furthermore, in Mexico, the handmade solid clay bricks are commonly used. Therefore, this technique is valid for confined clay brick masonry structures.

The method starts with the determination of inelastic displacement demands as usual. Then, these are checked with the performance criteria that are suggested by Alcocer *et al.* depending on the experimental results and damage observations in the laboratory and in the field. As it can be seen from Table 3.3, there are three limit states namely serviceability, reparability and safety. The short definitions of performance limit states as given in Alcocer *et al.* are summarized below.

- *Serviceability Limit State:* It is associated to the onset of masonry inclined cracking. This limit state is quite variable, depending on the type of masonry unit, flexure-to-shear capacity ratio of wall and others. At this stage, damage level is low.
- *Reparability Limit State:* It is associated with the formation of the full inclined cracking and the penetration of such cracking into the tie column ends. It has been observed in the laboratory that the residual crack width at this limit state is of order of 2 mm.
- *Safety Limit State:* It corresponds to wall shear strength, typically characterized by large masonry cracks (with a residual width of 5 mm) and considerable damage to tie column ends. Damage in tie columns occurs in the form of yielding of tie column longitudinal reinforcement due to shearing and onset of cracking, crushing and spalling.

Table 3.3. Performance Criteria for Confined Masonry Structures with Solid Clay Units

Limit State	Residual Crack Width (mm)	Drift Angle (%)
Serviceability	0.1	0.15
Reparability	2	0.25
Safety	5	0.40

3.5. Different Modeling Strategies

Two different strategies can be used for modeling masonry components.

1) Finite Element Method (Continuum)
2) Frame Model
   a. Lumped Plasticity
   b. Distributed Plasticity

Displacement-based design is a quite new concept for masonry structures. Therefore, there is no consensus about how to determine the capacity curve of the critical storey. Most of the time, the capacity curve is obtained by using pushover analysis instead of using more complicated finite element analysis for practical purposes, which will be dealt in the next chapter in detail. In this simplified analyses, the plastic behavior of masonry walls may be defined in various ways like lumped plasticity (with plastic hinges) (See Gilmore *et al.*, 2009; Salonikios *et al.*, 2003 and Penelis, 2006) and distributed plasticity (Belmouden & Lestuzzi, 2009).

3.5.1. Lumped Plasticity

In this section, two of the most commonly used lumped plasticity models are explained in detail. One way is to define inelastic behavior by using only one hinge at the bottom of piers. The spandrels are taken as elastic and rigid end zones are applied for only both ends of them. (See Figure 3.14) This method is established by Gilmore *et al.* (2009). In this technique, the degradation in stiffness should be predicted in advance, which sounds easy but it is not. Gilmore *et al.* claim that the stiffness degradation is dependent on the workmanship and the material quality, which shows a high scatter from region to region.

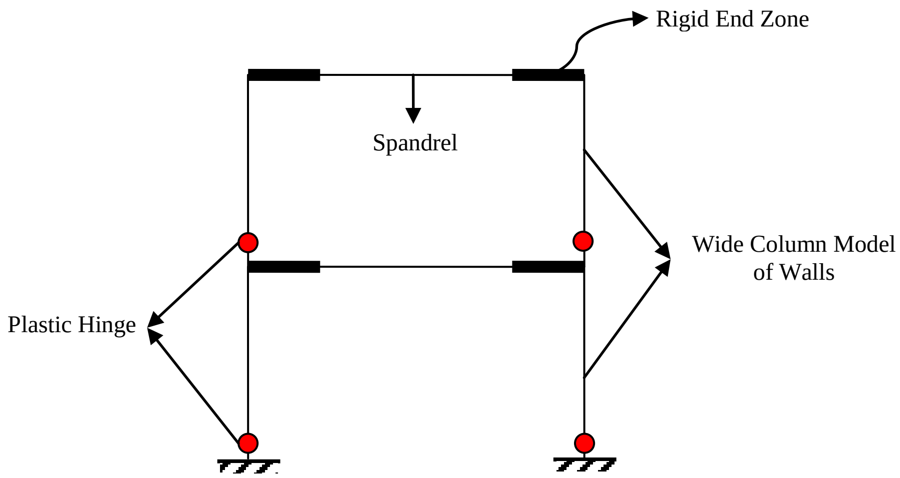

Figure 3.14. One Hinge Plasticity Frame Model

The other way is to use three different plastic hinges for every member (See Figure 3.15). In this technique, the end plastic hinges are used to simulate the flexural behavior. Therefore, these hinges are defined as moment versus rotation (M-θ). The moment capacities are found in a similar fashion to reinforced concrete case, i.e. the rectangular block concept is used. The maximum rotation capacity for flexural hinges is defined by experimental data as 1% according to Penelis (2006) or the region specific value can also be used. The other plastic hinge is placed in the middle and utilized to describe the shear behavior (V-Δ). More detailed explanation of this method can be found in Salonikios *et al.* (2003).

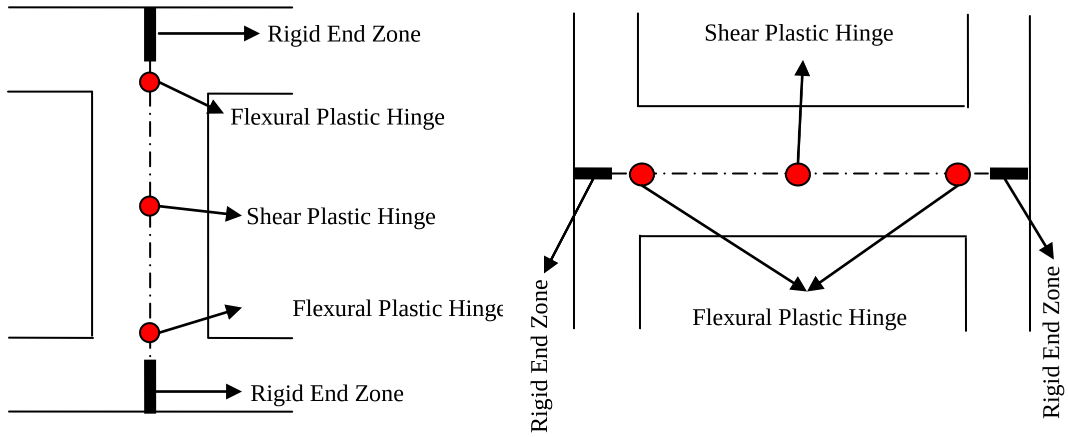

(a) Pier Frame Model (b) Spandrel Frame Model

Figure 3.15. Three Hinge Frame Model Details (Salonikios *et al.*, 2003)

After the analysis method is selected, the limit states for the critical storey should be determined and these limits ought to be compared with the displacement demands. In literature, there are many displacement limits given in different studies, five of which are summarized in this dissertation.

CHAPTER 4

FINITE ELEMENT MODELING OF THE IN-PLANE BEHAVIOR OF MASONRY WALL ELEMENTS

4.1. Introduction

In the first part of this chapter, a distinct finite element model for simulating the in-plane behavior of masonry walls is introduced after short definitions of in-plane modeling techniques common for masonry. Then, the assumptions and restrictions of this new model along with the material properties, i.e. plasticity, are summarized. Finally, the sufficiency of this model is tested by comparing its estimations with the experimental result of a wall tested in ETH Zurich.

4.2. Modeling Technique for Masonry Wall Elements

There is a need to estimate the behavior of masonry structures analytically because the design process demands the internal forces whereas the assessment process requires the simulation of the behavior of an existing structure in order to evaluate the expected performance under some external effects like earthquake, wind, explosion, etc. These analytical models can also be used to evaluate the code criteria and give researchers the chance to improve them.

Unfortunately, no analytical modeling technique has been able to simulate the behavior of the masonry structures exactly. This is because; the masonry structures have very complex non-homogeneous and anisotropic material properties as they are composed of mortar and masonry units.

In literature, there are three types of finite element based modeling techniques for modeling in-plane behavior of walls namely micro-modeling, simplified micro-modeling and macro-modeling. (See Figure 4.1)

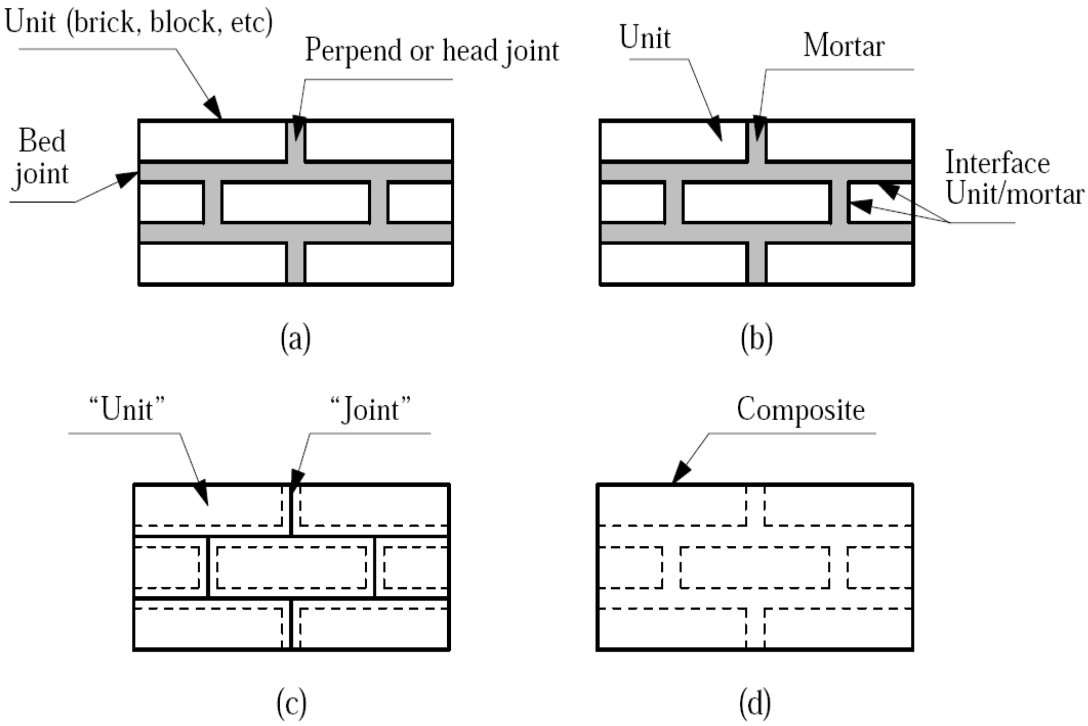

Figure 4.1. Modeling techniques for masonry structures: (a) masonry sample; (b) detailed micro-modeling; (c) simplified micro-modeling; (d) macro-modeling (Lourenco, 1996)

One contemporary idea about in-plane modeling of masonry walls is that this complex material can be solved by modeling its constituents one by one. So, a technique known as *micro-modeling* can be used for this purpose. This approach aims at including every part of wall in the model. Therefore, every unit, mortar and interface between mortar and units are taken into account in the analysis. (See Figure 4.1.b) As it is apparent that the interface has to be included to prevent the penetration of brick media into the mortar continuum or vice versa, these interface elements are given an artificial stiffness so as to assure all brick and mortar elements work together. In this strategy, every element has its individual material property like compressive strength, Poisson's ratio, modulus of elasticity, etc. However, it is almost impossible to create a micro-model of whole structure. Even if such a target were achieved, the solution of this model would probably take a couple of days.

Consequently, this technique is impractical and it is only used for small structural components, not for the whole structure.

In order to perform more practical analysis, the units and the mortar are not defined separately instead the units are modeled and between them interface elements are placed. This new strategy is called as *simplified micro-modeling*. (See Figure 4.1.c) Just like micro-modeling, simplified micro-modeling can also simulate the cracking pattern of walls. This is acquired by the interface elements. Whenever the interface element reaches its cracking or crushing capacity, the model shows a void between units. (See Figure 4.2.a) In this model, plasticity is lumped in the interface elements, leading the possible cracks and crushing planes to occur only along the interface elements. (See Figure 4.2.b) More detailed information about this modeling technique can be found in Lourenco (1996).

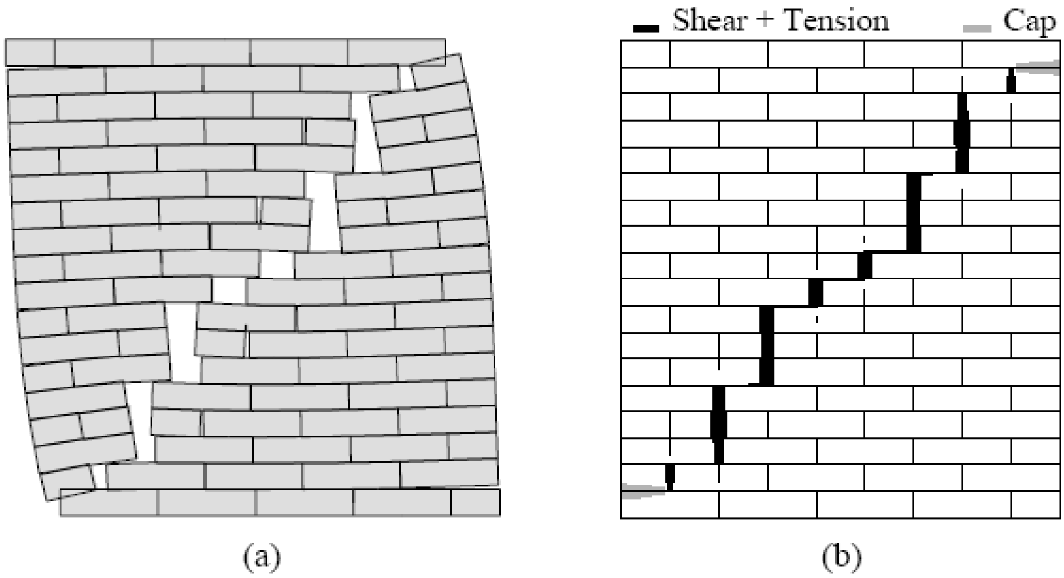

Figure 4.2. A typical wall modeled by simplified micro-model: (a) Deformed shape of the wall under vertical and horizontal load combination; (b) Damage pattern under the same load combination (Lourenco, 1996)

The third approach, which is the main concern for this study, is the modeling of masonry as if it is composed of a single homogeneous material. This method is called as macro-modeling or smeared model. As its name implies, only one material composed of brick and mortar is considered in this approach. (See Figure 4.3) Since the whole structure can be modeled by using this method, it can be utilized for assessing the structural performance of existing buildings under different loading conditions.

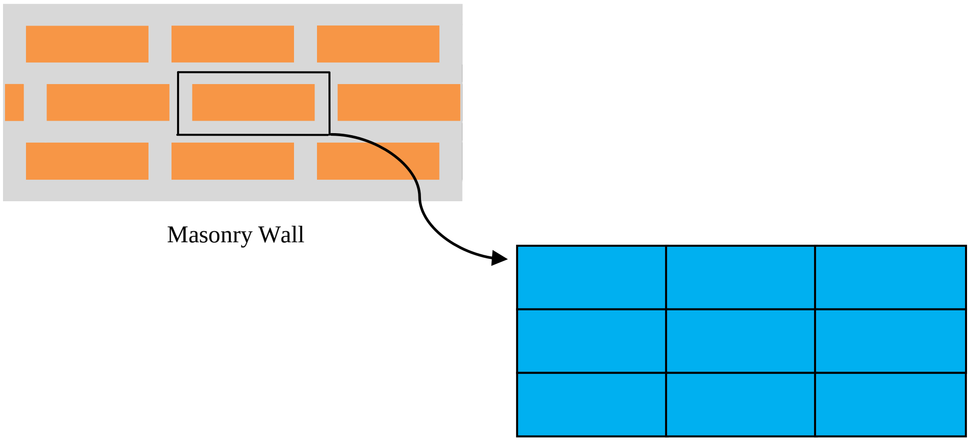

Figure 4.3. Sketch of Macro-modeling Technique

The main difficulty about the macro modeling is that the plastic behavior of a heterogeneous material (masonry) should be described by a single homogeneous element. Worse, there is no method which perfectly predicts the mechanical properties of the masonry by using the mechanical properties of its constituents namely, mortar and bricks. In fact, there are some efforts for generating empirical relationships but no consensus has been reached yet regarding this issue. Based on different experiments, some conclusions have been drawn about predicting masonry behavior. For example, Kaushik *et al*. (2007) state that the masonry, generally behaves in between the weak mortar and the strong brick. (See Figure 4.4)

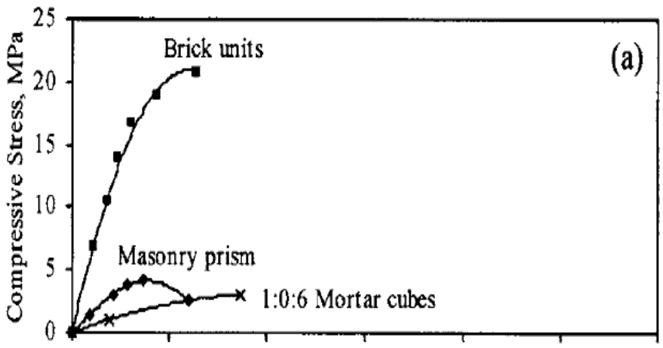

Figure 4.4. The Compressive Behavior of Masonry Prism, Mortar and Brick (Kaushik *et al.*, 2007)

The problem about estimating the plastic behavior of masonry is solved by using experimental data, viz. prism tests or full scale wall tests of the same wall. However, this remedy is not very economical and practical.

In this study, various walls are modeled with the Finite Element Program ANSYS 11 by using macro-modeling technique. The choice of macro-modeling is due to the time limitations based on the fact that more than 300 models are intended to be solved in this parametrical study.

Element type Solid 65 is selected from more than 100 different elements in ANSYS 11 as the most suitable one for modeling in-plane behavior of masonry walls. This is because; this element has the capability to exhibit crack and crush whenever its tensile and compressive capacity is reached. This property gives the opportunity to see the crack pattern and to identify the failure mode of a masonry wall. The other features of Solid 65 are summarized in the rest of this subsection.

4.3.1. Element Type Solid 65 that has been used in the Analyses

This element is designed for modeling reinforced or unreinforced concrete members. It is a three-dimensional brick element. (See Figure 4.5) It has eight nodes placed at its each corner. There are three translational degrees of freedom at each node (u_x, u_y and u_z).

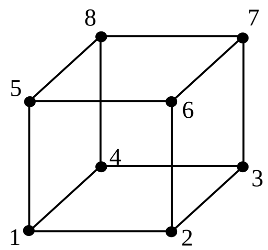

Figure 4.5. Solid 65 Element (3D 8 – node element)

According to ANSYS Element Reference, the most important aspect of this element is the treatment of nonlinear material properties. In other words, the element is capable of exhibiting cracking (in three orthogonal directions), crushing, plastic deformation and creep just like concrete. Three different reinforcement types can be defined in various orientations. These rebars contribute to only axial and bending response, but not the shear.

4.3.1.1. Assumptions and Restrictions of Solid 65 Element

The main properties and some restrictions given in ANSYS Element Reference and ANSYS Theoretical Reference are listed as follows:

- Zero volume elements are not allowed (2D is not allowed.).
- All elements must have eight nodes.
- A prism-shaped element may be formed by defining duplicate K and L and duplicate O and P node numbers. (See Figure 4.6) A tetrahedron shape is also available. The extra shapes (to be discussed later) are automatically deleted for tetrahedron elements.
- Whenever the rebar capability of the element is used, the rebar are assumed to be "smeared" throughout the element. The sum of the volume ratios for all rebar must not be greater than 1.0.
- The element is nonlinear and requires an iterative solution.
- When both cracking and crushing are used together, care must be taken to apply the load slowly to prevent possible fictitious crushing of the concrete before proper load transfer can occur through a closed crack. This usually happens when excessive cracking strains are coupled to the orthogonal uncracked directions through Poisson's effect. Also, at those integration points where crushing has occurred, the output plastic and creep strains are from the previous converged substep. Furthermore, when cracking has occurred, the elastic strain output includes the cracking strain. The lost shear resistance of cracked and/or crushed elements cannot be transferred to the rebar, which have no shear stiffness.
- The following two options are not recommended if cracking or crushing nonlinearities are present:
    - Stress-stiffening effects.

- Large strain and large deflection. Results may not converge or may be incorrect, especially if significantly large rotation is involved.

- Cracking is permitted in three orthogonal directions at each integration point.
- The concrete material is assumed to be initially isotropic.
- In addition to cracking and crushing, the concrete may also undergo plasticity. In this case, the plasticity is done before the cracking and crushing checks.

4.3.1.2. Shape Functions for Solid 65 Element

Solid 65 element has two options as far as shape functions are concerned. First one is the shape functions without extra shapes (See Equations 4.1.a-4.1.c) and the other one is the ones with extra shapes (See Equations 4.2.a-4.2.c). Note that when defining these equations, the notations in Figure 4.6 are used.

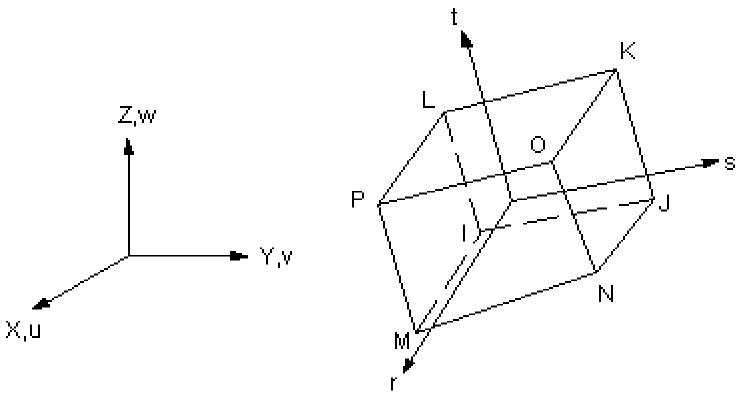

Figure 4.6. Local and Global Coordinates of 8 - node Brick Element [ANSYS Theory Reference]

$$u = \frac{1}{8}\begin{pmatrix} u_I(1-s)(1-t)(1-r) + u_J(1+s)(1-t)(1-r) + u_K(1+s)(1+t)(1-r) \\ +u_L(1-s)(1+t)(1-r) + u_M(1-s)(1-t)(1+r) + u_N(1+s)(1-t)(1+r) \\ +u_O(1+s)(1+t)(1+r) + u_P(1-s)(1+t)(1+r) \end{pmatrix} \tag{4.1.a}$$

$$v = \frac{1}{8}\begin{pmatrix} v_I(1-s)(1-t)(1-r) + v_J(1+s)(1-t)(1-r) + v_K(1+s)(1+t)(1-r) \\ +v_L(1-s)(1+t)(1-r) + v_M(1-s)(1-t)(1+r) + v_N(1+s)(1-t)(1+r) \\ +v_O(1+s)(1+t)(1+r) + v_P(1-s)(1+t)(1+r) \end{pmatrix} \tag{4.1.b}$$

$$w = \frac{1}{8}\begin{pmatrix} w_I(1-s)(1-t)(1-r) + w_J(1+s)(1-t)(1-r) + w_K(1+s)(1+t)(1-r) \\ +w_L(1-s)(1+t)(1-r) + w_M(1-s)(1-t)(1+r) + w_N(1+s)(1-t)(1+r) \\ +w_O(1+s)(1+t)(1+r) + w_P(1-s)(1+t)(1+r) \end{pmatrix} \tag{4.1.c}$$

As it can easily be inferred from Equations 4.1-4.2, there are three extra terms in every displacement shapes. (See last three terms in Equations 4.2.a-4.2.c) These additional variables are used to define the bending shape better. In other words, these extra polynomial terms prevent the parasitic shear occurring in the element known as shear locking. This remedy is also applied to the four-node plane elements (Q4) and Q4 element is turned to Q6 elements. However, this solution leads to the incompatible modes when more than one element is used to model a member, which is most of the time the case. (See Cook *et al.*, 2002 for details)

$$u = \frac{1}{8}\begin{pmatrix} u_I(1-s)(1-t)(1-r) + u_J(1+s)(1-t)(1-r) + u_K(1+s)(1+t)(1-r) \\ +u_L(1-s)(1+t)(1-r) + u_M(1-s)(1-t)(1+r) + u_N(1+s)(1-t)(1+r) \\ +u_O(1+s)(1+t)(1+r) + u_P(1-s)(1+t)(1+r) \\ +u_1(1-s^2) + u_2(1-t^2) + u_3(1-r^2) \end{pmatrix} \tag{4.2.a}$$

$$v = \frac{1}{8}\begin{pmatrix} v_I(1-s)(1-t)(1-r) + v_J(1+s)(1-t)(1-r) + v_K(1+s)(1+t)(1-r) \\ +v_L(1-s)(1+t)(1-r) + v_M(1-s)(1-t)(1+r) + v_N(1+s)(1-t)(1+r) \\ +v_O(1+s)(1+t)(1+r) + v_P(1-s)(1+t)(1+r) \\ +v_1(1-s^2) + v_2(1-t^2) + v_3(1-r^2) \end{pmatrix} \tag{4.2.b}$$

$$w = \frac{1}{8}\begin{pmatrix} w_I(1-s)(1-t)(1-r) + w_J(1+s)(1-t)(1-r) + w_K(1+s)(1+t)(1-r) \\ +w_L(1-s)(1+t)(1-r) + w_M(1-s)(1-t)(1+r) + w_N(1+s)(1-t)(1+r) \\ +w_O(1+s)(1+t)(1+r) + w_P(1-s)(1+t)(1+r) \\ +w_1(1-s^2) + w_2(1-t^2) + w_3(1-r^2) \end{pmatrix} \tag{4.2.c}$$

4.3.1.3. Quadrature Points for Solid 65 Element

In ANSYS, element and global stiffness matrices are formed and then their values are calculated by using the numerical methods (not the analytical ones) for the sake of less computer power and time consumption. The Gauss-Quadrature is employed in ANSYS as this numerical approach is one of the best methods for integrating the polynomials. Specifically, 2x2x2 point Gauss-Quadrature is used for Solid 65 formulation, which calculates the exact integral of polynomials up to third degree. (See Figure 4.7) Therefore, the exact stiffness matrix of Solid 65 is used in the analysis as the displacement shape polynomial has utmost second degree. (See Equations 4.1 and 4.2)

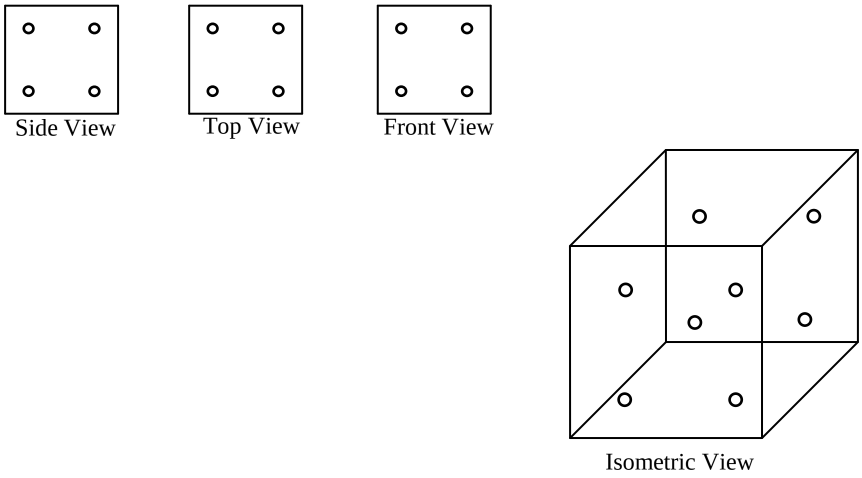

Figure 4.7. Quadrature Points used in the Solid 65 Element Solution (Circles are quadrature points.)

4.3.1.4. Modeling Cracking and Crushing in Solid 65 Element

According to ANSYS Theory Reference, a crack at an integration point means the modification of the original stress-strain matrix (See Equation 4.3) by inserting a plane of weakness in the normal direction to the crack face.

$$D = \frac{E}{(1+\upsilon)(1-2\upsilon)}\begin{bmatrix} 1-\upsilon & \upsilon & \upsilon & 0 & 0 & 0 \\ \upsilon & 1-\upsilon & \upsilon & 0 & 0 & 0 \\ \upsilon & \upsilon & 1-\upsilon & 0 & 0 & 0 \\ 0 & 0 & 0 & \frac{1-2\upsilon}{2} & 0 & 0 \\ 0 & 0 & 0 & 0 & \frac{1-2\upsilon}{2} & 0 \\ 0 & 0 & 0 & 0 & 0 & \frac{1-2\upsilon}{2} \end{bmatrix} \tag{4.3}$$

When a crack occurs, the concept of shear transfer is also born. Therefore, in ANSYS, a shear transfer coefficient is introduced for both open crack (β_t) and closed crack (β_c) cases in order to bring about sliding across the crack face. This coefficient is applied to shear terms in the directions lying on the crack plane. This coefficient can take values between 0, meaning perfectly smooth crack that is not able to transfer shear (complete loss of shear transfer), and 1, representing a rough crack that can transfer all of shear (no shear transfer loss). The stress-strain relationship for an element that has cracked in only one direction becomes as given in Equation 4.4.

$$D^{ck} = \frac{E}{(1+\upsilon)} \begin{bmatrix} R^t \frac{1+\upsilon}{E} & 0 & 0 & 0 & 0 & 0 \\ 0 & \frac{1}{1-\upsilon} & \frac{\upsilon}{1-\upsilon} & 0 & 0 & 0 \\ 0 & \frac{\upsilon}{1-\upsilon} & \frac{1}{1-\upsilon} & 0 & 0 & 0 \\ 0 & 0 & 0 & \frac{\beta_t}{2} & 0 & 0 \\ 0 & 0 & 0 & 0 & \frac{1}{2} & 0 \\ 0 & 0 & 0 & 0 & 0 & \frac{\beta_t}{2} \end{bmatrix} \quad (4.4)$$

In this equation, the superscript *ck* signifies that the stress strain relations refer to a coordinate system parallel to principal stress directions with the x^{ck} axis perpendicular to the crack face. If the stress relaxation after cracking option, which is used to ease the convergence, is canceled, R^t becomes theoretically zero but, for numerical stability purposes, it is taken as $1x10^{-6}$. For other case, R^t is the slope (secant modulus). (See Figure 4.8) R^t works with adaptive descent and diminishes to 0.0 ($1x10^{-6}$) as the solution converges. (ANSYS Theory Reference)

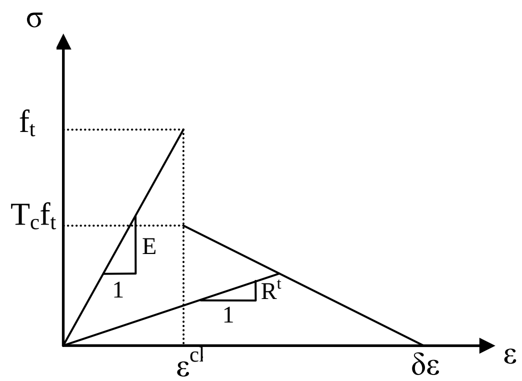

Figure 4.8. Concept of Stress Relaxation after Cracking (f_t is the uniaxial tensile strength and T_c is the multiplier for amount of tensile stress relaxation.) [ANSYS Theory Reference]

If the crack closes, then all compressive stresses normal to the crack plane are transmitted across the crack and only a shear transfer coefficient for the closed crack (β_c) is introduced. Thus, the stress-strain relationship turns out to Equation 4.5.

$$D^{ck} = \frac{E}{(1+\upsilon)(1-2\upsilon)} \begin{bmatrix} 1-\upsilon & \upsilon & \upsilon & 0 & 0 & 0 \\ \upsilon & 1-\upsilon & \upsilon & 0 & 0 & 0 \\ \upsilon & \upsilon & 1-\upsilon & 0 & 0 & 0 \\ 0 & 0 & 0 & \beta_c \frac{1-2\upsilon}{2} & 0 & 0 \\ 0 & 0 & 0 & 0 & \frac{1-2\upsilon}{2} & 0 \\ 0 & 0 & 0 & 0 & 0 & \beta_c \frac{1-2\upsilon}{2} \end{bmatrix} \tag{4.5}$$

In summary, if a crack closes then all of the axial terms in the constitutive relation returns to their original values but the shear terms have a coefficient related to the shear transfer capability of the crack. (See Equations 4.3 and 4.5)

In ANSYS, the cracked direction is treated as if it is not closed in the following first iteration and checks whether it is closed or not by controlling the strains. By using this algorithm, the constitutive relations are changed to catch the real behavior.

As the element can crack in all three principal directions at any integration point, it is beneficial to show the stress-strain relations of two directional and three directional cracks. (See Equations 4.6 and 4.7)

$$D^{ck} = E \begin{bmatrix} \frac{R^t}{E} & 0 & 0 & 0 & 0 & 0 \\ 0 & \frac{R^t}{E} & 0 & 0 & 0 & 0 \\ 0 & 0 & 1 & 0 & 0 & 0 \\ 0 & 0 & 0 & \frac{\beta_t}{2(1+\upsilon)} & 0 & 0 \\ 0 & 0 & 0 & 0 & \frac{\beta_t}{2(1+\upsilon)} & 0 \\ 0 & 0 & 0 & 0 & 0 & \frac{\beta_t}{2(1+\upsilon)} \end{bmatrix} \tag{4.6}$$

$$D^{ck} = E \begin{bmatrix} \frac{R^t}{E} & 0 & 0 & 0 & 0 & 0 \\ 0 & \frac{R^t}{E} & 0 & 0 & 0 & 0 \\ 0 & 0 & \frac{R^t}{E} & 0 & 0 & 0 \\ 0 & 0 & 0 & \frac{\beta_t}{2(1+\upsilon)} & 0 & 0 \\ 0 & 0 & 0 & 0 & \frac{\beta_t}{2(1+\upsilon)} & 0 \\ 0 & 0 & 0 & 0 & 0 & \frac{\beta_t}{2(1+\upsilon)} \end{bmatrix} \tag{4.7}$$

If the cracks in all directions close, the relations for both two directional and three directional cases turn out to be Equation 4.8.

$$D^{ck} = \frac{E}{(1+\upsilon)(1-2\upsilon)} \begin{bmatrix} 1-\upsilon & \upsilon & \upsilon & 0 & 0 & 0 \\ \upsilon & 1-\upsilon & \upsilon & 0 & 0 & 0 \\ \upsilon & \upsilon & 1-\upsilon & 0 & 0 & 0 \\ 0 & 0 & 0 & \beta_c \frac{1-2\upsilon}{2} & 0 & 0 \\ 0 & 0 & 0 & 0 & \beta_c \frac{1-2\upsilon}{2} & 0 \\ 0 & 0 & 0 & 0 & 0 & \beta_c \frac{1-2\upsilon}{2} \end{bmatrix} \tag{4.8}$$

If the uniaxial, biaxial or triaxial compressive strength of material is exceeded at an integration point, the material crushes, (fails in compression). In ANSYS, crushing is defined as the complete deterioration of the structural integrity of the material e.g. material spalling (ANSYS Theory Reference). The stiffness contribution of a crushed element is ignored by taking its value as $1x10^{-6}$.

4.3.1.5. Concrete Material used in Solid 65 Element

This material model is used for predicting the behavior of brittle materials. It is defined as an isotropic material. The failure criterion due to a multiaxial stress state is determined by Willam-Warnke (William & Warnke, 1975). (See Equation 4.9)

$$\frac{F}{f_c} - S \geq 0 \tag{4.9}$$

Where F is a function of the principal stress state (σ_{xp}, σ_{yp} and σ_{zp}), S is failure surface expressed in terms of principal stresses and five input parameters, f_c is uniaxial crushing strength and σ_{xp}, σ_{yp} and σ_{zp} are principal stresses in principal directions (ANSYS Theory Reference).

If Equation 4.9 is satisfied, the material fails in tension or compression.

The failure surface (S) is defined by five strength parameters (temperature dependent or independent) with an ambient hydrostatic stress state. (See Table 4.1)

Table 4.1. Willam-Warnke Failure Surface Parameters [ANSYS Theory Reference]

Parameter	Definition
f_t	Ultimate uniaxial tensile strength
f_c	Ultimate uniaxial compressive strength
f_{cb}	Ultimate biaxial compressive strength
f_1	Ultimate compressive strength for a state of biaxial compression superimposed on hydrostatic stress state (σ_h)
f_2	Ultimate compressive strength for a state of uniaxial compression superimposed on hydrostatic stress state (σ_h)

If the parameters f_{cb}, f_1 and f_2 are not known, then the default values given by Willam-Warnke can also be used as far as the hydrostatic stress state is less than or equal to $\sqrt{3}f_c$. (See Equation 4.10)

$$f_{cb} = 1.2 f_c \quad (4.10.a)$$

$$f_1 = 1.45 f_c \quad (4.10.b)$$

$$f_2 = 1.725 f_c \quad (4.10.c)$$

valid if Equation 4.11 holds.

$$Hydrostatic\ Stress\ State = |\sigma_h| = \left|\frac{1}{3}\left(\sigma_{xp} + \sigma_{yp} + \sigma_{zp}\right)\right| \leq \sqrt{3}f_c \quad (4.11)$$

After sorting the principal stresses from maximum to minimum (See Equation 4.12), the failure domains of concrete reduce to four.

$$\sigma_1 = \max\left(\sigma_{xp}, \sigma_{yp}, \sigma_{zp}\right) \quad (4.12.a)$$

$$\sigma_3 = \min\left(\sigma_{xp}, \sigma_{yp}, \sigma_{zp}\right) \quad (4.12.b)$$

I. $0 > \sigma_1 > \sigma_2 > \sigma_3 \quad (Compression - Compression - Compression)$
II. $\sigma_1 > 0 > \sigma_2 > \sigma_3 \quad (Tension - Compression - Compression)$
III. $\sigma_1 > \sigma_2 > 0 > \sigma_3 \quad (Tension - Tension - Compression)$
IV. $\sigma_1 > \sigma_2 > \sigma_3 > 0 \quad (Tension - Tension - Tension)$

In every domain, different functions for principal stress state (F) and failure surface(S) exist. These four functions for F and S will be called with subscripts i=1,2,3 and 4. Before these functions are investigated in detail, some properties of failure surface(S) are mentioned. The functions S_i have the properties that the surface they describe is continuous while the surface gradients are not continuous when any one of the principal stresses changes sign (ANSYS Theory Reference). (See Figures

4.9, 4.10 and 4.11) In other words, they are not differentiable at points where they intersect the coordinate axes.

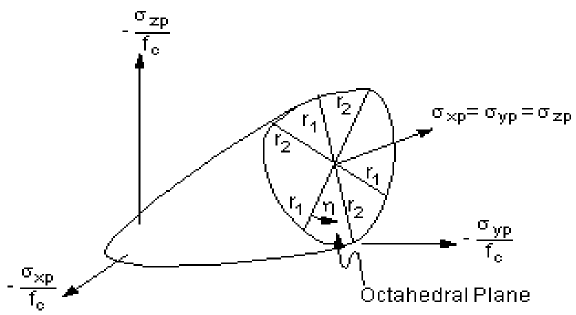

Figure 4.9. 3D Failure Surface in Principal Stress Space [ANSYS Theory Reference]

For biaxial or nearly biaxial stress states, the failure surface can be depicted as given in Figure 4.10. If the most significant principal stresses are σ_{xp} and σ_{yp}, there will be only three choices of failure surfaces for zero, little positive or little negative σ_{zp} values. The projections of the 3D failure surfaces on the σ_{xp} - σ_{yp} plane for the aforementioned σ_{zp}'s are close to each other. However, the failure mode, viz. cracking or crushing, differs depending on the sign of σ_{zp}. If σ_{zp} is zero or little negative in the third quadrant of 2D failure surface, the mode of failure will undoubtedly be crushing whereas it will be cracking or crushing for little positive σ_{zp} values.

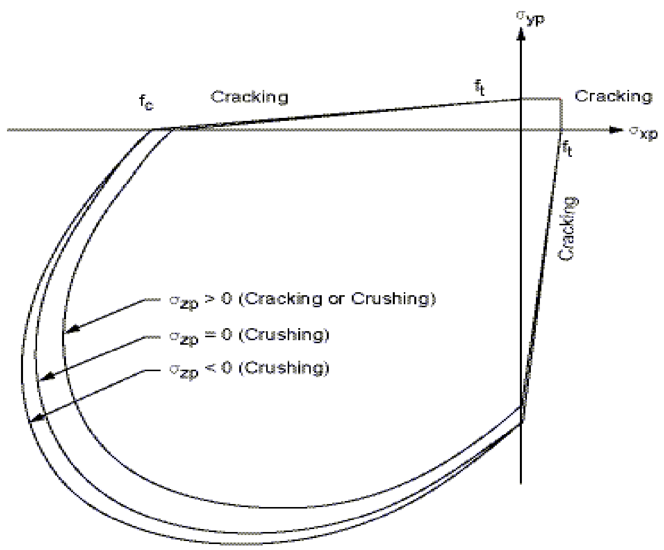

Figure 4.10. Failure Surface in Principal Stress Space with nearly Biaxial Stress [ANSYS Theory Reference]

4.3.1.5.1. Compression - Compression - Compression Domain

In this regime, the principal stress state (F) and failure surface (S) take the form given in Equation 4.13 and Equation 4.14, respectively, according to Willam-Warnke criterion (ANSYS Theory Reference).

$$F_1 = \frac{1}{\sqrt{15}}\left(\sqrt{(\sigma_1-\sigma_2)^2+(\sigma_2-\sigma_3)^2+(\sigma_3-\sigma_1)^2}\right) \quad (4.13)$$

$$S_1 = \frac{2r_2(r_2{}^2-r_1{}^2)cos\eta+r_2(2r_1-r_2)\sqrt{4(r_2{}^2-r_1{}^2)cos^2\eta+5r_1{}^2-4r_1r_2}}{4(r_2{}^2-r_1{}^2)cos^2\eta+(r_2-2r_1)^2} \quad (4.14)$$

In the above equations, $cos\eta$, r_1, r_2 and ξ are given in Equations 4.15-4.18, σ_h is the hydrostatic stress state, η is the angle of similarity, a_0, a_1, a_2, b_0, b_1, and b_2 are undetermined coefficients, σ_i (i=1, 2, 3) are the principal stresses and f_c is the compressive strength.

$$cos\eta = \frac{2\sigma_1-\sigma_2-\sigma_3}{\sqrt{2}\sqrt{(\sigma_1-\sigma_2)^2+(\sigma_2-\sigma_3)^2+(\sigma_3-\sigma_1)^2}} \quad (4.15)$$

$$r_1 = a_0 + a_1\xi + a_2\xi^2 \quad (4.16)$$

$$r_2 = b_0 + b_1\xi + b_2\xi^2 \quad (4.17)$$

$$\xi = \frac{\sigma_h}{f_c} \quad (4.18)$$

The angle of similarity (η) is related to the relative magnitudes of principal stresses. For example, $\eta = 0°$ contains every stress state formed by $\sigma_3 = \sigma_2 > 0 > \sigma_1$ (e.g. uniaxial compression, biaxial tension) while $\eta = 60°$ comprises any stress states consisting of $\sigma_3 > 0 > \sigma_2 = \sigma_1$ (e.g. uniaxial tension, biaxial compression). All other multiaxial stress states have angles of similarity between 0° and 60°. When $\eta = 0°$ and $\eta = 60°$, S_1 coincide with r_1 and r_2, respectively. (See Equation 4.14) In other words, the function r_1 (r_2) is the boundary of the failure surface when $\eta = 0°$ (60^o). The profile of the failure surface is depicted on Figure 4.11. For more details about how to determine the undetermined coefficients, see references ANSYS Theory Reference and Chen (1982).

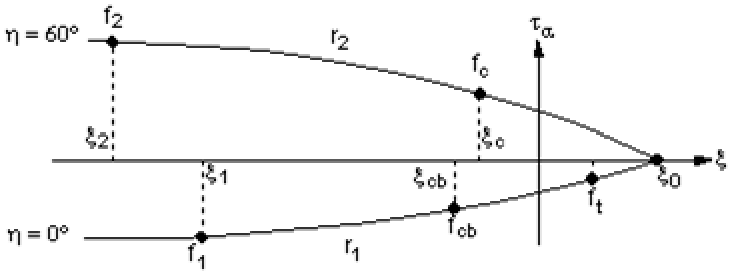

Figure 4.11. A Profile of the Failure Surface [ANSYS Theory Reference]

If the failure criterion in this regime is satisfied, the material crushes.

4.3.1.5.2. Tension - Compression - Compression Domain

The principal stress state (F) and failure surface (S) for the second domain are given below. (See Equation 4.19 and Equation 4.20)

$$F_2 = \frac{1}{\sqrt{15}}\left(\sqrt{(\sigma_2-\sigma_3)^2+{\sigma_2}^2+{\sigma_3}^2}\right) \tag{4.19}$$

$$S_2 = \left(1-\frac{\sigma_1}{f_t}\right)\frac{2p_2({p_2}^2-{p_1}^2)cos\eta+p_2(2p_1-p_2)\sqrt{4({p_2}^2-{p_1}^2)cos^2\eta+5{p_1}^2-4p_1p_2}}{4({p_2}^2-{p_1}^2)cos^2\eta+(p_2-2p_1)^2} \tag{4.20}$$

In these equations, cosη, p_1, p_2 and χ are given in Equations 4.21-4.24, η is the angle of similarity, a_0, a_1, a_2, b_0, b_1, and b_2 are undetermined coefficients and σ_i (i=2 and 3) are the principal stresses.

$$cos\eta = \frac{2\sigma_1-\sigma_2-\sigma_3}{\sqrt{2}\sqrt{(\sigma_1-\sigma_2)^2+(\sigma_2-\sigma_3)^2+(\sigma_3-\sigma_1)^2}} \tag{4.21}$$

$$p_1 = a_0 + a_1\chi + a_2\chi^2 \tag{4.22}$$

$$p_2 = b_0 + b_1\chi + b_2\chi^2 \tag{4.23}$$

$$\chi = \frac{1}{3}(\sigma_2+\sigma_3) \tag{4.24}$$

If the failure criterion is satisfied, cracking occurs in the plane perpendicular to principal stress σ_1 (ANSYS Theory Reference). The crushing ability of this domain is explained in details in Willam and Warnke (William & Warnke, 1975).

4.3.1.5.3. Tension - Tension - Compression Domain

The principal stress state (F) and failure surface (S) for this regime can be found by using the Equations 4.25 and 4.26.

$$F_3 = \sigma_i \qquad for\ i = 1\ and\ 2 \tag{4.25}$$

$$S_3 = \frac{f_t}{f_c}\left(1 + \frac{\sigma_3}{f_c}\right) \tag{4.26}$$

In the above equations, σ_i (i=1, 2 and 3) are the principal stresses, f_c is the uniaxial compressive strength and f_t is the uniaxial tensile strength.

In this criterion, a crack plane perpendicular to the principal direction 1 occurs if the failure criterion is satisfied for σ_1 and two crack planes perpendicular to principal directions 1 and 2 exist if both σ_1 and σ_2 satisfy it. The crushing is also applicable to this domain as it is explained by Willam-Warnke (William & Warnke, 1975).

4.3.1.5.4. Tension - Tension - Tension Domain

The principal stress state (F) and failure surface (S) for the last domain is determined by the Equations 4.27 and 4.28.

$$F_4 = \sigma_i \qquad for\ i = 1, 2\ and\ 3 \tag{4.27}$$

$$S_4 = \frac{f_t}{f_c} \tag{4.28}$$

In these equations, σ_i (i=1, 2 and 3) are the principal stresses, f_c is the uniaxial compressive strength and f_t is the uniaxial tensile strength.

There are no crushing possibilities in this regime as no compressive principal stresses exist. However, up to three crack planes could appear at an instant if the criterion is satisfied. The crack sequence always starts with the first principal direction as, in the beginning, the principal stresses are sorted from largest to smallest.

4.3.2. Plasticity definitions in ANSYS

Engineering materials show a linear stress-strain behavior till the proportional limit is reached. After that point, the stress-strain relationship shows nonlinearity but the strains continue to be recoverable up to the yield point. In other words, the plasticity (unrecoverable strains) starts with the yielding of materials. However, in ANSYS, the yield point and the proportional limit are assumed to be coincident. This assumption is not too wrong as, for most of the materials; there is a little difference between the proportional limit and the yield point. (See Figure 4.12)

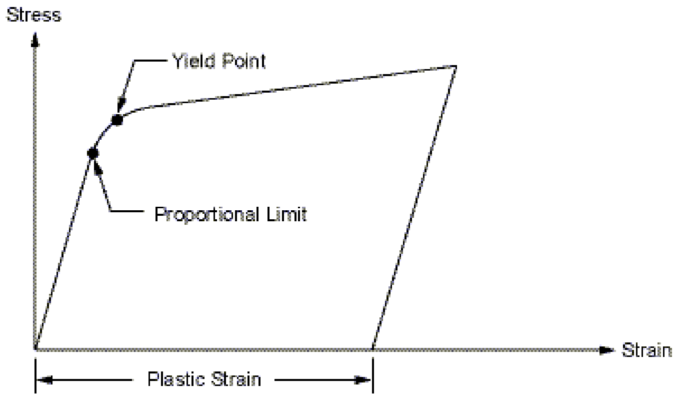

Figure 4.12. Proportional Limit and Yield Point

In ANSYS Structural Analysis Guide, plasticity is described as a non-conservative and path-dependent phenomenon. Therefore, the result is completely dependent on the load application sequence and load steps.

In ANSYS, several plasticity formulations can be combined to catch the inherent behavior of different materials. There exist tables in ANSYS Element Reference about limitations on the various plasticity combinations and explanations of how to obtain the desired plasticity. Specifically, bilinear isotropic hardening, multilinear isotropic hardening, bilinear kinematic hardening, multilinear kinematic hardening and Drucker-Prager plasticities can be used with Solid 65 element.

This study uses a combination of two material models namely Willam – Warnke, which is the 5 parameter concrete model used worldwide, (See Figures 4.9-4.11) and multilinear isotropic hardening. (See Figure 4.14) As it is stated in Theory Reference for ANSYS 11, two models are combined in such a way that the inner plasticity model is always effective in finding the solution. (See Figure 4.13)

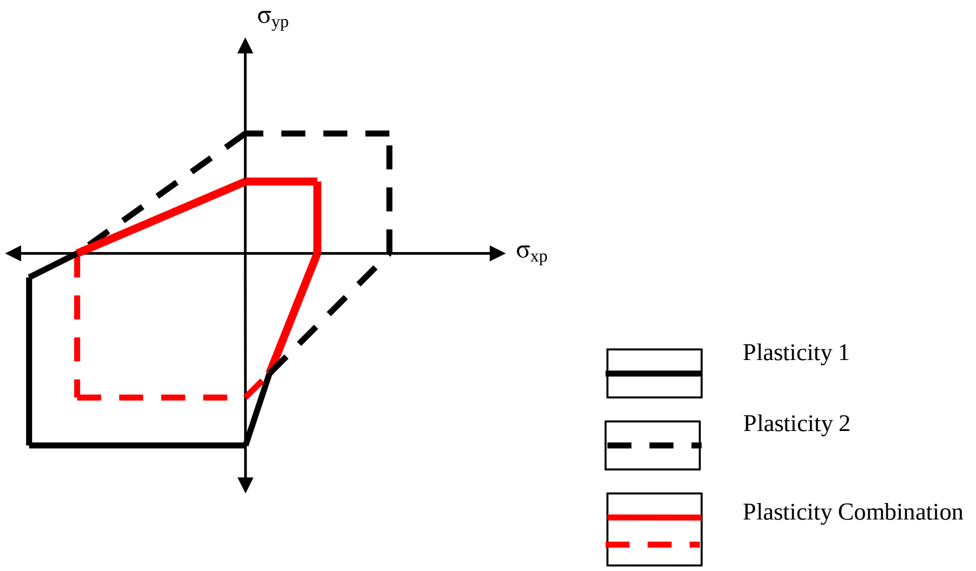

Figure 4.13. Sketch of a Sample Plasticity Combination done in ANSYS 11

4.3.3. Input parameters for modeling masonry walls in ANSYS

When modeling the unreinforced masonry walls in ANSYS 11, the element Solid 65 is used and the aforementioned properties of it are adjusted as follows:

- Extra displacement shapes are excluded in the shape functions.
- The stress relaxation after cracking is cancelled as it is only needed to accelerate the convergence.
- The shear transfer is neglected when there exist cracks on any integration point in any directions because there are no preferences in ANSYS 11 that classifies the cracks according to their strains. In other words, a crack is recognized as open whenever its strain is higher than the cracking strain but it is not meaningful to trust a highly opened crack in unreinforced masonry with transmitting the shear force. Therefore, the open shear transfer coefficient is assumed as zero. However, it is taken as 0.01 in the analysis in order to prevent numerical instability.

- The closed crack is assumed to transmit the whole shear as the cracks in masonry are rough. Thus, the closed shear transfer coefficient is taken as 1.
- The concrete material is defined by its compressive strength and its tensile strength and the other parameters are taken as default values given in Willam-Warnke (William & Warnke, 1975). This is because; the hydrostatic stress state for masonry walls is low.
- The plasticity is defined as multilinear isotropic hardening. (See Figure 4.14)

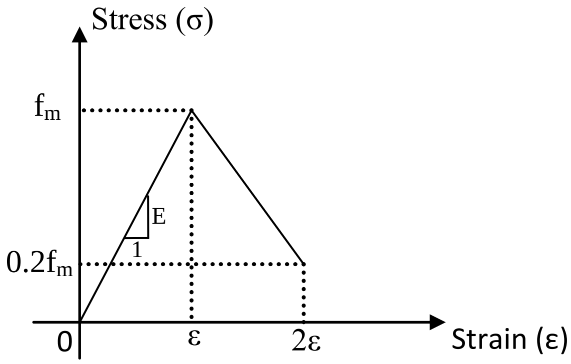

Figure 4.14. Multilinear Isotropic Plasticity Model used in Analytical Model

4.3.4. Verification of FEM Model by experimental data

The next step is to use the analytical model explained in previous section in order to estimate the in-plane behavior of unreinforced masonry walls in this study. But, first the proposed model should be verified by using experimental data. The most suitable experimental program for this purpose is a series of tests conducted in ETH Zurich on unreinforced brick masonry walls. The details of this test program can be found elsewhere (Lourenco, 1996).

The test wall is composed of hollow clay bricks. A masonry wall panel (3600x2000x150 [mm^3]) and two flanges (150x2000x600 [mm^3]) make up the test specimen, whose geometrical properties are sketched in Figure 4.15. Mechanical properties of the wall specimen are given in Table 4.2. A reinforced concrete slab and foundation also exist as this wall is tested as if it is a part of real masonry structure. Initially, a uniformly distributed pressure (p=0.61 N/mm^2), whose resultant is 415 kN, is applied on top of the wall. After that, the wall is monotonically pulled rightwards (Displacement-controlled test). At the ultimate stage, diagonal shear cracks appear and some of the blocks in the middle part of the wall sally from wall panel. (See Figure 4.16)

Table 4.2. The Mechanical Properties of ETH Zurich Wall

E (MPa)	ν	G (MPa)	f_m (MPa)	f_{mt} (MPa)
2460	0.18	1130	7.61	0.28

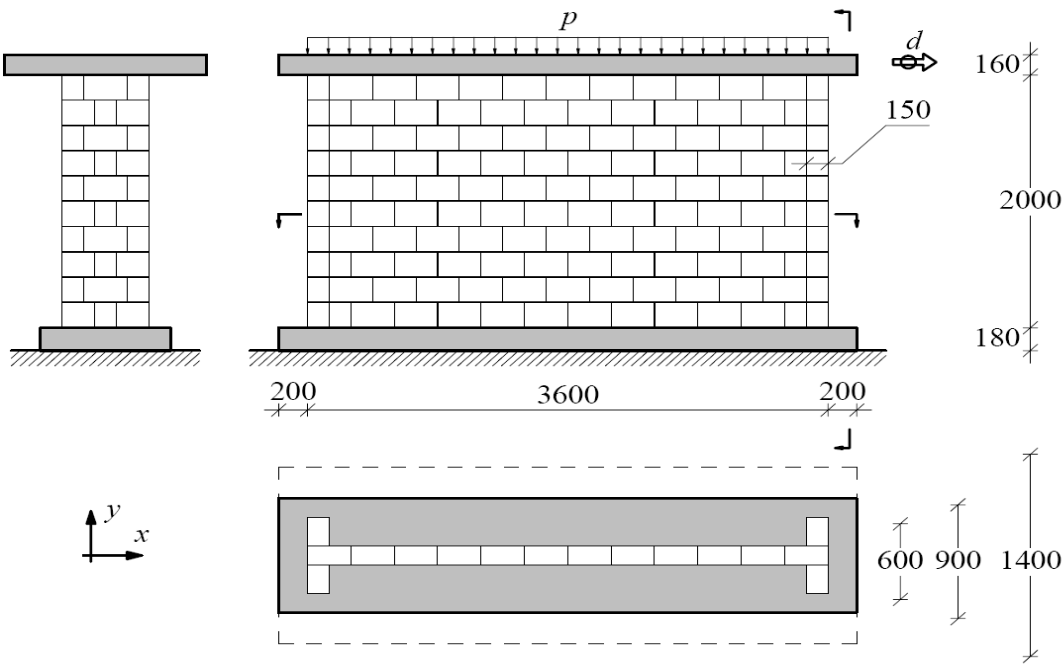

Figure 4.15. The Sizes of Wall tested in ETH Zurich (All dimensions are in mm and p=0.61 N/mm^2) (Lourenco, 1996)

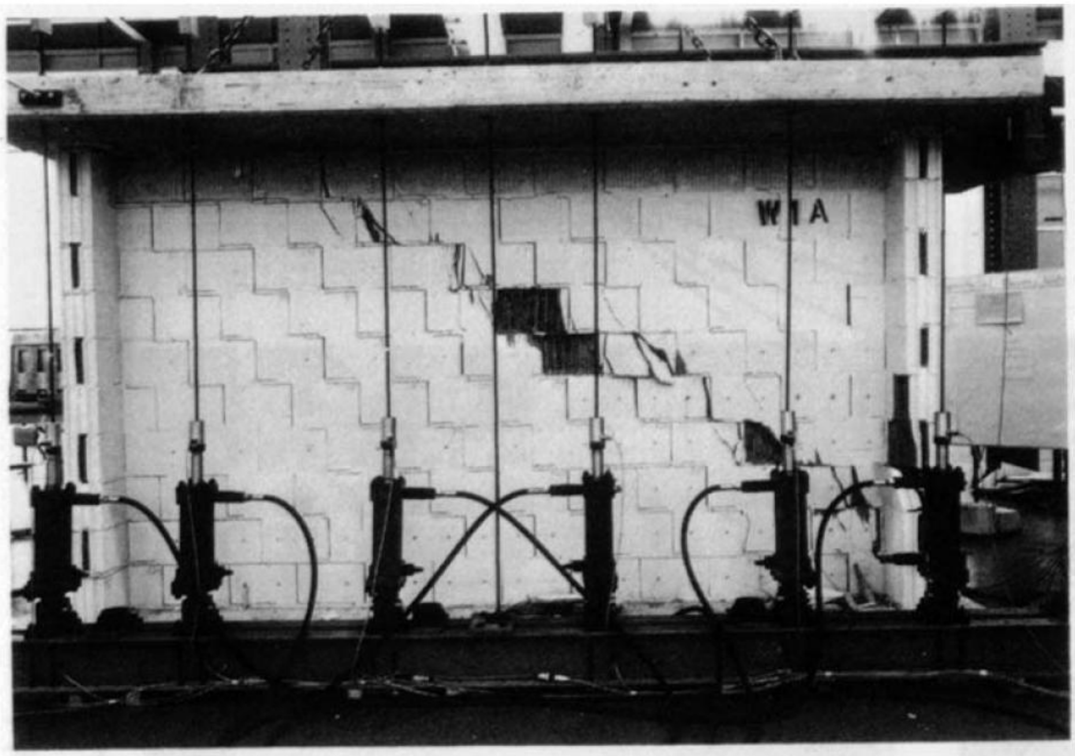

Figure 4.16. The Failure of Wall tested in ETH Zurich (Lourenco, 1996)

4.3.4.1. Analytical Model

In the 3D finite element model, the bottom of the wall is taken as fixed to the base, which is reasonable as the concrete block is attached to the base by strong bolts. (See Figure 4.17) The top concrete slab is modeled by concrete elements having a compressive strength of 30 MPa, tensile strength of 1.9 MPa, a Modulus of Elasticity of 25000 MPa and a Poisson's Ratio of 0.20 (See Figure 4.18). Besides, in modeling slab, Solid 65 elements are used with only Willam-Warnke plasticity as it is composed of only concrete.

The mesh density is very important for the finite element analysis because a coarse mesh leads to an analysis with approximate or unrealistic results whereas a very fine mesh causes impractical analysis in terms of computation time and effort. In this study, the mesh density is determined by using a trial and error process. At the first stage, a very coarse mesh is selected and the displacements are obtained under a combination of a vertical load and a lateral load. Then, a finer mesh is conducted.

The optimum mesh density is achieved when the error in the lateral displacement resulted from fine and coarse mesh is less than or equal to one-tenth of a millimeter. After the trial and error procedure, it is found that there should be 1380 elements, 1080 of which is used to model the masonry wall. The remaining 300 elements are used to model the concrete slab.

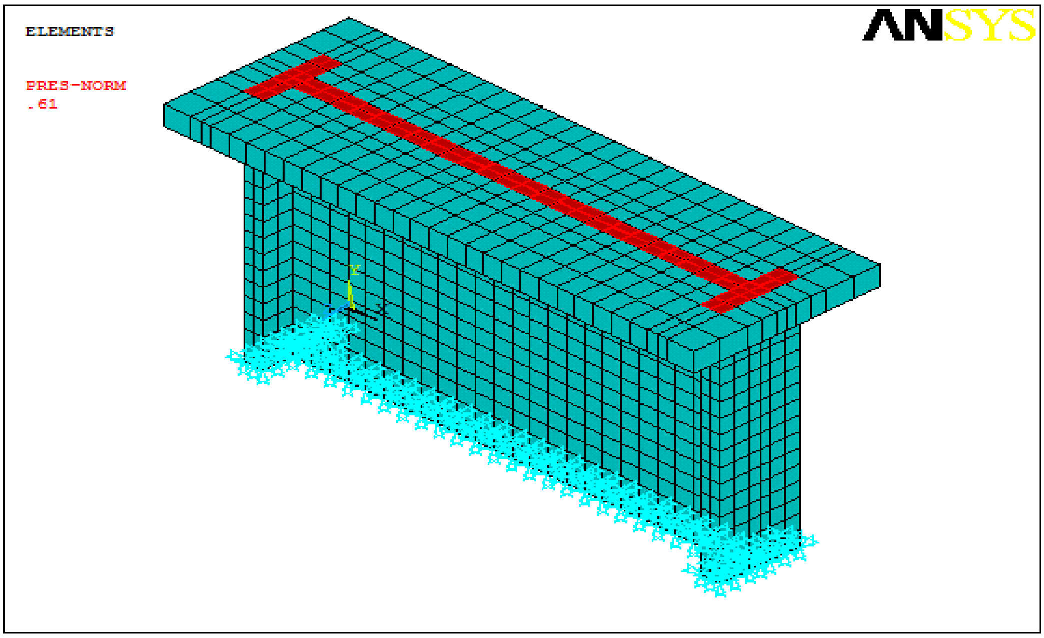

Figure 4.17. The Support Conditions and Vertical Load used in the Model

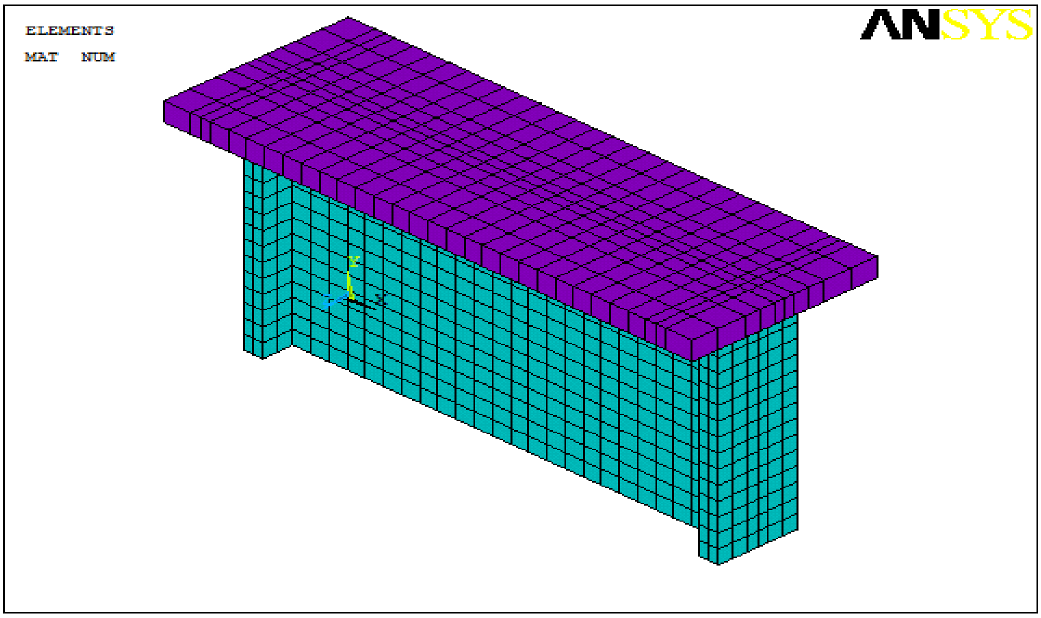

Figure 4.18. The Different Materials used in the Model (Purple is concrete slab and blue is the masonry.)

The analysis is done by applying displacements at the top nodes in increments. (See Figure 4.19) The top nodes are pulled up to 15 mm in 1000 steps. If the convergence is not satisfied for 1000 steps, the automatic time stepping feature of ANSYS 11 activates and decreases the step size.

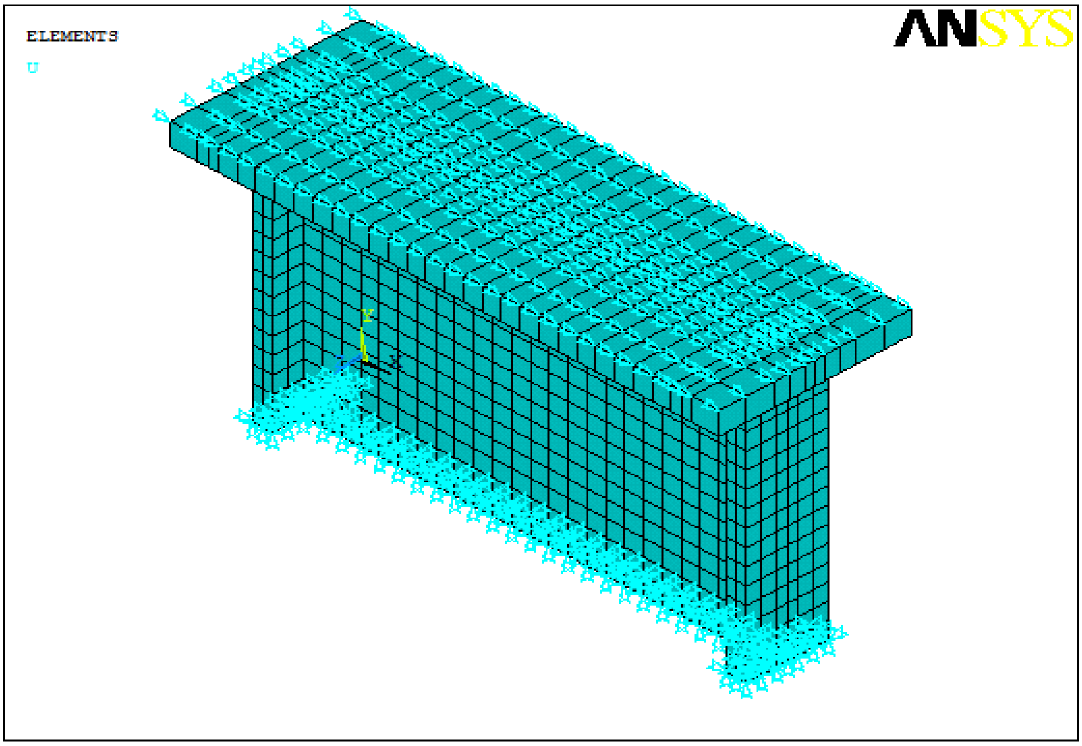

Figure 4.19. The Top Displacement Application

4.3.4.2. Results

The comparison of the capacity curve obtained from the analysis and the experiment is given in the Figure 4.20. It can be inferred that the analytical model simulates the behavior of the wall acceptably. The maximum lateral load found in the experiment is 265 kN, which is 272.8 kN from the analytical model. The percentage error in the maximum lateral load prediction is 2.94%. This amount of error is acceptable for masonry structures for which material uncertainty is significant. However, it is not possible to predict the degrading behavior (descending portion after maximum load) by using this model. This is because; in ANSYS, Newton-Raphson method is used to make iterations in an increment. This method always finds the point above the preceding point. Therefore, the capacity curve cannot comprise the falling branch. Moreover, the model estimates the displacement capacity as 14.2 mm whereas the experiment gives it as 14 mm. The percentage error in lateral displacement capacity is 1.43%. These results indicate that this model can be used for the assessment of in-plane behavior of the tested masonry wall.

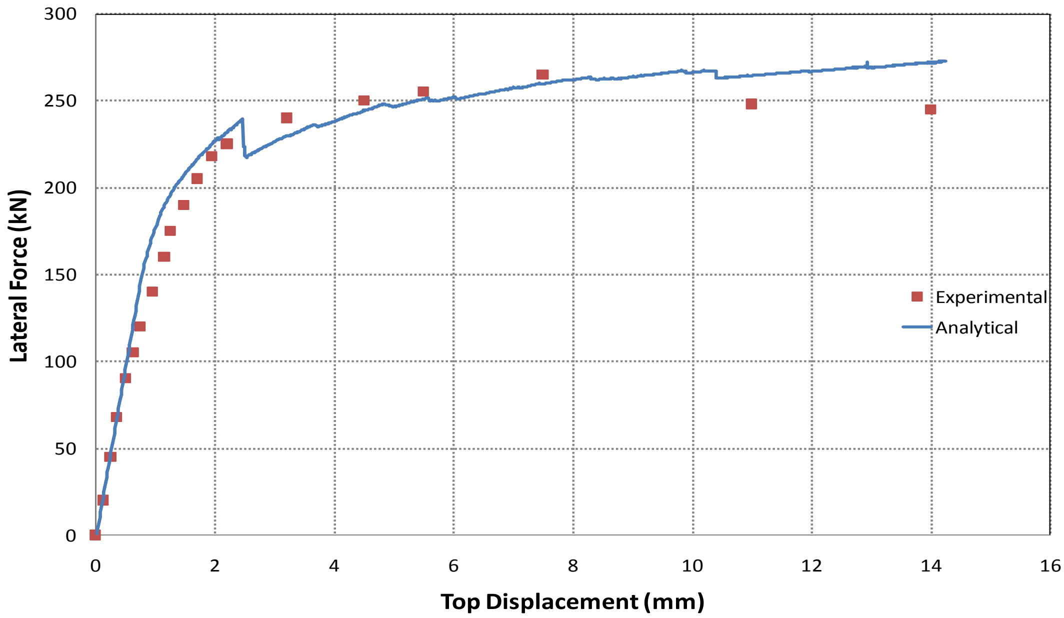

Figure 4.20. The Capacity Curves from Analysis and Experiment

The crack pattern of the analytical model at the failure is given in Figure 4.21. (The lowest values of tensile strains are discarded in order to obtain a legible picture.) As it can be seen, a well-defined diagonal crack is predicted by the analytical model, which agrees well with the experimental result. (See Figure 4.16 and Figure 4.21)

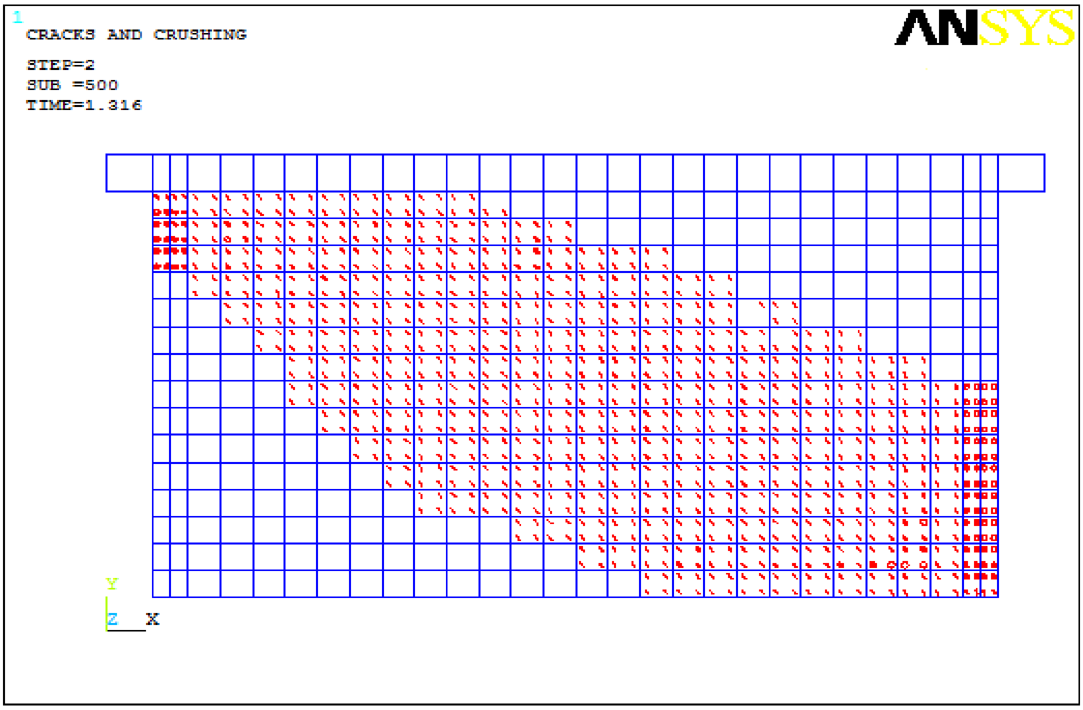

Figure 4.21. The Crack Pattern from the Analytical Model

CHAPTER 5

DEVELOPMENT OF A PERFORMANCE BASED TECHNIQUE FOR UNREINFORCED BRICK MASONRY BUILDINGS IN TURKEY

5.1. Introduction

This chapter begins with a brief discussion about the material characteristics of brick masonry units in Turkey. Then, referring to this information, mechanical properties of masonry walls required for analytical modeling are obtained. The rest of this chapter is mainly devoted to the development of a displacement-based procedure for the seismic evaluation of existing unreinforced brick masonry buildings. If properly adopted, the procedure can also be used for design purposes. The main feature of this procedure is that it enables determination of the capacity and performance of an unreinforced masonry building based on detailed modeling of the in-plane behavior of its piers and walls. Although detailed finite element based analysis are performed on piers, these are implicit in the method and their results are employed in the proposed procedure by using approximate and simple formulations.

The proposed procedure also constitutes the outline of this chapter, which is explained as follows:

1) Capacity curves of different piers (with different aspect ratios, compressive strength and loading conditions) are obtained by utilizing the previously mentioned analysis technique in ANSYS (for details refer to Chapter 4).
2) These curves are then bilinearized according to FEMA356.
3) The analytical database obtained is utilized to create a simplified version of capacity curve generation as the analysis done in ANSYS takes too much time to be utilized in practice. In this simplified method, empirical formulations for yield lateral load (F_y), yield displacement (u_y), ultimate

lateral load (F_u) and ultimate displacement (u_u) are developed by performing nonlinear regression analyses.

4) Local limit states are defined for each pier based on the obtained values of the yield displacement (u_y) and the ultimate displacement (u_u) such that the yield displacement represents serviceability limit state whereas the ultimate displacement stands for ultimate limit state.
5) The capacity curve is constructed by gathering the contribution from each pier in a specific direction. It also becomes possible to decide on the global limit state of the building by considering local limit states of individual piers.
6) If a performance assessment is required, then the capacity curve is converted to ADRS format and compared with demand (in terms of acceleration spectrum). The point where the capacity and the demand for that specific building intersects is regarded as the "performance point" and it is used in order to assess the seismic performance of the building.

Last part of this chapter is devoted to the implementation of this technique to an existing unreinforced masonry building located in Istanbul.

5.2. Assumptions involved in the Simple Method

The proposed approach depends on several simplifications as stated below:

- This method is valid for only unreinforced brick masonry structures.
- The masonry material is assumed to be isotropic.
- It is assumed that out-of-plane failure of the masonry walls has been prevented by proper measures (rigid floor diaphragm, proper wall-to-wall connections, proper wall-to-floor connections, presence of horizontal RC bond beams).
- It is assumed that the plastic deformation or damage accumulates on piers. This is a reasonable assumption since it has been observed that generally piers are weaker than spandrels in traditional unreinforced masonry construction (Tomazevic, 1999).

- In determining the effective pier heights, the offset method proposed by Dolce (1989) is employed.
- It is assumed that a reinforced concrete slab or a slab type capable of providing rigid diaphragm action exist in the masonry structures.
- The mass is assumed to be lumped at the storey levels when performing the modal analysis.
- In demand calculations, the viscous damping is taken as 10% of the critical if the damage is occured. Otherwise, it is 5%.

5.3. Material Characteristics of Brick Masonry Units in Turkey

In Turkish masonry construction practice, there are two types of clay bricks: local and factory bricks. The former type is manufactured in local furnaces and was very popular during 1970's but they are rarely produced nowadays. Therefore, such type of bricks is usually encountered in old masonry structures. These bricks are burned at low temperatures (maximum 900C^{o}) due to lack of technology. As it is a known fact that the compressive strength of bricks depends on the temperature during production, it is lower than the factory bricks'. However, the fracture of local bricks is less brittle and they can experience considerable plastic deformation prior to failure (Sucuoğlu & Erberik, 1997).

The second type of bricks is divided into many subcategories such as solid bricks, bricks with vertical holes, bricks with horizontal holes, etc. As the name implies, this type of bricks is being produced in factories and burnt up to 1200 C^{o}, which makes it stronger but more brittle when compared to local bricks.

In TS EN 771 (Turkish Standards Institution, 2004), the recommended compressive strength values for different types of clay brick have been tabulated for national use. Only the values for two types are given in this document (Tables 5.1 and 5.2) as the other types (clay bricks with horizontal holes) are not permitted in the load bearing wall construction. Moreover, it is a common practice to use the high density clay bricks with vertical holes as load bearing elements due to their reasonable compressive strength.

Table 5.1. Compressive Strength of Local Clay Bricks [TS EN 771]

Class		Compressive Strength (MPa) Average	Minimum
Solid	***Moderate***	5	4
	Low	3	2.5
Hollow	***Moderate***	5	4
	Low	3	2.5

Table 5.2. Compressive Strength of Clay Bricks with Vertical Holes [TS EN 771]

	Density (kg/m^3)	Class	Compressive Strength (MPa) Average	Minimum
Low Density	700	I	3	2.4
		II	4	3.2
	800	I	4	3.2
		II	5	4
	900	I	5	4
		II	6	4.8
	1000	I	6.5	5.2
		II	8	6.4
High Density	1200	I	15	4.5
		II	6	12
	1400	I	20	6.5
		II	8	16
	1600	I	22	8
		II	10	17.5
	1800	I	22	8
		II	10	17.5
	2000	I	24	9.5
		II	12	19

Unfortunately, there exist few laboratory tests for the determination of mechanical properties of masonry units to be used in Turkish construction practice and most of them were performed in 1960's and 1970's when masonry construction was popular.

Between years 1964-1975, a series of experiments were carried out on local bricks in Materials Laboratory of Ministry of Public Works and Settlement in order to determine their compressive strength. The average compressive strength for all local brick groups was obtained as 5.5 MPa with a standard deviation of 1.8 MPa. The minimum and maximum average values were detected as 2.3 MPa and 10.5 MPa, respectively (Bayülke, 1992). Although all the local brick batches had been taken from local furnaces near Ankara, one can clearly see that even average values can vary by an order of magnitude of 3 or 4. This clearly indicates that the uncertainty in mechanical properties of local clay brick is very high.

In another series of tests, Postacıoğlu (1962) used 37 local brick specimens and he concluded that the probabilities that the strength of the specimen being smaller than 1.6 MPa, 4 MPa and 7.5 MPa are 5%, 17% and 69%, respectively.

For factory bricks, similar tests had been performed in Materials Laboratories of Ministry of Public Works and Settlement. The results are listed in Table 5.3 for different types. As it can be observed from the table, coefficient of variation (cov) for nearly all types of factory bricks is very high (Bayülke, 1992).

Table 5.3. Compressive Strength Values for Factory Bricks (Bayülke, 1992)

Type	Number of Specimens	Average Compressive Strength (MPa)	Coefficient of Variation (MPa)	Maximum Value of Compressive Strength (MPa)	Minimum Value of Compressive Strength (MPa)
Solid	9	22.6	0.57	50.0	11.6
Vertical Holes	19	19.5	0.26	29.0	8.0
Horizontal Holes	46	4.4	0.41	8.0	1.5

Postacıoğlu (1962) obtained an average compressive strength of 28.8 MPa with a standard deviation of 10.5 MPa for solid factory bricks. For perforated factory bricks with vertical holes, he obtained an average value of 18 MPa whereas for perforated factory bricks with horizontal holes, the average value was 5 MPa.

As the experimental results imply, there are significant variations in the compressive strength values of brick masonry units. This is not surprising, especially in Turkey, where there exist limited standardization and control over the construction material technologies. Such a high material uncertainty is inherent for this type of construction materials and perhaps this is their major weakness when compared to other types of construction materials.

There have also been some attempts in Turkey to estimate the compressive strength of masonry walls from the corresponding strength values of units and mortar. For instance, Tolunay (1966) obtained the following empirical formulations for factory bricks with 1:3 lime mortar (Equation 5.1.a) and for factory bricks with 1:2:8 mortar (Equation 5.1.b).

$$f_m = 0.27 f_b \tag{5.1.a}$$

$$f_m = 0.22 f_b \tag{5.1.b}$$

In the above equations, f_m is the compressive strength of wall and f_b is the compressive strength of brick.

Bayülke (1992) recommended a simple formulation for the estimation of the wall compressive strength, which is valid for solid and hollow factory bricks.

$$f_m = (0.32\ to\ 0.75) f_b \tag{5.2}$$

In this study, brick masonry units constructed in Turkey are classified in three groups according to their compressive strengths namely Low, Medium and High by using the limited data available from the aforementioned studies. The mean compressive strength values assigned to these groups are 2 MPa (for local bricks), 5 MPa (for local bricks and low quality factory bricks) and 8 MPa (for high quality factory bricks).

According to Costa (2007), the tensile strength of masonry walls of any type may be taken as 3%-9% of its compressive strength. Unfortunately, there exists no reliable documentation regarding this mechanical property of masonry in Turkey. Therefore, it is assumed that the range of values stated by Costa holds also for the Turkish masonry construction.

There is also no consensus about how to calculate the Modulus of Elasticity of masonry walls from its components' mechanical properties. Some previous studies proposed relations depending on the compressive strength of masonry wall but the coefficients are so different from each other that, for the same wall, the estimated modulus of elasticity may be three times the others. For example, Plowman (1965) and Sahlin (1971) recommend coefficients in the range 400-1000 for the compressive strength (Equation 5.3) whereas the formulations proposed by Schubert (1982) and Sinha and Pedreschi (1983) are given in Equations 5.4 and 5.5, respectively.

$$E_m = (400 - 1000)f_m \tag{5.3}$$

$$E_m = 2116\sqrt{f_m} \tag{5.4}$$

$$E_m = 1180{f_m}^{0.83} \tag{5.5}$$

In these formulations, E_m is the Modulus of Elasticity of masonry wall and f_m is the compressive strength of the wall (in MPa in Equations 5.3-5.5).

There are also some code-based formulations similar to the above formulas like the one in TEC2007 (Equation 5.6) and the one in Eurocode 6 (Equation 5.7).

$$E_m = 200f_m \tag{5.6}$$

$$E_m = 1000f_m \tag{5.7}$$

In this study, the Modulus of Elasticity for the previously mentioned masonry brick unit classes is assumed to be between 400 MPa and 8000 MPa by considering the above formulations. The dispersion in estimated values is huge so an average value for every class is decided to be used. Consequently, the Modulus of Elasticity is taken as 2000 MPa in this study.

5.4. Capacity Evaluation of Masonry Piers

First step in the procedure is to obtain the capacity curves of brick masonry piers by taking into consideration different structural parameters such as compressive strength, aspect ratio and vertical stress. The analysis tool used is ANSYS as explained in the previous chapter. Material properties of the finite element models are determined in accordance with the typical construction practice for unreinforced masonry buildings in Turkey as discussed in the previous section.

5.3.1. Classification of Masonry Piers

Masonry piers are classified according to the aforementioned structural parameters. The first classification for piers is according to compressive strength: low, moderate and high. The physical quantification of these classes in terms of the mean values is 2 MPa, 5 MPa and 8 MPa as stated before (See Table 5.4).

Table 5.4. Classification of piers according to compressive strength

Pier Category	Compressive Strength (MPa)
Low Strength	2
Medium Strength	5
High Strength	8

The second classification is according to aspect ratio. By definition, it is the ratio of the wall height to wall length in horizontal direction. In this category, masonry piers with 8 different aspect ratios ranging from 0.25 to 2.0 are considered (See Table 5.5). The reason for this broad range of classification is that the mode of failure highly depends on the aspect ratio and that many different aspect ratios can be encountered in practice. It is impossible to define an analytical model by using a predefined aspect ratio, i.e. length or height along with the thickness should also be known. Thus, a reference length of 1 m and a reference thickness of 0.2 m are assumed. Pier categories are named as Squat, Ordinary and Slender in terms of aspect ratio as shown in the table.

Table 5.5. Classification of piers according to aspect ratio

Pier Category	Aspect Ratio of Pier
Squat	0.25
Squat	0.5
Ordinary	0.75
Ordinary	1.0
Ordinary	1.25
Ordinary	1.5
Slender	1.75
Slender	2.0

The last classification of piers is made according to vertical stress (level of axial load). This is because; just like reinforced concrete members, the unreinforced masonry panels tested under higher axial loads exhibit larger lateral load capacity with a less ductile displacement response than their counterparts, which have been subjected to lower vertical stresses. Furthermore, the level of axial load can also change the failure mode. For example, a wall tested under low levels of axial load is expected to fail in flexure whereas it would probably fail in diagonal tension under high axial loads. In view of these discussions, six different categories are considered in this study (See Table 5.6). Pier categories are named as Low, Moderate and High according to the level of axial load as shown in the table. Level of axial load is given as a percentage of the compressive strength of masonry pier under consideration.

Table 5.6. Classification of piers according to the level of axial load (f_m is the compressive strength of pier.)

Pier Category	Level of Axial Load
Low	0.05 f_m
Low	0.10 f_m
Moderate	0.20 f_m
Moderate	0.30 f_m
High	0.40 f_m
High	0.50 f_m

The combination of these three classes makes up 144 different masonry piers to be modeled analytically. All of the models are three dimensional and formed by using the previously mentioned Solid 65 elements in ANSYS. Figure 5.1 presents the stress-strain characteristics of subclasses in terms of compressive strength. The modulus of elasticity is taken as 2000 MPa for all cases as discussed before. Theses bilinear curves are used as multilinear isotropic plasticity models in ANSYS. At first glance, the ultimate strains especially for f_m=5 MPa and f_m=8 MPa seem to be large for unreinforced masonry that has been known to behave in a brittle manner. However, these plastic strains are utilized for modeling the biaxial state of stress on unreinforced masonry piers and recent experiments done by Senthivel & Uzoegbo (2004) show that the ultimate axial strain under biaxial state of stress may reach the value of 0.008 (See Figure 5.2). For all analytical models, the Poisson's ratio has been assumed as constant and equal to 0.2.

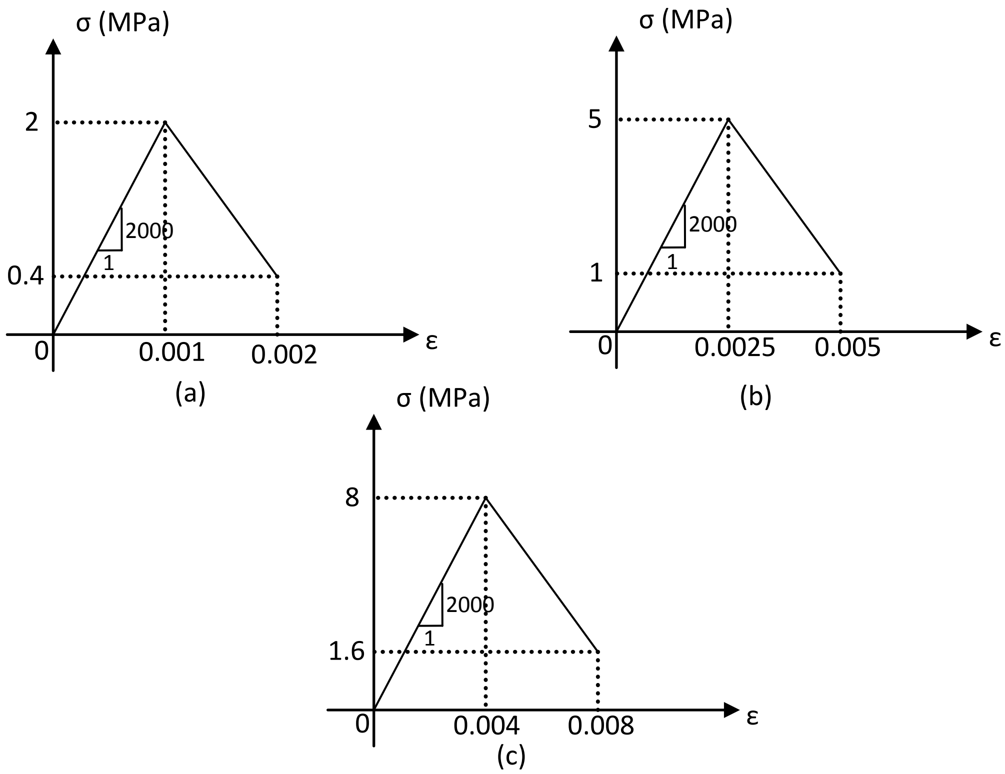

Figure 5.1. Stress-strain characteristics for subclasses according to compressive strength values of (a) 2 MPa, (b) 5 MPa and (c) 8 MPa

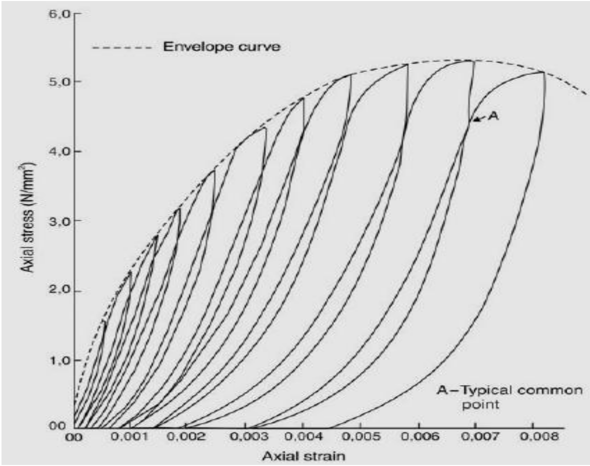

Figure 5.2. Typical Stress-Strain Hysteresis Curves for an Unreinforced Masonry Wall under Pseudo-Dynamic Biaxial Compression (Senthivel & Uzoegbo, 2004)

Every analytical model should be re-meshed whenever its geometrical properties change. Therefore, there are eight different meshes in this study as eight categories of aspect ratios have been selected. When determining the mesh density, adaptive meshing is applied manually. In adaptive meshing, the analytical model is coarsely meshed and analyzed under a combination of vertical and lateral loads. Then, the mesh size of every element is halved and the model is solved under the same loading effect. If the displacements from these two successive models are close to each other, the former meshing is assumed as the optimum mesh because the little error in the displacements implies that the mesh density lose its effect on the results. If not, the mesh sizes should be reduced to half of their previous values until the error between two successive models is less than an acceptable limit.

5.3.2. Restraints and Loading Conditions for Analytical Models

In all models, the bottom of piers is assumed to be fixed and the top of piers is taken as a free end. (See Figure 5.3)

After the vertical load is applied to the piers as a pressure load, which is shown by red rectangles in Figure 5.3, horizontal displacement is imposed to piers until failure. (See blue arrows on top of piers in Figure 5.3.e-h)

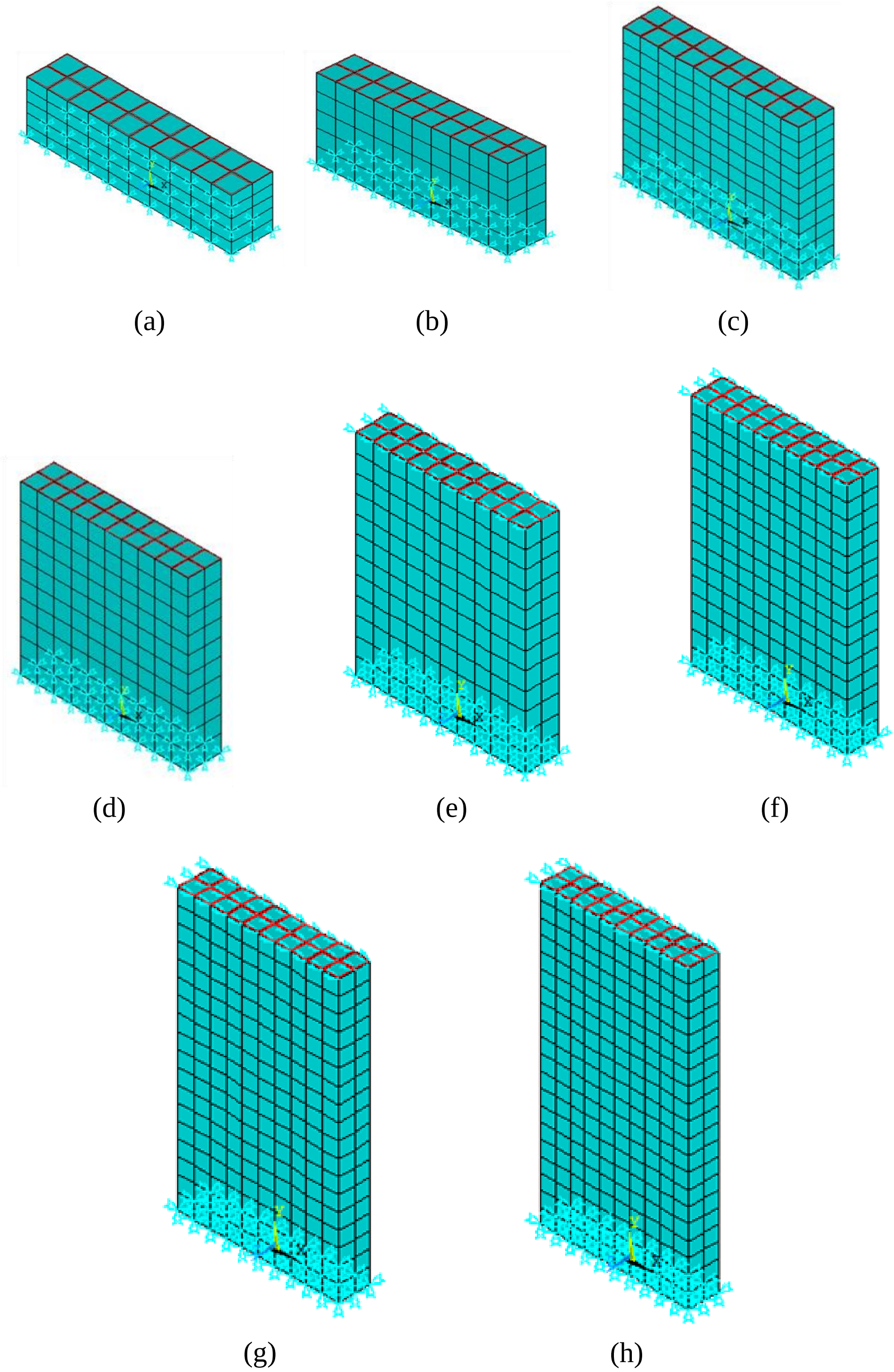

Figure 5.3. The analytical models for a reference length=1 m and thickness=0.2 m for different aspect ratios (a) λ=0.25; (b) λ=0.50; (c) λ=0.75; (d) λ=1.00; (e) λ=1.25; (f) λ=1.50; (g) λ=1.75; (h) λ=2.00

5.3.3. Solution Technique for Analytical Models

The small displacement nonlinear static analysis is selected as the solution technique since masonry is a brittle material. Masonry components are not capable of experiencing large deformations with respect to their sizes. Nonlinear static analysis (pushover) is employed in order to obtain the capacity curves for masonry pier models.

The built-in nonlinear solution techniques of ANSYS 11 are used in the analysis. The details of these solution techniques are as follows:

- The sparse direct equation solver is preferred because according to Basic Analysis Guide for ANSYS 11 (2007), sparse direct solver is suited for analyses in which robustness and solution speed are required (nonlinear analyses), and for linear analyses in which iterative solvers are slow to converge (especially for ill-conditioned matrices, such as poorly shaped elements).
- Degree of freedom solution predictor is used for the numerical integration technique whenever the number of iterations in a solution step starts getting higher values.
- Line search is used whenever the solution does not converge.
- If the solution does not converge in any steps given above, the displacement convergence criterion along with the force convergence criterion is increased.
- Maximum number of iterations is chosen as 100 in order to prevent premature convergence problems in any substeps.

5.5. Idealization of Capacity Curves for Masonry Piers

The performance of a wall (pier) element may be determined by comparing its state of deformation (deformation demand) with its deformation capacity. Traditionally, the criteria about the performance limits are recommended by international or national standards. In most of the codes, three performance states, namely immediate occupancy, life safety and collapse prevention are advised and all of these limits are assigned in terms of deformation or drift ratio.

In this study, only two performance limits are used namely: serviceability and ultimate. This is due to the fact that it is not possible to obtain force-displacement data after reaching the maximum capacity by using ANSYS. However, the observations regarding the actual behavior of masonry components indicate that there should be a descending branch in the load-deformation curve due to degradation of mechanical properties at later stages of loading. The start of descending branch after reaching the ultimate capacity should correspond to an intermediate limit state such as "Life Safety" in actual behavior. However, since it is not possible to obtain any further data, the point of maximum capacity has been taken as ultimate limit state in this study. This is a gross assumption due to lack of additional data but it is conservative and simple enough to be used for a population of buildings, not for the detailed analysis of an individual building.

As a general rule, the serviceability limit state is related to minor structural damage. This minor structural damage can be detected by investigating the crack pattern from ANSYS. In other words, hairline cracks appear in the initial stages of loading in the linear elastic range and the serviceability limit is reached with the propagation of cracks that alter the stiffness of the component significantly (Figure 5.4). However, this is not practical as the strain values at the cracked elements should be checked for every wall, which is comprised by thousands of nodes. Therefore, a simplification is intended to be used for serviceability limit such that the assumed yield point at the idealized capacity curve is taken as the serviceability limit for each wall. The determination of the yield point by using idealization is explained in the following paragraphs.

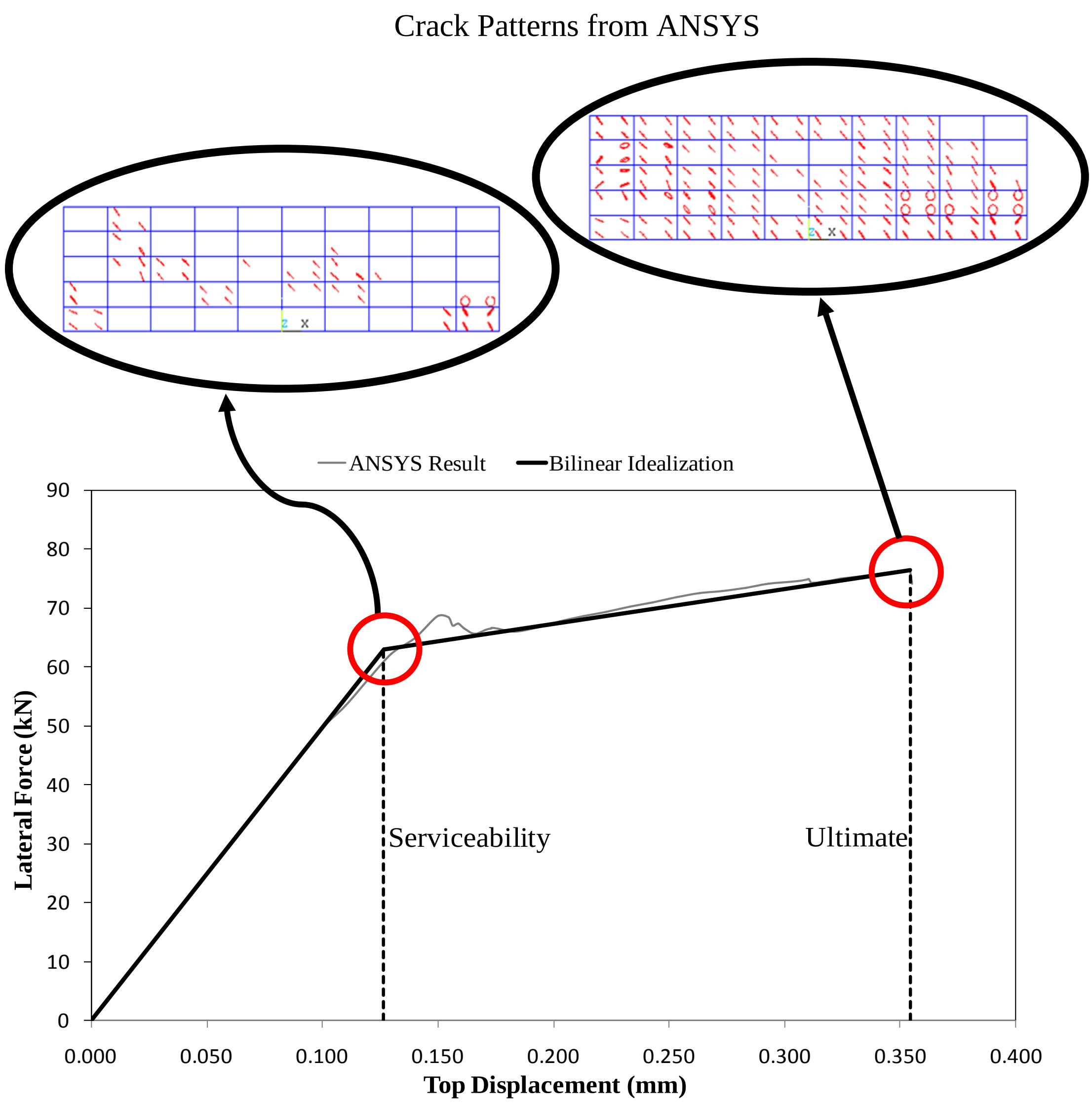

Figure 5.4. Serviceability and Ultimate Performance Limits

The ultimate limit is taken as the end of the capacity curve reached in the analytical model. This limit is dictated by the numerical convergence of the ANSYS model rather than a physical state due to actual behavior. The ANSYS results reveal that at this point the drift of the masonry component is likely to be in the range of maximum capacity. However, since there exists no data beyond this point, it is conservatively assumed as the ultimate limit state after which most of the capacity is suddenly lost.

Since two limit states have been considered, it is appropriate to represent the capacity curves of masonry piers that have been obtained from finite element analyses by an idealized bilinear envelope. This type of idealization for masonry components have been used before by other researchers (Tomazevic, 1999). For this purpose, the bilinearization method proposed by FEMA356 is utilized. It is quite easy-to-use procedure with only four rules (See Figure 5.5). However, the area equality rule compels an iterative solution. The main rules stated are as follows:

1. The area between the curve and its bilinear version should be equal to each other.
2. The initial line of the bilinearized figure should intersect the actual curve at a point that is equal to 60% of the yield force (V_y).
3. The yield force never exceeds the actual maximum capacity.
4. The last point of both actual and idealized curves should be coincident.

By the use of this bilinearization procedure, each capacity curve can simply be represented by four parameters: the yield lateral load capacity (F_y), the yield displacement capacity (u_y), the ultimate lateral load capacity (F_u) and the ultimate displacement capacity (u_u). (See Figure 5.6) Exceeding the point of ultimate capacity, it is further assumed that strength suddenly drops 20% of the maximum value. Physically this means that the component loses its load carrying capacity after this point.

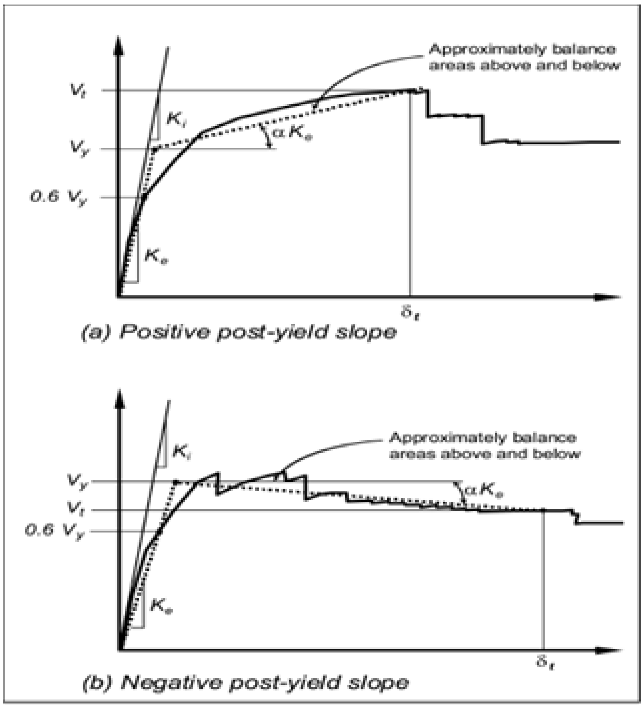

Figure 5.5. Bilinearization of an Actual Curve [FEMA356]

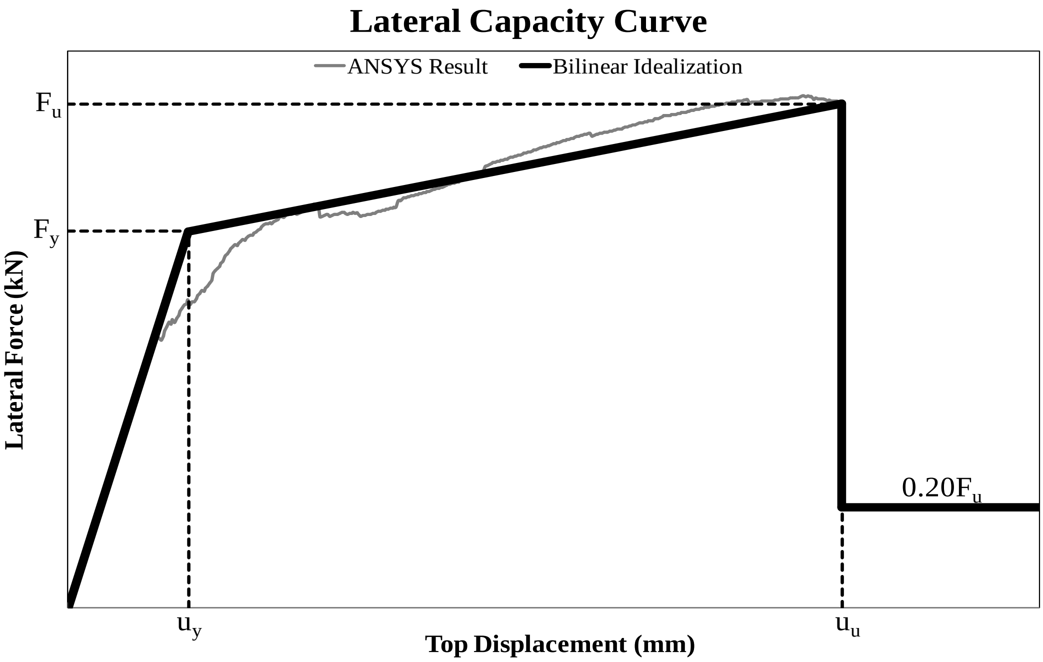

Figure 5.6. Lateral Capacity Curve of a typical pier with f_m=5 MPa, λ=1 and p=0.5 MPa

Hence, the previously obtained analytical results can be used as a database for generating simple relationships between the yield lateral load capacity, the yield displacement capacity, the ultimate lateral load capacity and the ultimate displacement capacity, and different geometrical and mechanical properties of piers. (See Equation 5.8)

$$F_y = F(L, t, \lambda, f_m, p) \quad (5.8.a)$$

$$F_u = F(L, t, \lambda, f_m, p) \quad (5.8.b)$$

$$\delta_y = F(L, t, \lambda, f_m, p) \quad (5.8.c)$$

$$\delta_u = F(L, t, \lambda, f_m, p) \quad (5.8.d)$$

In above equations, L is the length, t is the thickness, λ is the aspect ratio, f_m is the compressive strength of pier and p is the axial pressure on the pier.

5.4.1. Effect of Length and Thickness on Capacity Curve Parameters of Masonry Piers

As mentioned previously, the database comprises capacity curves of piers that have a reference length of 1 m and a reference thickness of 0.2 m. However, these geometrical properties may differ in practice. Consequently, the influence of these parameters on the aforementioned capacity curve parameters should be investigated.

The effect of length is determined by analyzing three different lengths of 1 m, 2 m and 3 m for aspect ratios of 0.5, 1 and 2 and for all load levels and for compressive strength of 5 MPa. (See Figure 5.7 and Table 5.7)

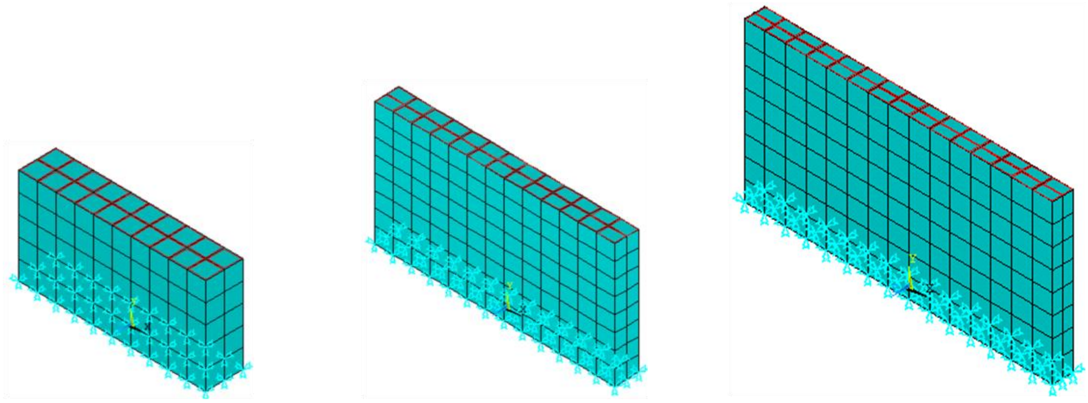

(a) (b) (c)

Figure 5.7. Different Wall Lengths for λ=0.5: (a) L=1 m; (b) L=2 m; (c) L=3 m

Table 5.7. Pier categories for different reference lengths
(Thickness is 0.2 m for all cases.)

Aspect Ratio	Compressive Strength (MPa)	Axial Load Level	Reference Length (m)
0.5	5	$0.05f_m$ $0.10f_m$ $0.20f_m$ $0.30f_m$ $0.40f_m$ $0.50f_m$	1 2 3
1	5	$0.05f_m$ $0.10f_m$ $0.20f_m$ $0.30f_m$ $0.40f_m$ $0.50f_m$	1 2 3
2	5	$0.05f_m$ $0.10f_m$ $0.20f_m$ $0.30f_m$ $0.40f_m$ $0.50f_m$	1 2 3

The effect of thickness on capacity curve parameters is also examined by varying thicknesses only and using other variables as constant just like in the previous case. (See Figure 5.8 and Table 5.8)

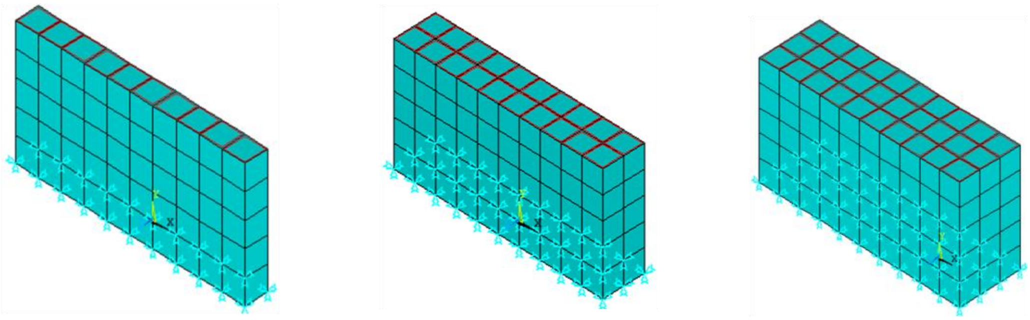

(a) (b) (c)

Figure 5.8. Different Wall Thicknesses for λ=0.5 : (a) t=0.1 m; (b) t=0.2 m; (c) t=0.3 m

Table 5.8. Pier categories for different reference thicknesses
(Length is 1 m for all cases.)

Aspect Ratio	Compressive Strength (MPa)	Axial Load Level	Reference Thickness (mm)
0.5	5	$0.05f_m$ $0.10f_m$ $0.20f_m$ $0.30f_m$ $0.40f_m$ $0.50f_m$	100 200 300
1	5	$0.05f_m$ $0.10f_m$ $0.20f_m$ $0.30f_m$ $0.40f_m$ $0.50f_m$	100 200 300
2	5	$0.05f_m$ $0.10f_m$ $0.20f_m$ $0.30f_m$ $0.40f_m$ $0.50f_m$	100 200 300

For every combination in Tables 5.7 and 5.8, one analytical model is constructed in ANSYS and the effect of length and thickness on the ultimate force capacity, ultimate displacement capacity, the yield force capacity and the yield displacement capacity are compared, separately. (See Figures 5.9 – 5.32)

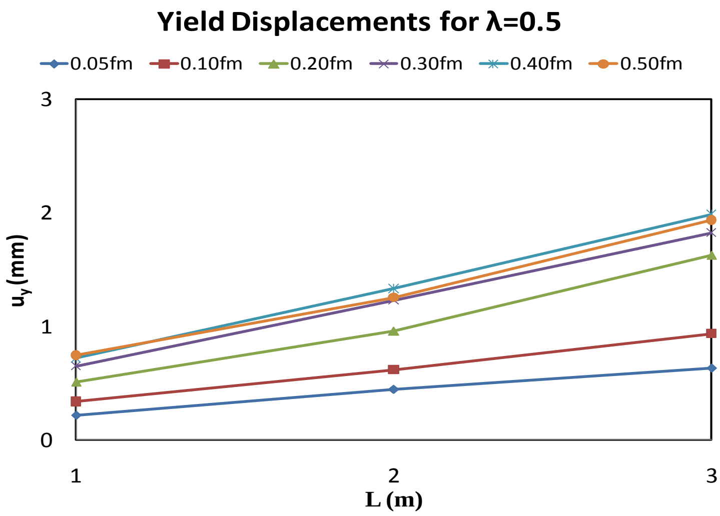

Figure 5.9. Effect of different reference lengths on the yield displacement for λ=0.5

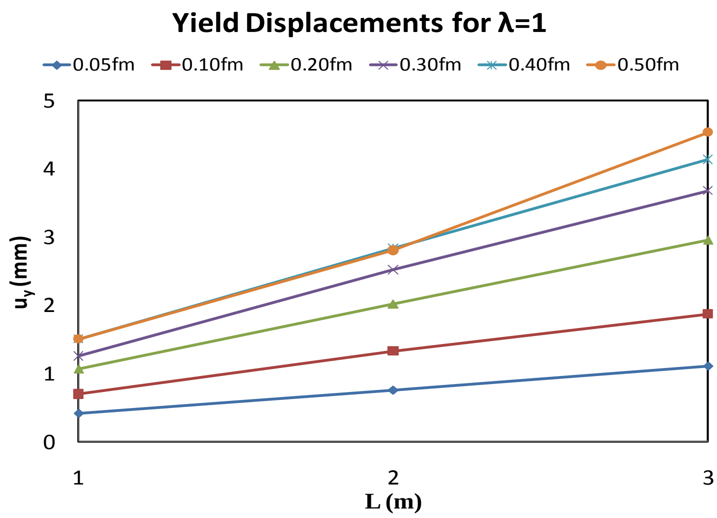

Figure 5.10. Effect of different reference lengths on the yield displacement for λ=1

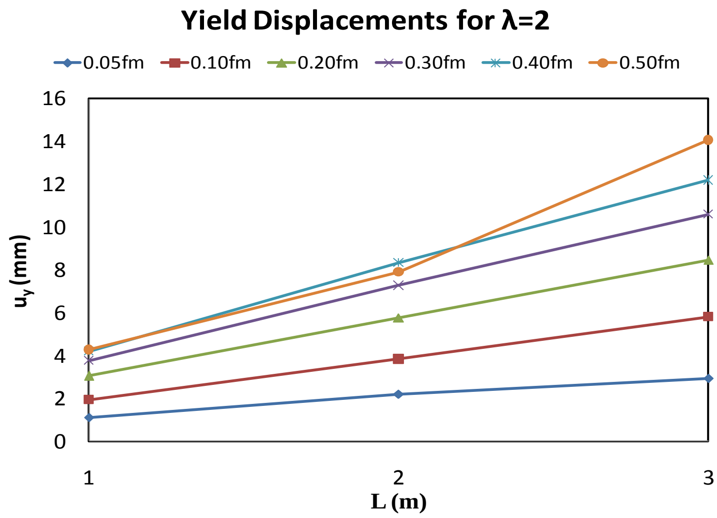

Figure 5.11. Effect of different reference lengths on the yield displacement for λ=2

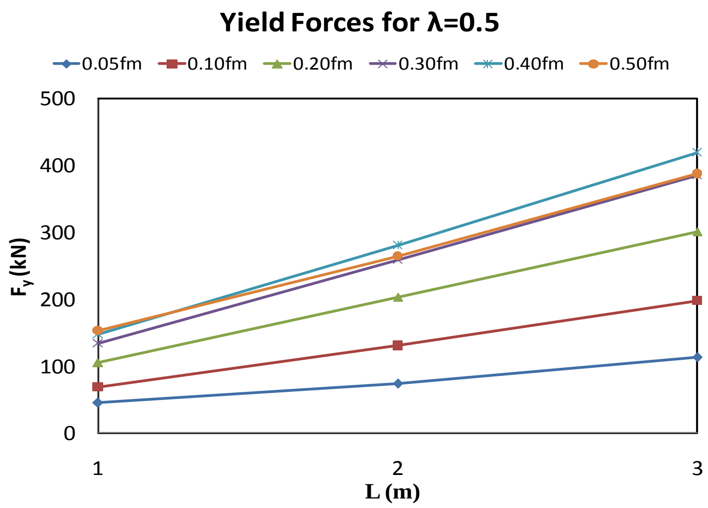

Figure 5.12. Effect of different reference lengths on the yield force capacity for λ=0.5

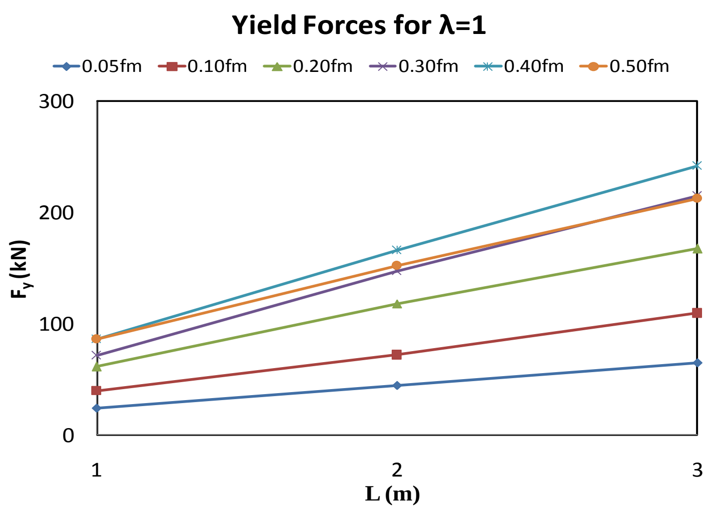

Figure 5.13. Effect of different reference lengths on the yield force capacity for λ=1

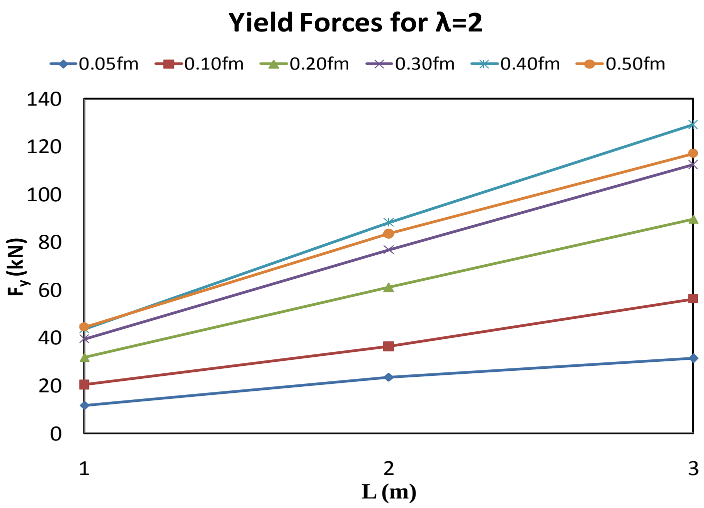

Figure 5.14. Effect of different reference lengths on the yield force capacity for λ=2

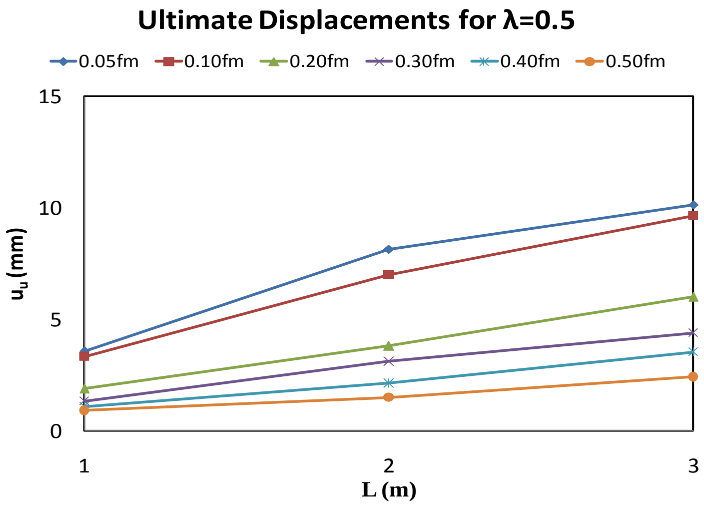

Figure 5.15. Effect of different reference lengths on the ultimate displacement for λ=0.5

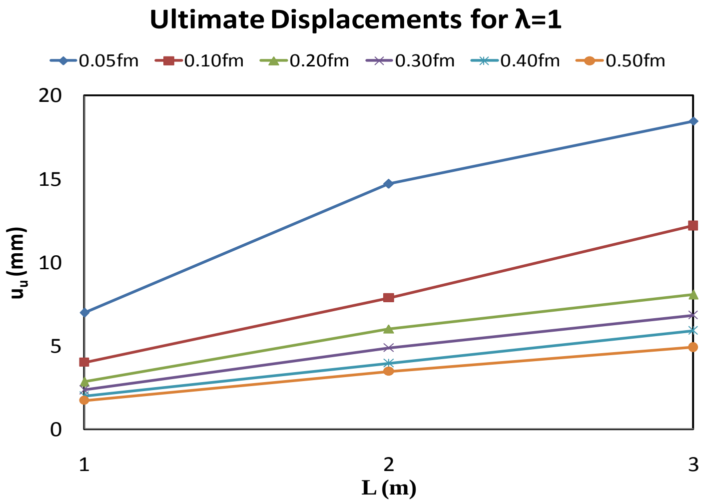

Figure 5.16. Effect of different reference lengths on the ultimate displacement for λ=1

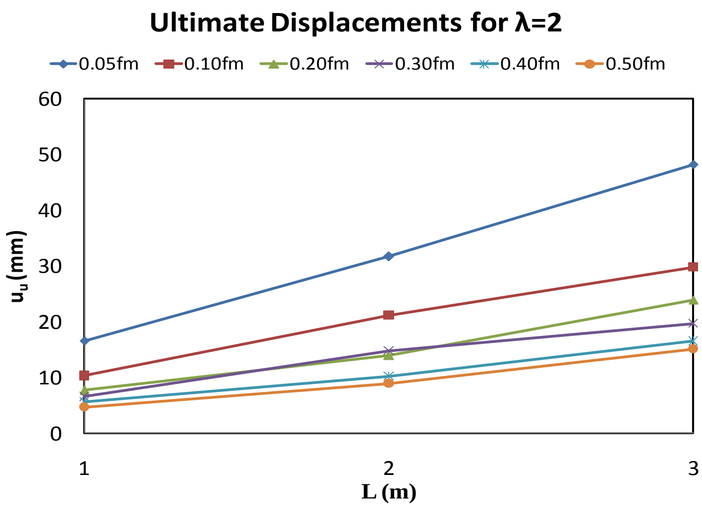

Figure 5.17. Effect of different reference lengths on the ultimate displacement for λ=2

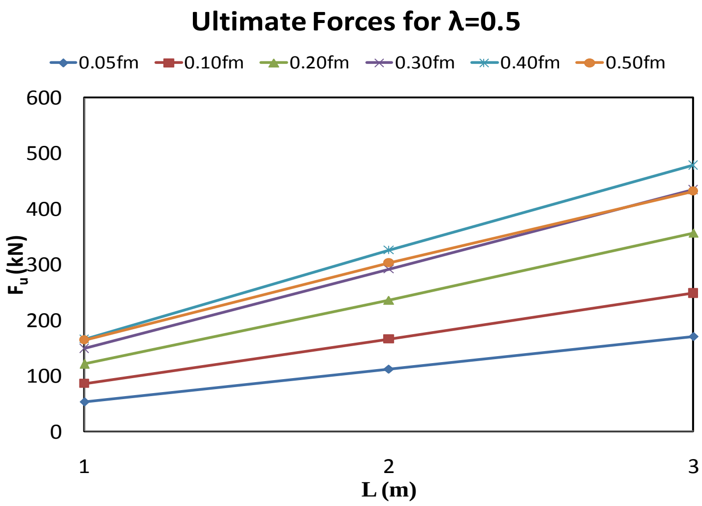

Figure 5.18. Effect of different reference lengths on the ultimate force capacity for λ=0.5

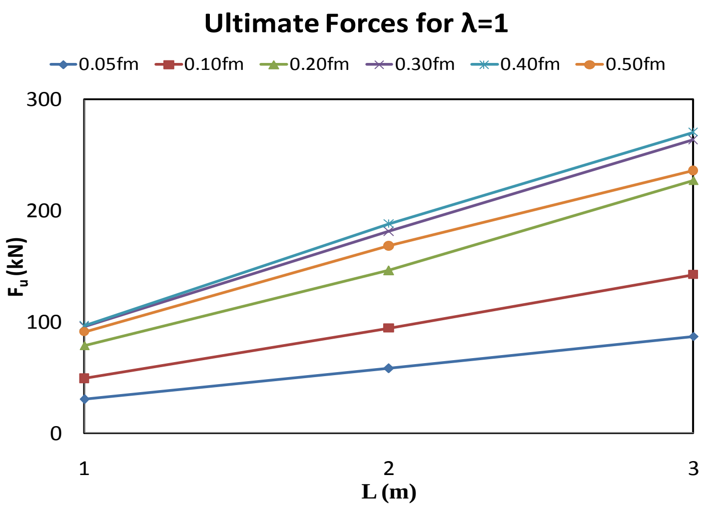

Figure 5.19. Effect of different reference lengths on the ultimate force capacity for λ=1

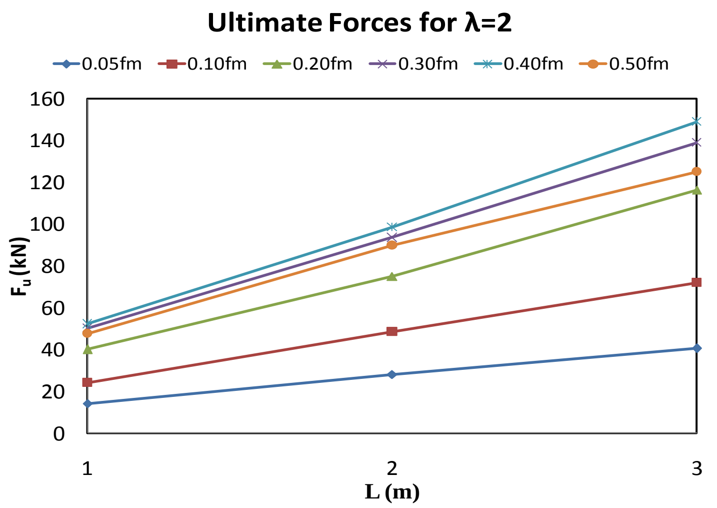

Figure 5.20. Effect of different reference lengths on the ultimate force capacity for λ=2

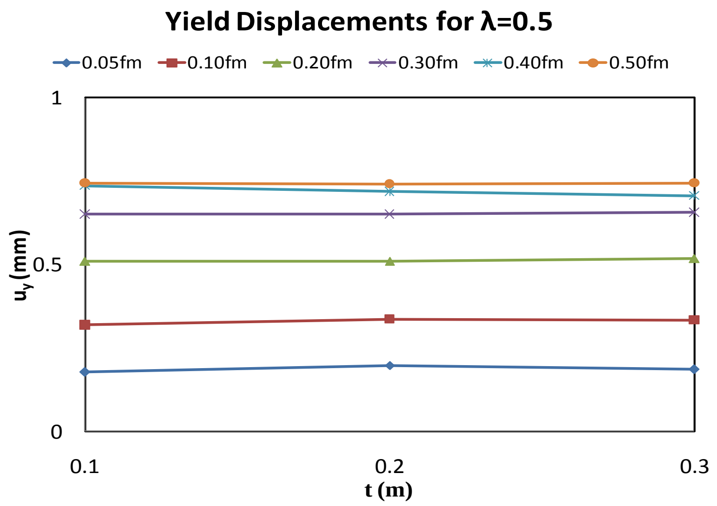

Figure 5.21. Effect of different reference thicknesses on the yield displacement for λ=0.5

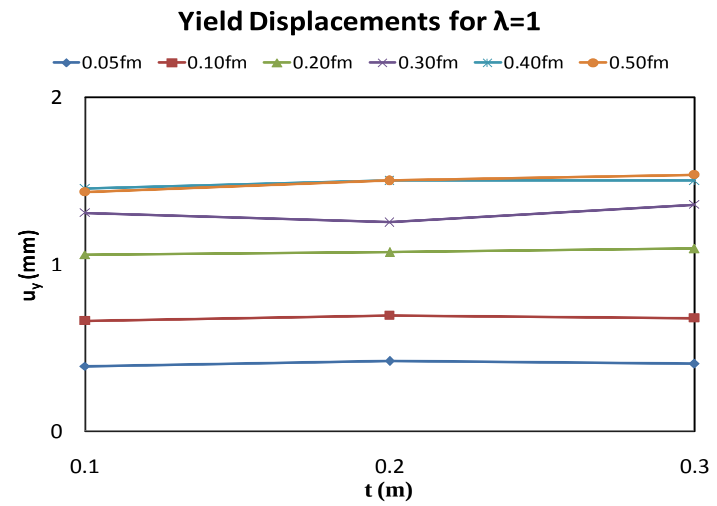

Figure 5.22. Effect of different reference thicknesses on the yield displacement for λ=1

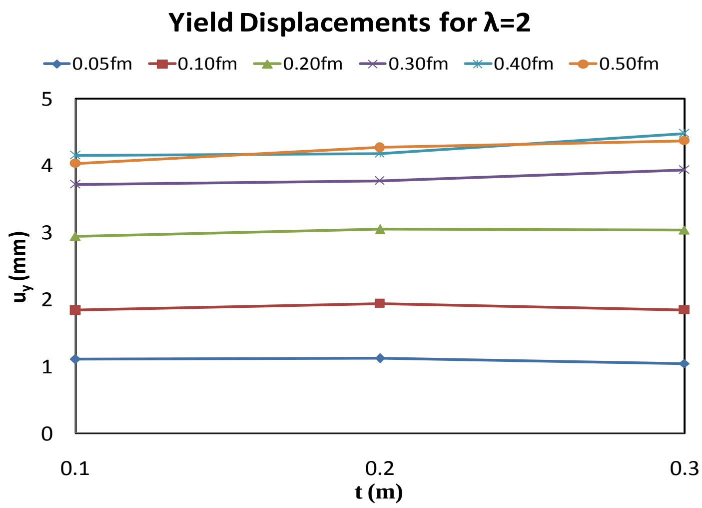

Figure 5.23. Effect of different reference thicknesses on the yield displacement for λ=2

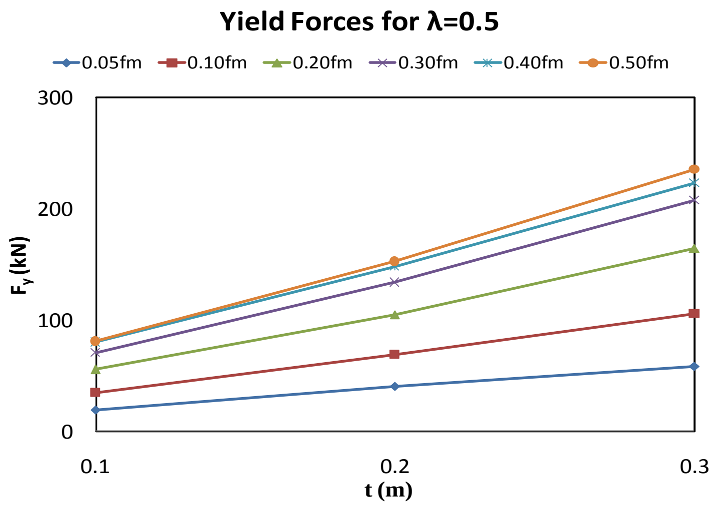

Figure 5.24. Effect of different reference thicknesses on the yield force capacity for λ=0.5

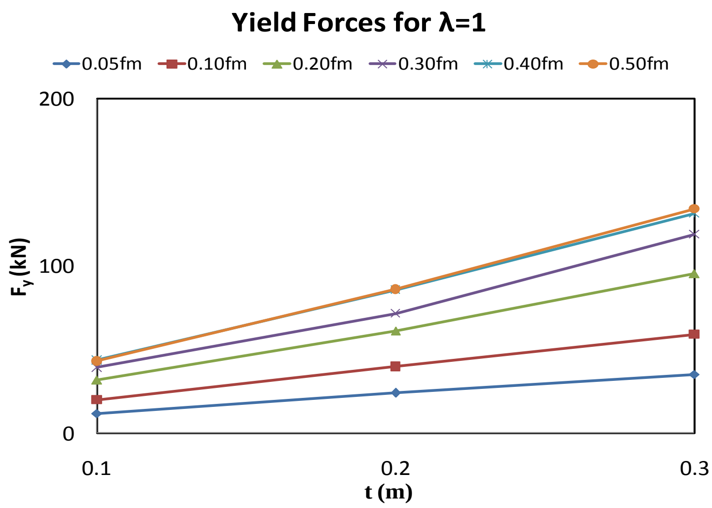

Figure 5.25. Effect of different reference thicknesses on the yield force capacity for λ=1

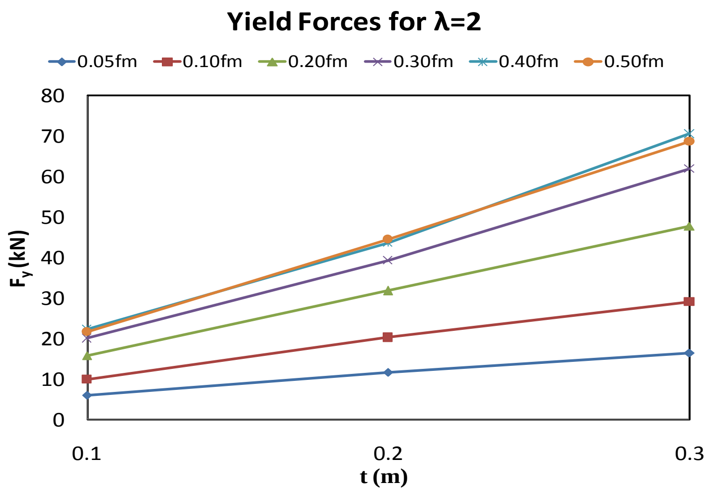

Figure 5.26. Effect of different reference thicknesses on the yield force capacity for λ=2

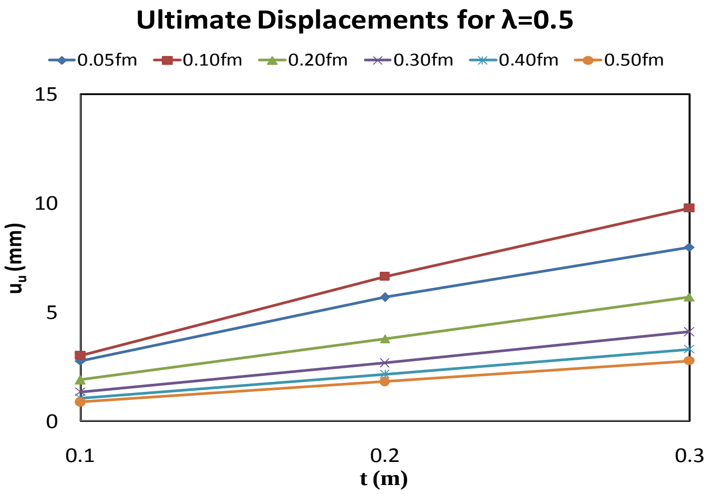

Figure 5.27. Effect of different reference thicknesses on the ultimate displacement for λ=0.5

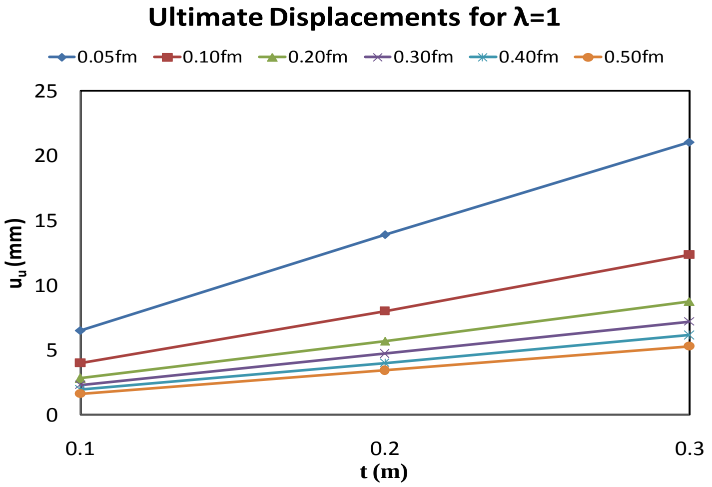

Figure 5.28. Effect of different reference thicknesses on the ultimate displacement for λ=1

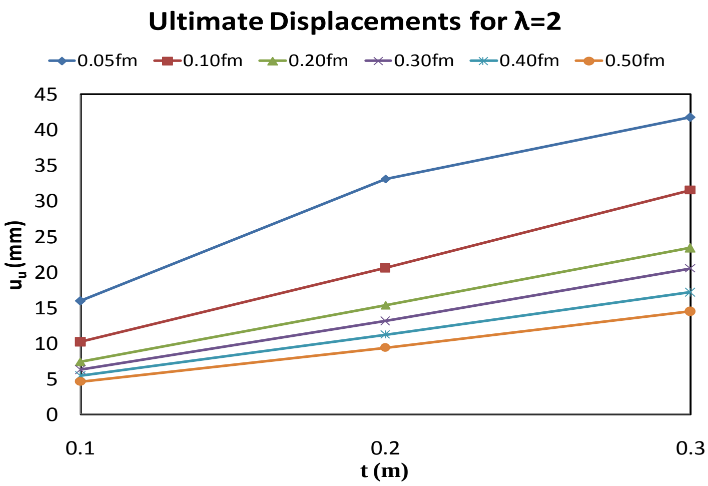

Figure 5.29. Effect of different reference thicknesses on the ultimate displacement for λ=2

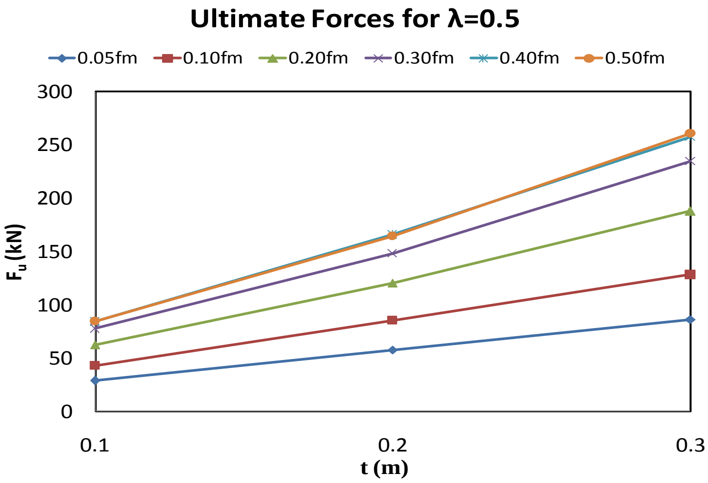

Figure 5.30. Effect of different reference thicknesses on the ultimate force capacity for λ=0.5

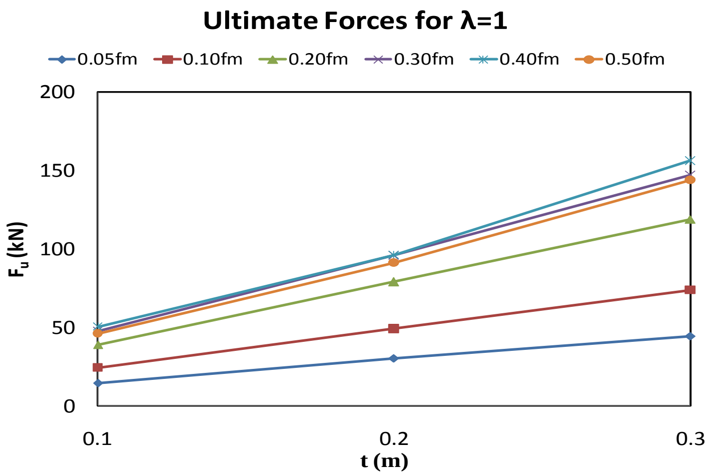

Figure 5.31. Effect of different reference thicknesses on the ultimate force capacity for λ=1

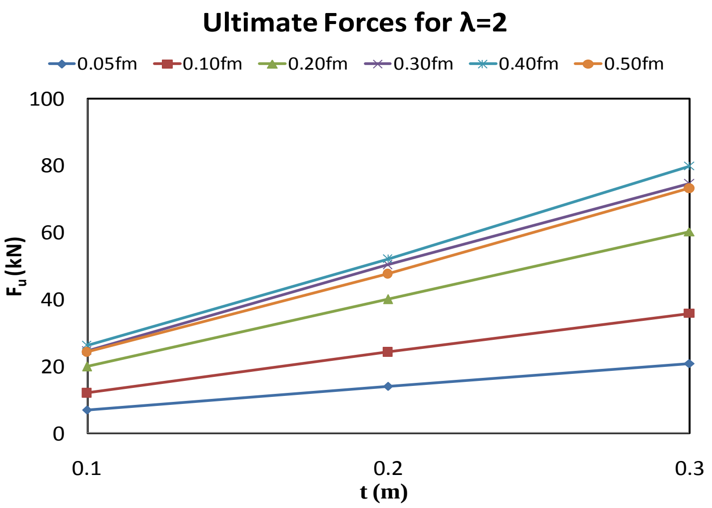

Figure 5.32. Effect of different reference thicknesses on the ultimate force capacity for λ=2

As the results in these figures show a nearly directly proportional trend for all of the mentioned variables except for the influence of thickness on the yield displacement, the effect of length or thickness is incorporated by simply multiplying them by their ratios to their reference counterparts.

5.4.2. Comparison of Failure Modes from ANSYS with the Literature

The failure mode plays an important role on the load deformation characteristics of any masonry piers. Therefore, the analyses results should be capable of describing mode of failure. To check it, the analyzed piers are inspected according to their predicted failure modes by using the analyses results of this dissertation and the literature formulas (See Equations 5.9 – 5.11).

$$R_{ss} = L * t * \left(V_{bo} + \mu * \sigma_y\right) \tag{5.9}$$

$$R_{dt} = L * t * \frac{f_{mt}}{b} * \sqrt{\frac{\sigma_y}{f_{mt}} + 1} \tag{5.10}$$

$$R_f = \frac{\sigma_y * t * L^2}{2 * \alpha * H}\left(1 - \frac{\sigma_y}{f_m}\right) \tag{5.11}$$

where V_{bo} is the shear bond strength at zero compression (recommended as 0.15MPa in TEC2007), μ is the coefficient of friction (taken as 0.4), b is the shear stress distribution factor (takes values between 1 and 1.5 depending on the aspect ratio) and α is the effective height determination factor (taken as 0.5 for cantilever piers).

In order to show the procedure, three examples showing three different modes of failures are investigated in details. In Table 5.9, the characteristics and the predicted failure modes of these piers are summarized. In this table, the mode of failure is determined by the minimum of the above formulas. (See Equations 5.9 – 5.11)

Table 5.9. The Properties of Piers and the Predicted Failure Modes

Pier	Aspect Ratio	Compressive Strength (MPa)	Axial Load Ratio (MPa)	Failure Mode
1	0.5	2	0.2	Diagonal Tension
2	1	5	0.1	Sliding
3	2	8	0.2	Flexure

The failure modes from the analyses would be determined by inspecting

1) Crack Patterns
2) Strain Distributions

The following figures summarize both the crack patterns and the strain distributions at the ultimate stage of the selected masonry piers. (See Figures 5.33 - 5.34)

It can easily be inferred from Figures 5.33.a and 5.34.a that the dominant mode of failure is diagonal tension as an inclined crack pattern is observed along the diagonal of the pier, which is the same as the literature prediction.

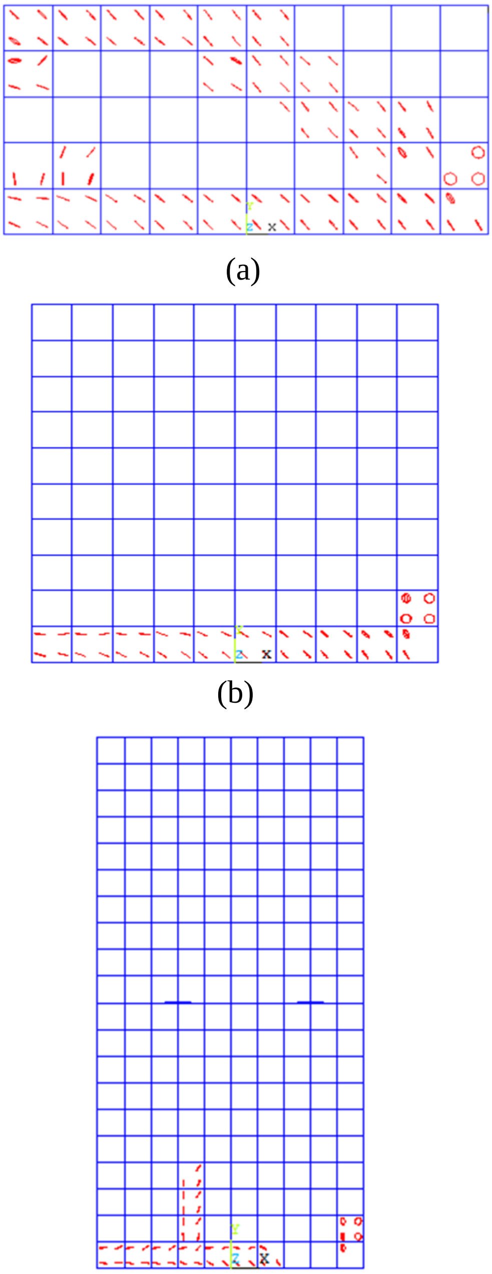

(a)

(b)

(c)

Figure 5.33. The Crack Patterns (a) Pier 1; (b) Pier 2; (c) Pier 3

The sliding shear failure mode is dominant as far as the pier 2 is concerned because a nearly horizontal cracking pattern manifests at the ultimate stage (See Figure 5.33.b). This phenomenon is also realized if the total principal strain vector plots given in Figure 5.34.b is inspected.

The third failure mode, flexure, is observed in Pier 3 although it is not apparent from the crack pattern (See Figure 5.33.c). However, the flexural failure is prominent as high axial elongation (marked by two- headed arrows) occurs on side of the pier whereas axial contraction (marked by blue arrows) is seen on the other side (See Figure 5.34.c).

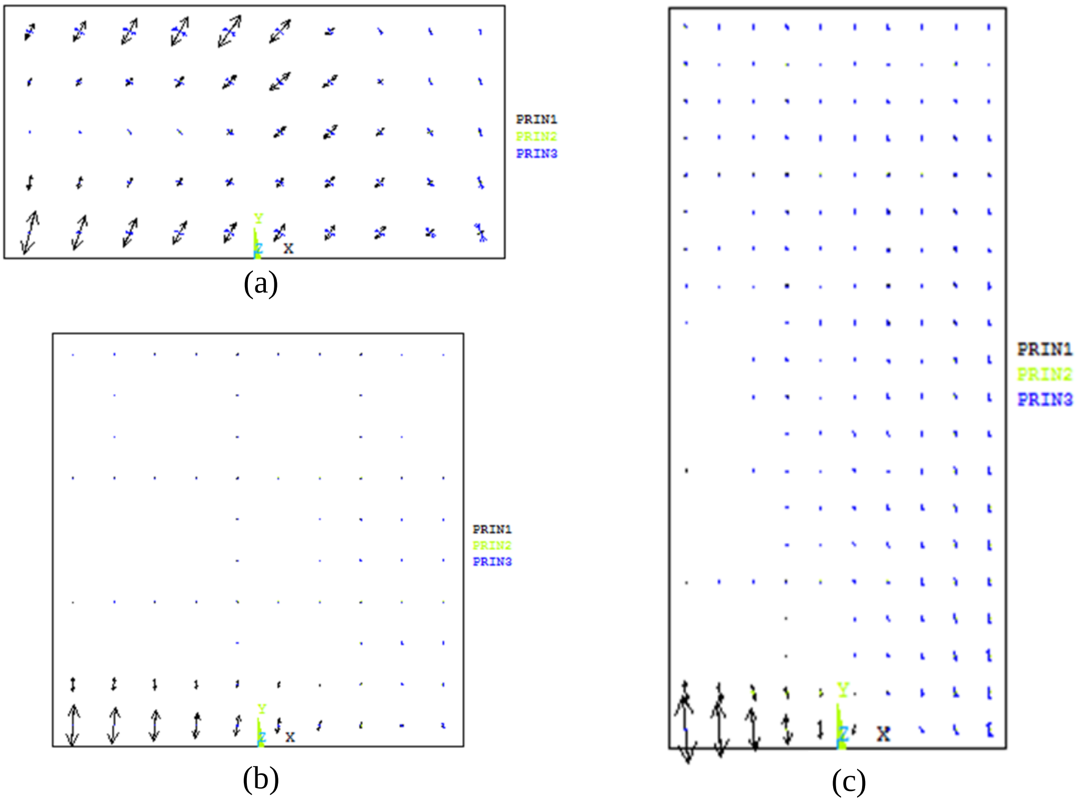

Figure 5.34. The Total Principal Strain Vector Plots (a) Pier 1; (b) Pier 2; (c) Pier 3

The finite element analyses and the literature formulas come up with pretty different lateral load capacity estimations. (See Table 5.10) This is because; the literature formulas are purely dependent on constants like V_{bo}, μ, b, etc. whose true values for the selected pier set are not known.

Table 5.10. The Properties of Piers and the Predicted Failure Modes

Pier	**$F_{u,literature}$ (kN)**	**$F_{u,FEM}$ (kN)**	**Percentage Error (%)**
1	70.000	41.934	-35.299
2	54.991	45.291	-23.743
3	128.000	56.821	-55.608

5.4.3. Mathematical Models used for Nonlinear Regression Analysis

Nonlinear regression analysis is used in order to obtain empirical relationships for capacity curve parameters (F_y, u_y, F_u and u_u) in terms of aforementioned structural parameters (f_m, λ, L, t and p). The analyses are performed by using Statistical Package for the Social Sciences (SPSS 15) and the following non-linear regression models (See Equation 5.12) are intended to be used in the trial and error process.

$$\hat{y} = (C_1(p + C_2)^2 + C_3(f_m + C_4)^2 + C_5(\lambda + C_6)^2) * L * t \qquad (5.12.a)$$
$$\hat{y} = (C_1(p + C_2)^3 + C_3(f_m + C_4)^3 + C_5(\lambda + C_6)^3) * L * t \qquad (5.12.b)$$
$$\hat{y} = C_1 * p^{C_2} * {f_m}^{C_3} * \lambda^{C_4} * L * t \qquad (5.12.c)$$
$$\hat{y} = C_1 * e^{C_2 p} * e^{C_3 f_m} * e^{C_4 \lambda} * L * t \qquad (5.12.d)$$
$$\hat{y} = C_1 * e^{C_2 p} * {f_m}^{C_3} * \lambda^{C_4} * L * t \qquad (5.12.e)$$
$$\hat{y} = C_1 * p^{C_2} * e^{C_3 f_m} * \lambda^{C_4} * L \qquad (5.12.f)$$
$$\hat{y} = C_1 * p^{C_2} * e^{C_3 f_m} * \lambda^{C_4} * L * t \qquad (5.12.g)$$
$$\hat{y} = C_1 * p^{C_2} * {f_m}^{C_3} * e^{C_4 \lambda} * L * t \qquad (5.12.h)$$
$$\hat{y} = C_1 * p^{C_2} * e^{C_3 f_m} * e^{C_4 \lambda} * L * t \qquad (5.12.i)$$
$$\hat{y} = (C_1 * (p + C_2)^2 + C_3 {f_m}^{C_4} * e^{C_5 \lambda}) * L * t \qquad (5.12.j)$$

In the above equations, p (in MPa), f_m (in MPa), λ, L (in m) and t (in m) are the abbreviations for the structural parameters defined previously. C_i's are coefficients to be determined in the regression analysis and $\hat{y}$ represents the estimated value of one of the capacity curve parameters. [F_y (in kN), u_y (in mm), F_u (in kN) and u_u (in mm)]

According to SPSS Manual (2006), nonlinear regression is a method of finding a nonlinear model of the relationship between the dependent variable and a set of independent variables. Nonlinear regression utilizes iterative estimation algorithms so the starting values of the undetermined constants are vital. Therefore, the trial values for coefficients should be selected with caution.

The mathematical expressions in Equations 5.12.a-j are examined for obtaining best fit equations in terms of the yield lateral load, the yield lateral displacement, the ultimate lateral load capacity and the ultimate lateral displacement capacity, separately. Then, the model with the highest coefficient of determination (R^2) is accepted as the most appropriate formulation.

The regression analyses for force parameters indicate result that the model represented by Equation 5.12.h is superior to the other models as R^2 values have been obtained as 0.984 and 0.982 for the yield lateral force and ultimate lateral force equations, respectively. Such high values of coefficient of determination mean that most of the dependent variables (force capacities in this case) are well represented by the regression equations so the regression lines can be assumed to meet the expectations.

The regression coefficients in Equation 5.12.h for the yield lateral force capacity and the ultimate lateral load capacity from regression analysis are summarized in Table 5.11.

Table 5.11. Regression coefficients of Equation 5.12.h for yield lateral load and ultimate lateral load capacity

Coefficients	Yield Lateral Load	Ultimate Lateral Load Capacity
C_1	353.147	352.156
C_2	0.604	0.498
C_3	0.414	0.501
C_4	-0.931	-0.856

The most suitable models for the yield displacement and the ultimate lateral displacement capacity are given in Equation 5.12.f and Equation 5.12.g with R^2=0.982 and R^2=0.962, respectively. The reason why the yield displacement estimation equation does not comprise a term related to thickness is that the analyses results obtained from different models with changing thicknesses show that the effect of thickness on the yield displacement is negligible. (See Figures 5.21 - 5.23)

The regression coefficients for the yield displacement and the ultimate lateral displacement capacity from regression analysis are also given in Table 5.12.

Table 5.12. Regression coefficients of Equations 5.12.f and 5.12.g for yield displacement and ultimate displacement capacity

Coefficients	Yield Displacement	Ultimate Displacement Capacity
C_1	0.587	2.385
C_2	0.543	-0.540
C_3	0.0949	0.319
C_4	1.426	1.414

Hence, these simple formulations can replace detailed finite element analyses in order to estimate idealized capacity curve parameters of masonry piers of any geometry. For instance, the comparison of results obtained from both above simple equations and ANSYS for a pier of λ=1, f_m=5 MPa and p=0.5 MPa yields a conclusion that the errors of these estimations are acceptable. (See Table 5.13)

Table 5.13. Comparison of capacity curve parameter estimations

	Simple Equations	**ANSYS**	**Error (%)**
Yield Displacement (mm)	0.622	0.648	4.204
Yield Force (kN)	33.821	35.710	5.585
Ultimate Displacement (mm)	3.985	3.424	14.058
Ultimate Force (kN)	45.291	47.456	4.780

Then, the lateral load capacity of the critical storey of an unreinforced masonry building in one direction can be obtained by combining the contributions coming from each pier of different geometry after obtaining the simple and idealized capacity curves of these piers as explained above. It is also possible to determine the performance limits of the critical storey since limit states for all piers have already been defined. Finally, this information can be used to attain the global limit states of the building under construction.

After determining the seismic demand on the building, the performance state can be obtained by using any of the proposed methods in literature (single-degree-of-freedom idealization, capacity spectrum method, displacement coefficient method, etc.). Since the proposed method is simple (with bilinear capacity curves as function of simple structural parameters) and approximate (including many assumptions at different stages), it is very suitable to assess the seismic safety of a population of buildings. For individual buildings which require detailed evaluation, this method may yield misleading results (generally on the conservative side).

The application of the method will be presented by considering an actual unreinforced masonry building in Istanbul, which was investigated during Istanbul Masterplan Project.

5.6. Application of the Procedure to an Existing Masonry Building

The previously explained procedure is used to estimate the lateral capacity curve of an existing masonry building located in Istanbul. According to the procedure, the piers in the building should be considered but it is not an easy task to decide on the height of a masonry pier in a perforated building (that means a building where the walls are pierced with window and door openings). Therefore, the effective height concept developed by Dolce (1989) is utilized. This method developed by Dolce starts with drawing lines joining the tops and bottoms of adjacent voids. If there is no adjacent void but the edge of the building exists then the line is drawn to the edge of building. (See Figure 5.35) After that the angle between these lines and the horizontal axis is measured and a new line is drawn with a horizontal deviation of 30^o whenever the angle is higher than 30^o.

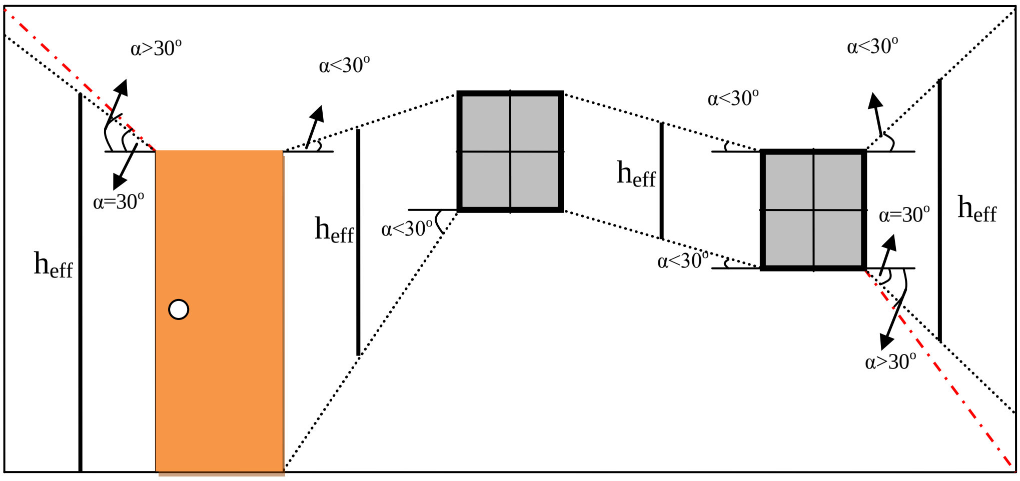

Figure 5.35. Effective Height Determination

In other words, the support conditions for a single pier is determined by its neighbour spandrels and the effective height concept dictates the height that is capable of flexural deformation and other parts are assumed as rigid (or non-deformable). (See Figure 5.36)

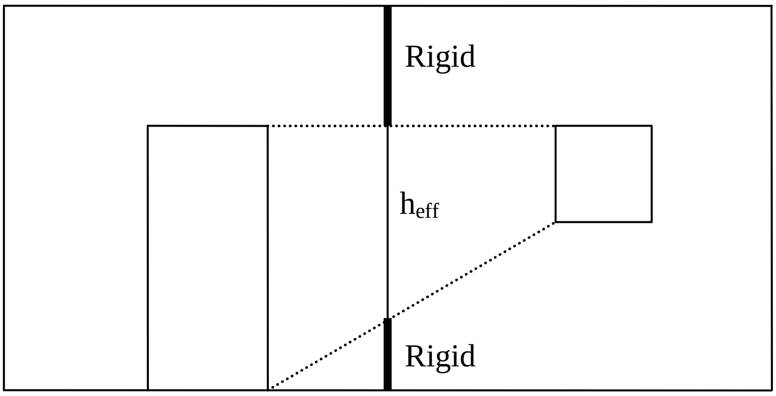

Figure 5.36. Effective Height of a Pier and Flexurally Rigid Parts

5.6.1. The Mechanical and Physical Properties of Case Structure

This building is an unreinforced masonry made up of local clay bricks. It has three stories, first of which is 2.9 m in height and others have 3 meters height. Referring to the previous discussions about the characteristics of Turkish masonry construction, the modulus of elasticity, Poisson’s ratio, the compressive strength and the tensile strength are assumed as 2000 MPa, 0.20, 5 MPa and 0.35 MPa, respectively.

Figure 5.37. Picture of the masonry building used as a case study

A frontal photo of the masonry building under concern and its plan view are shown in Figures 5.37 and 5.38, respectively.

The piers are labeled according to orthogonal directions. Figures 5.39 and 5.40 show the walls in X and Y directions as dashed lines, respectively. (The labeling of frames in x and y directions starts from bottom left, respectively. i.e. X1 is the leftmost frame in X direction.) The effective heights of piers determined by the Dolce Method are also shown in Figures 5.41-5.46.

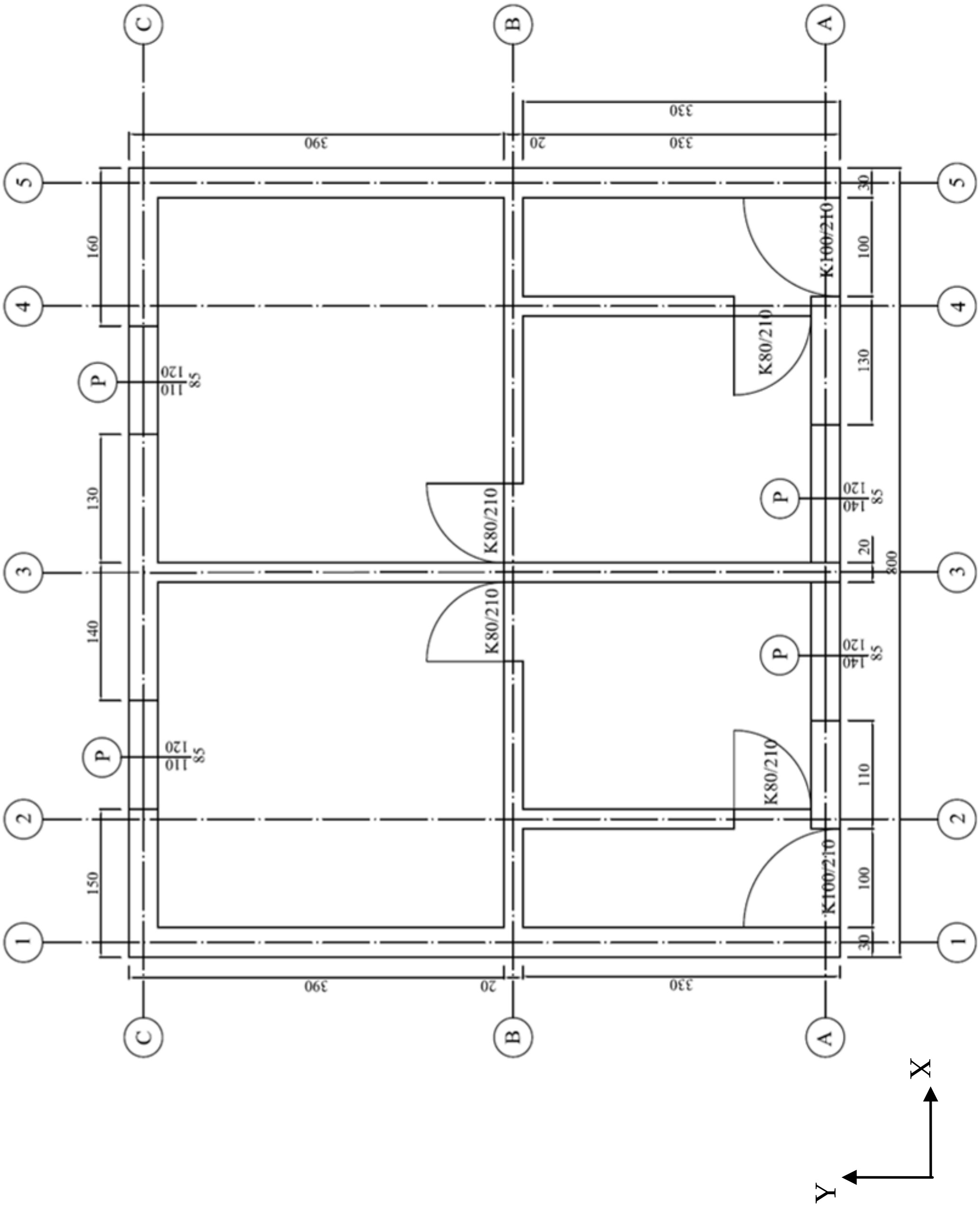

Figure 5.38. Plan View of Building

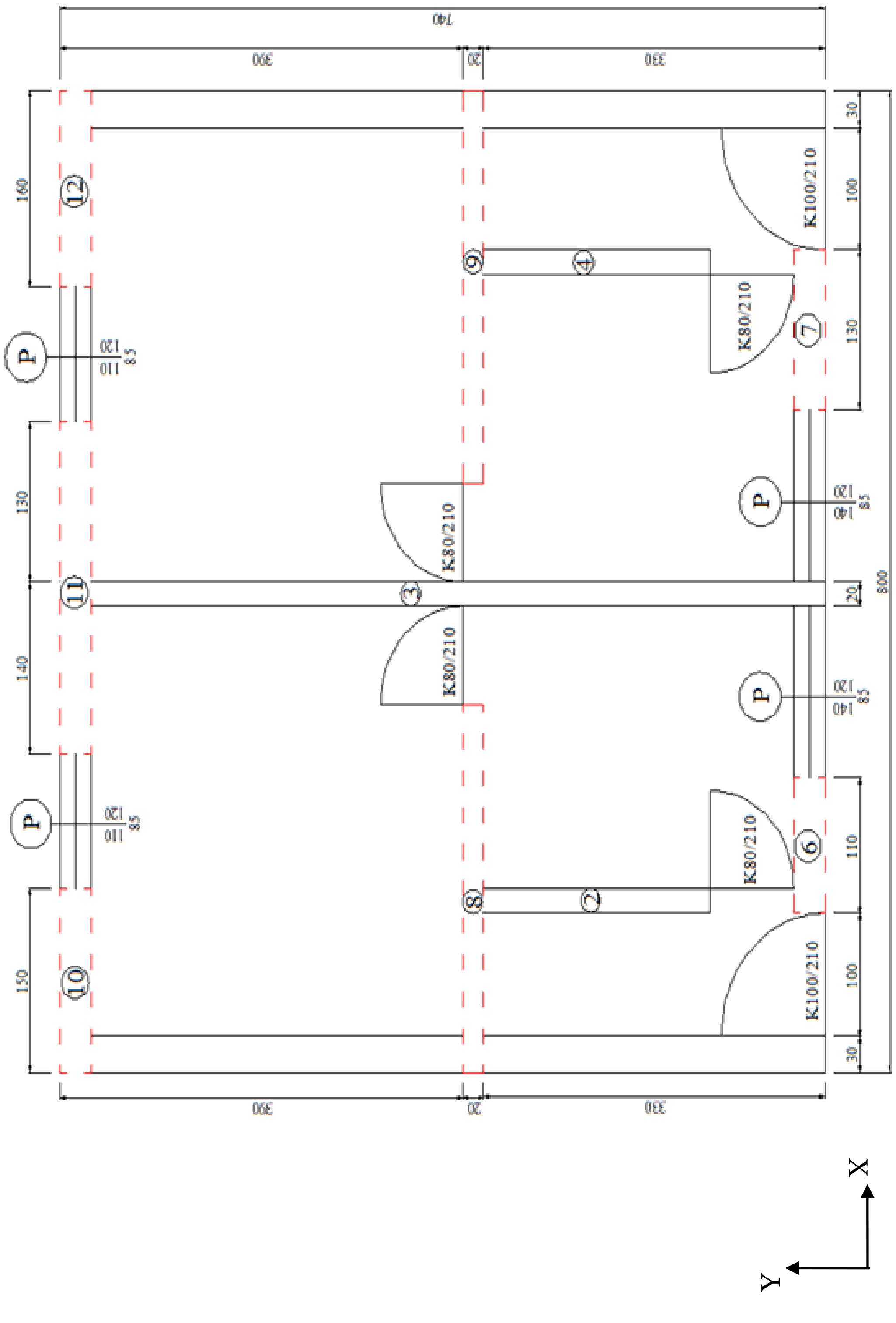

Figure 5.39. Walls in X Direction

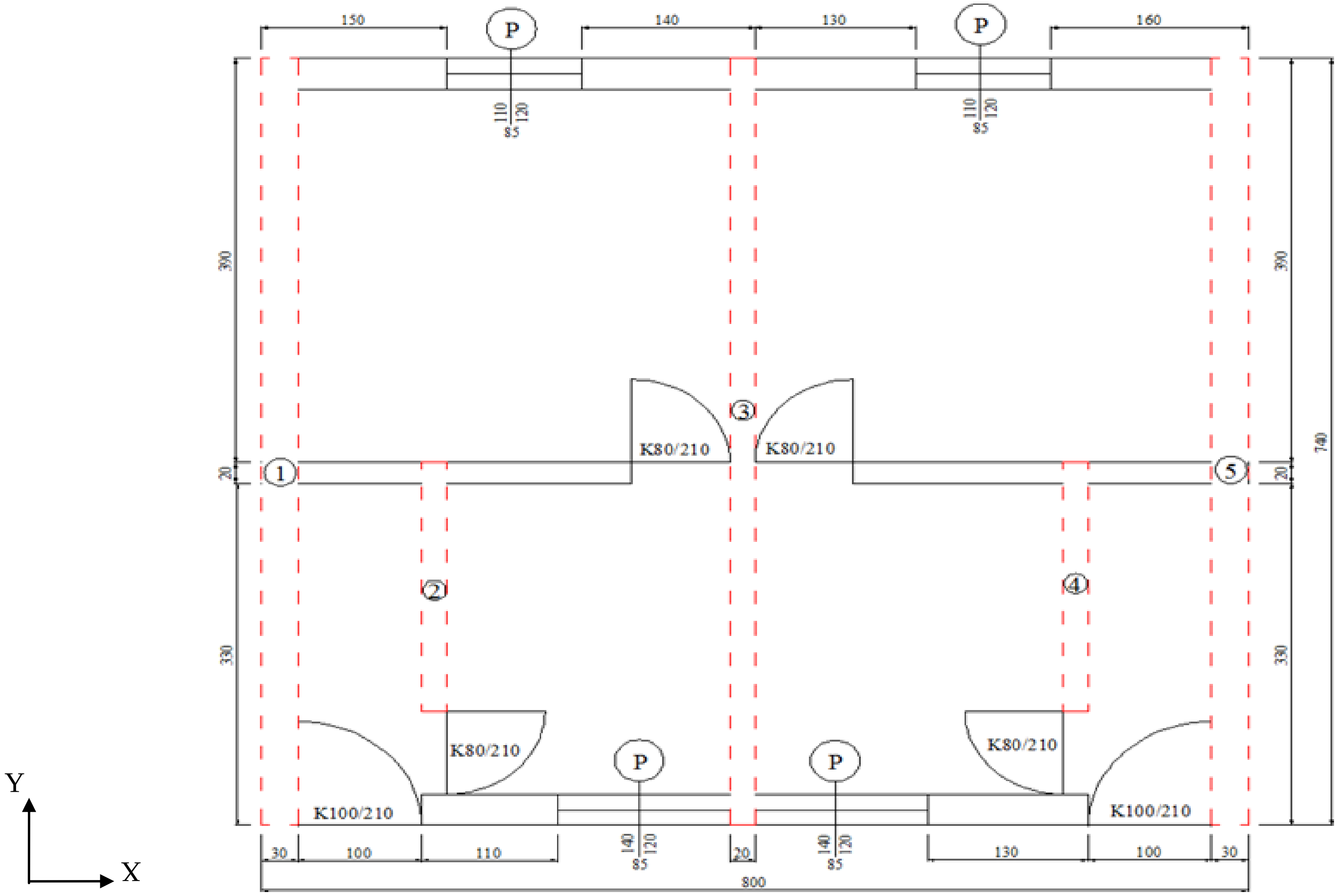

Figure 5.40. Walls in Y Direction

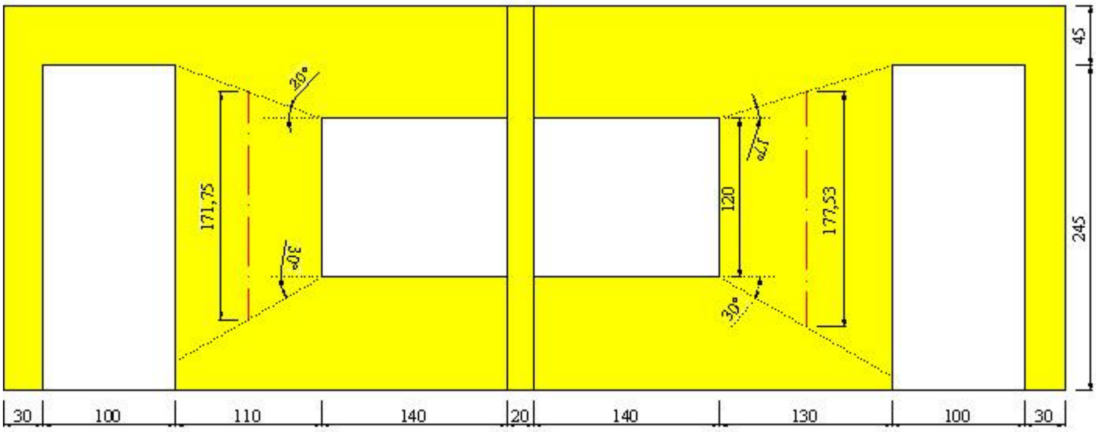

Figure 5.41. Effective Heights in X1 for First Storey (All dimensions are in mm.)

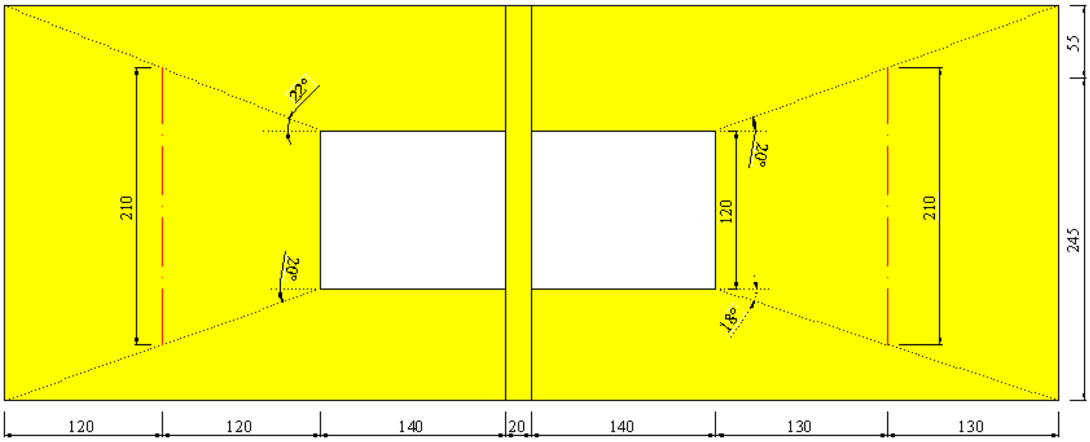

Figure 5.42. Effective Heights in X1 for Second and Third Stories

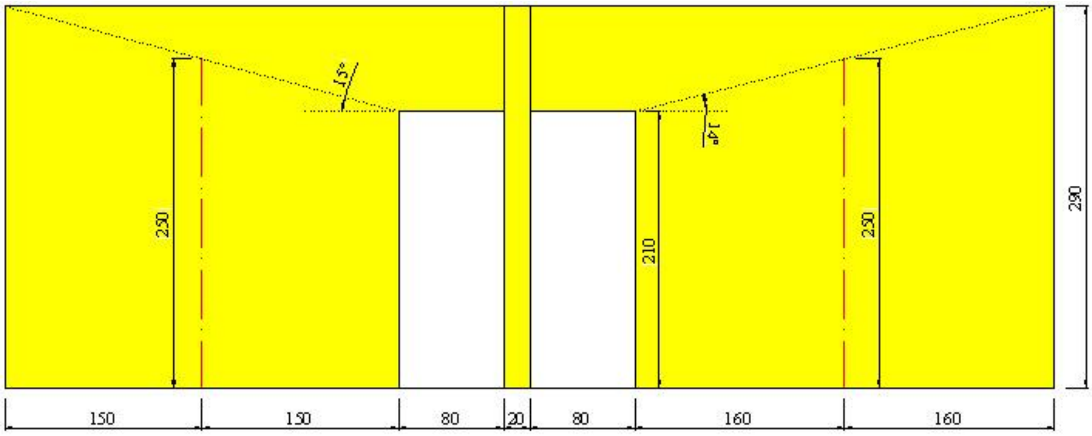

Figure 5.43. Effective Heights in X2 for All Stories (All dimensions are in mm.)

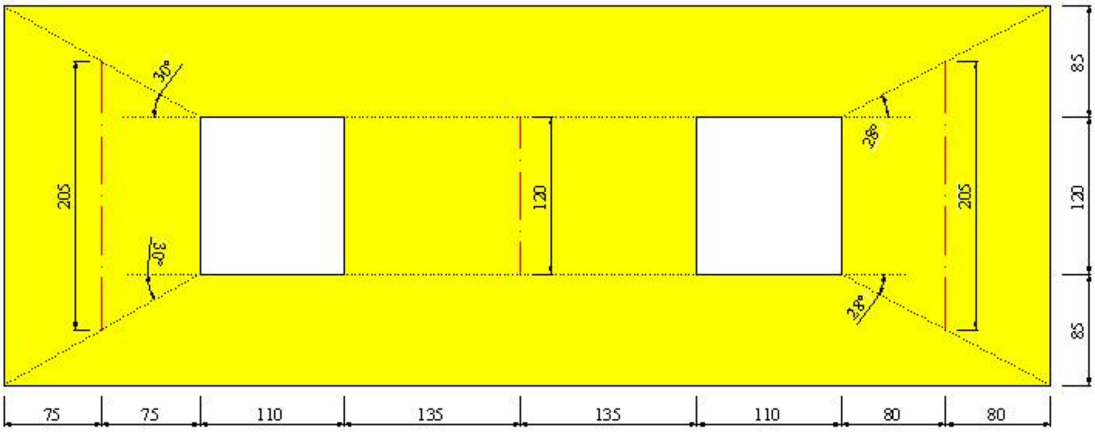

Figure 5.44. Effective Heights in X3 for All Stories (All dimensions are in mm.)

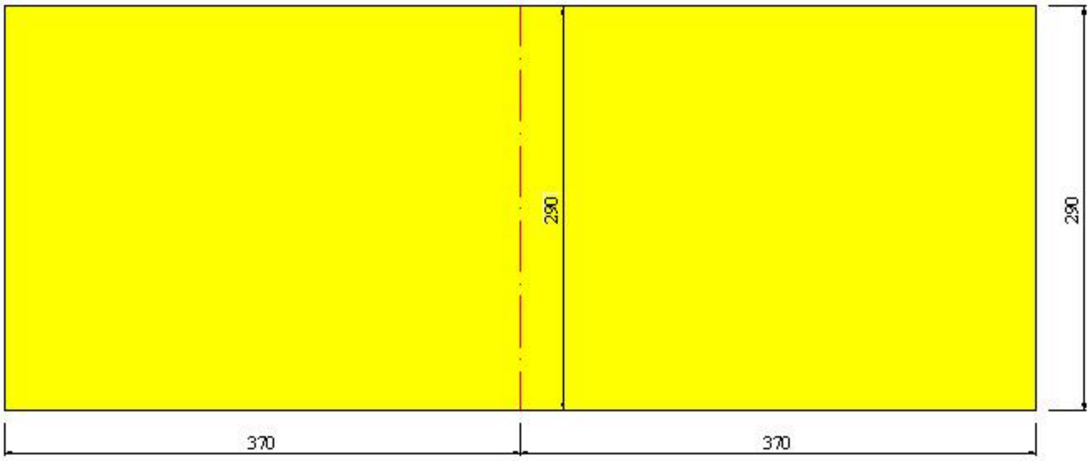

Figure 5.45. Effective Heights in Y1, Y3 and Y5 for All Stories
(All dimensions are in mm.)

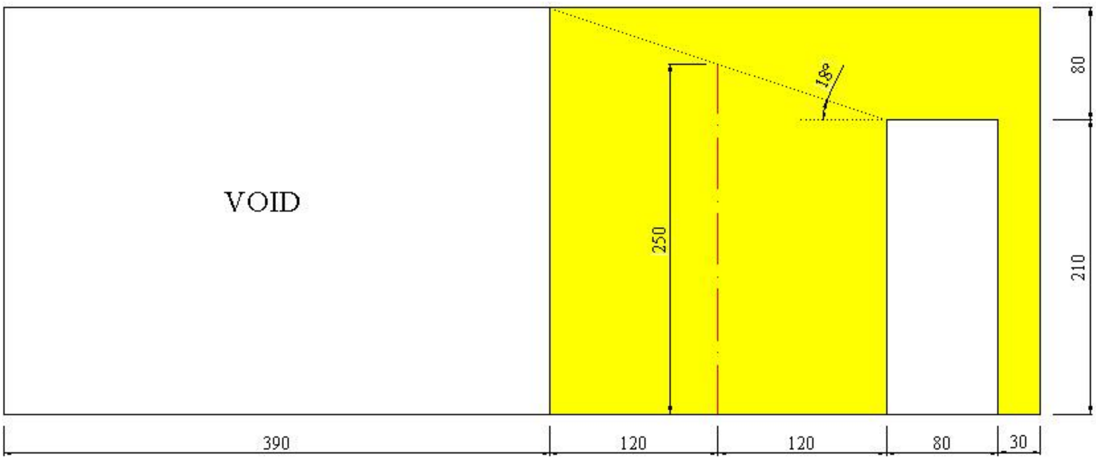

Figure 5.46. Effective Heights in Y2 and Y4 for All Stories
(All dimensions are in mm.)

5.6.2. Analysis Results

In this study, all piers are, firstly, modeled in ANSYS and the capacity curves are determined from these analyses results. After that the same building is analyzed by the previously found simple formulas to form the capacity curves. Then, the capacity curves are compared for both orthogonal directions. In Figures 5.47 and 5.48, the capacity curves of first-storey piers generated by utilizing both ANSYS (bilinearized states) and simple method are summarized.

At this point, it should be stated that all of the piers are modeled in ANSYS as the axial load on piers change from storey to storey, which are calculated by combining the slab loads and the total weight of each wall. (See Table 5.14)

Table 5.14. Axial loads and Axial Pressures on each Pier

Pier	***N_{total1}(ton)***	***N_{total2}(ton)***	***N_{total3}(ton)***	***p_1 (ton/m^2)***	***p_2 (ton/m^2)***	***p_3 (ton/m^2)***	***Direction***
1	51.035	34.290	17.145	22.989	15.446	7.723	Y
2	15.998	10.723	5.362	33.330	22.340	11.170	Y
3	62.173	41.626	20.813	42.009	28.126	14.063	Y
4	16.208	10.863	5.432	33.767	22.631	11.316	Y
5	51.359	34.506	17.253	23.135	15.543	7.772	Y
6	13.163	10.757	5.378	39.886	14.940	7.470	X
7	14.847	11.934	5.967	38.070	15.300	7.650	X
8	21.098	14.137	7.069	35.163	23.562	11.781	X
9	23.478	15.729	7.864	36.684	24.576	12.288	X
10	11.462	7.695	3.848	25.470	17.100	8.550	X
11	20.853	13.999	7.000	25.744	17.283	8.641	X
12	12.480	8.377	4.189	25.999	17.453	8.726	X

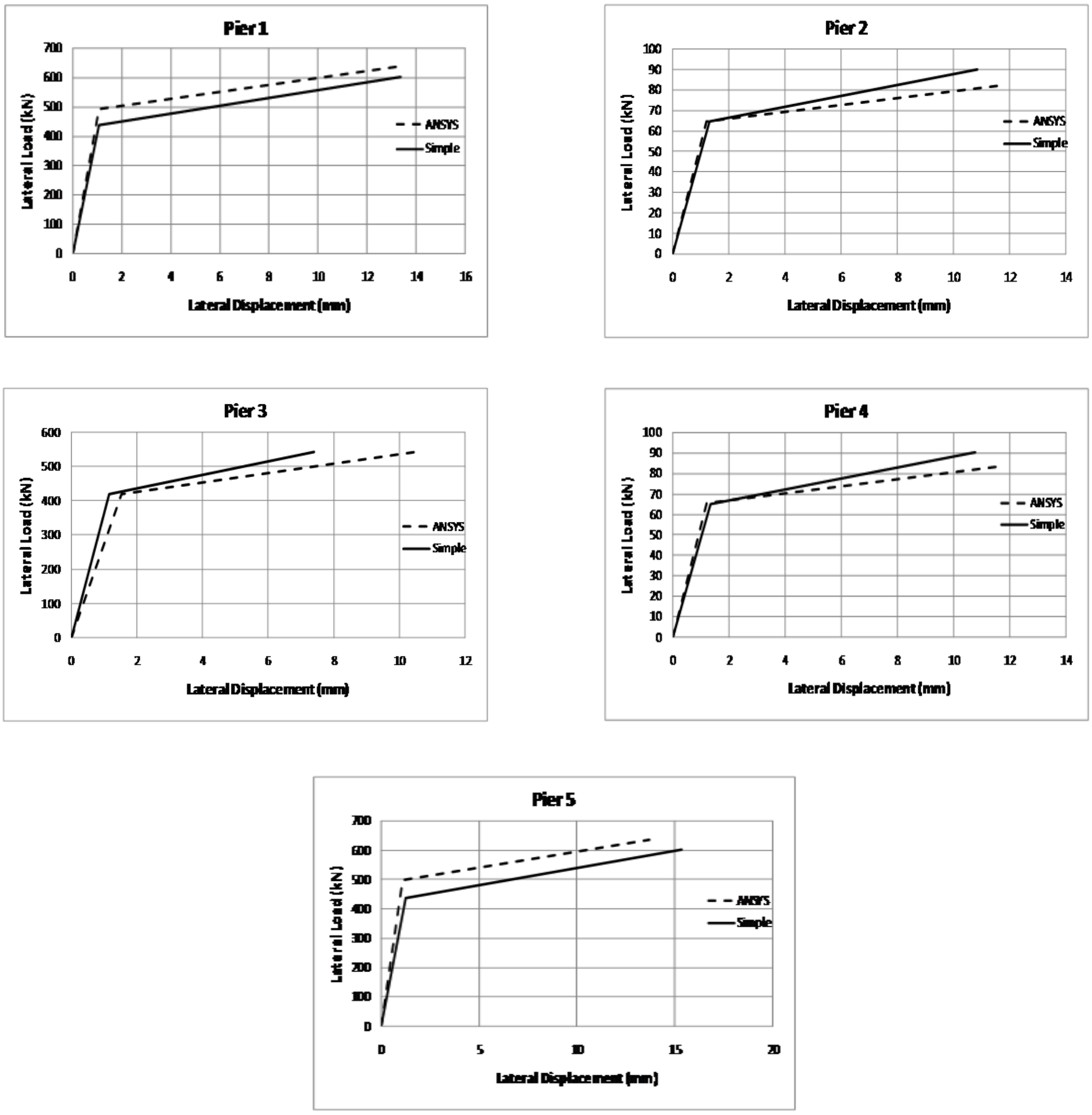

Figure 5.47. The Comparison of Capacity Curves from ANSYS and Simple Method for Piers working along Y direction (First Storey)

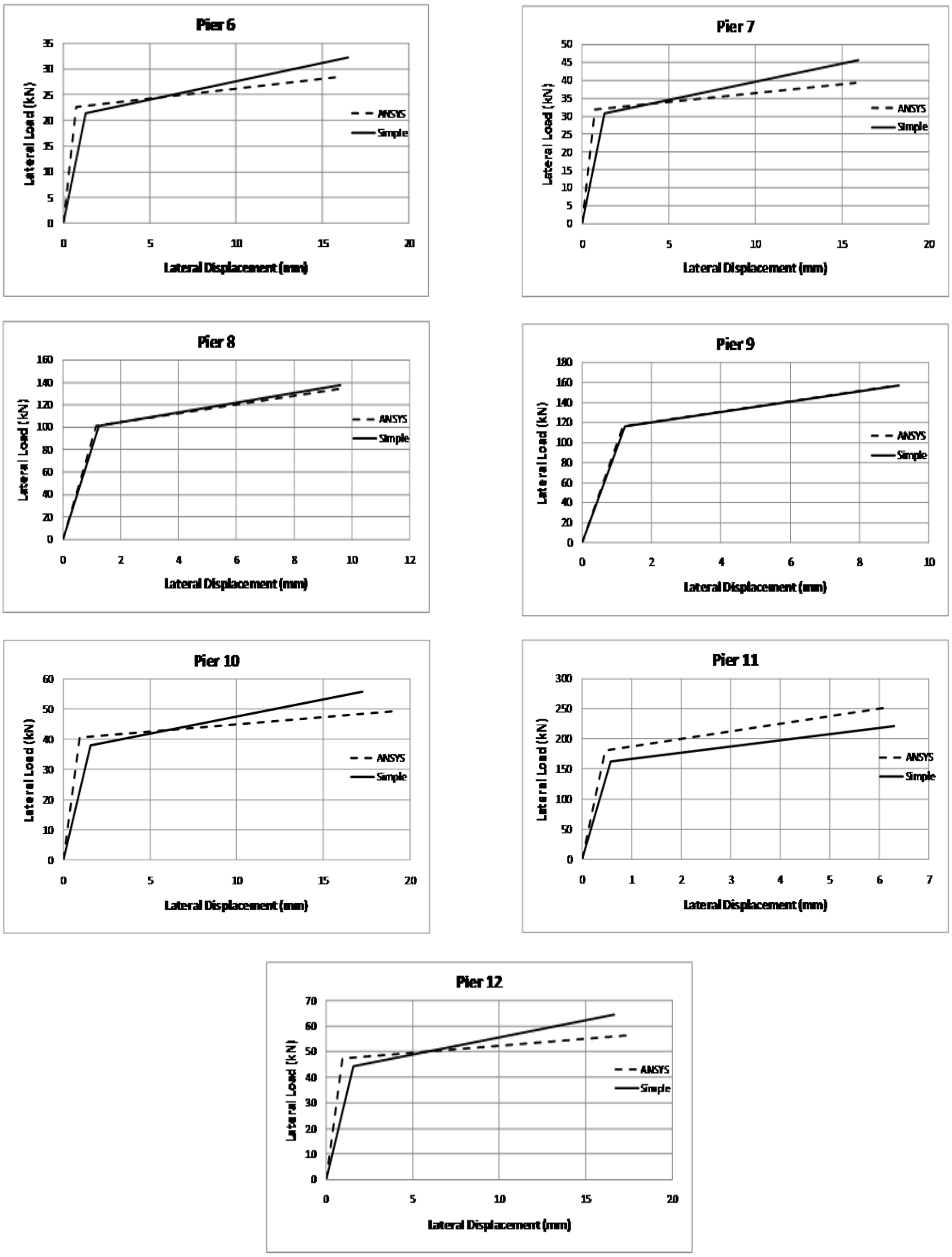

Figure 5.48. The Comparison of Capacity Curves from ANSYS and Simple Method for Piers working along X direction (First Storey)

It can easily be inferred that the simple method estimates the capacity curve parameters for every pier with reasonable errors, which increase with the decreasing axial load ratio (less than 30% in the worst case). This indicates that analytical models of piers do not have to be constructed one by one so as to acquire their capacity curves if some error is tolerable, which is always the case when dealing with a population of buildings. As a consequence, the simple method may be preferred regarding practicality and computational effort.

Afterwards, the capacity curves of this building for both orthogonal directions are determined by using the simplified approach. In this simple analysis, the piers along the in-plane direction are modeled side by side in SAP2000 v14 (2009). (See Figures 5.49 and 5.50) If the piers have spandrels between them, the spandrels are modeled by rigid elements (See Figures 5.53 and 5.54).

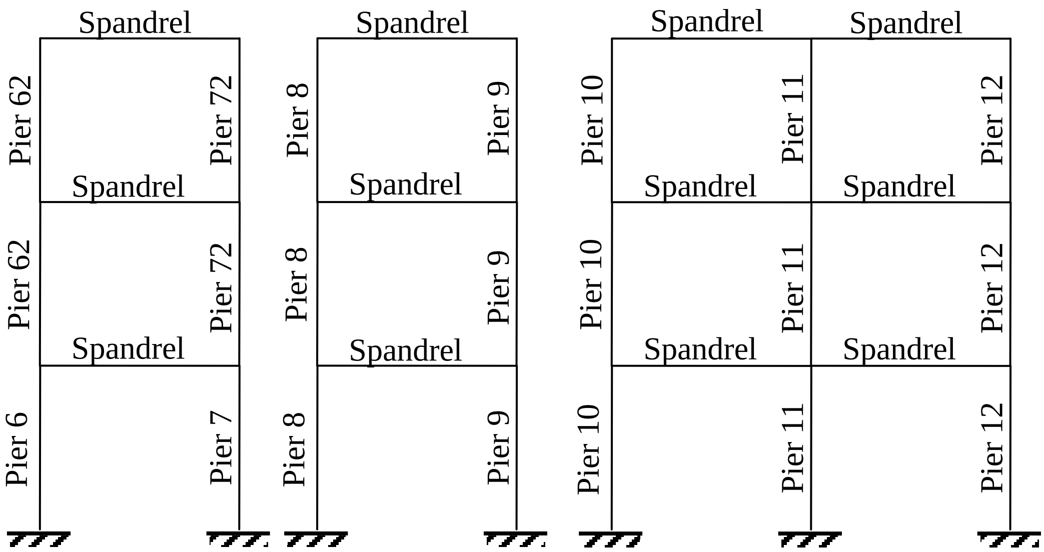

Figure 5.49. Pier Labels along X Direction (Pier 62 and Pier 72 stand for the geometrical property change of Pier 6 and Pier 7.)

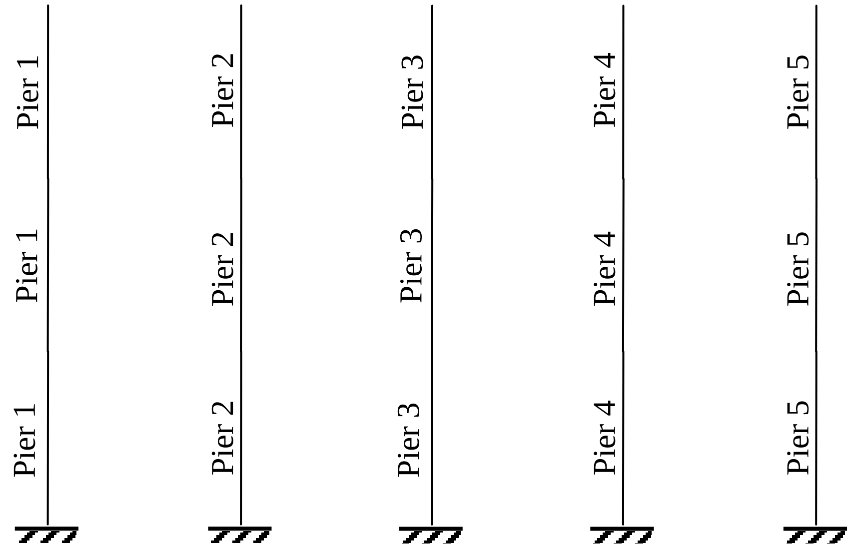

Figure 5.50. The Pier Labels along Y Direction

The lateral connection between different frames is satisfied by using diaphragm constraint as the building has a reinforced concrete slab (See Figures 5.51 and 5.52).

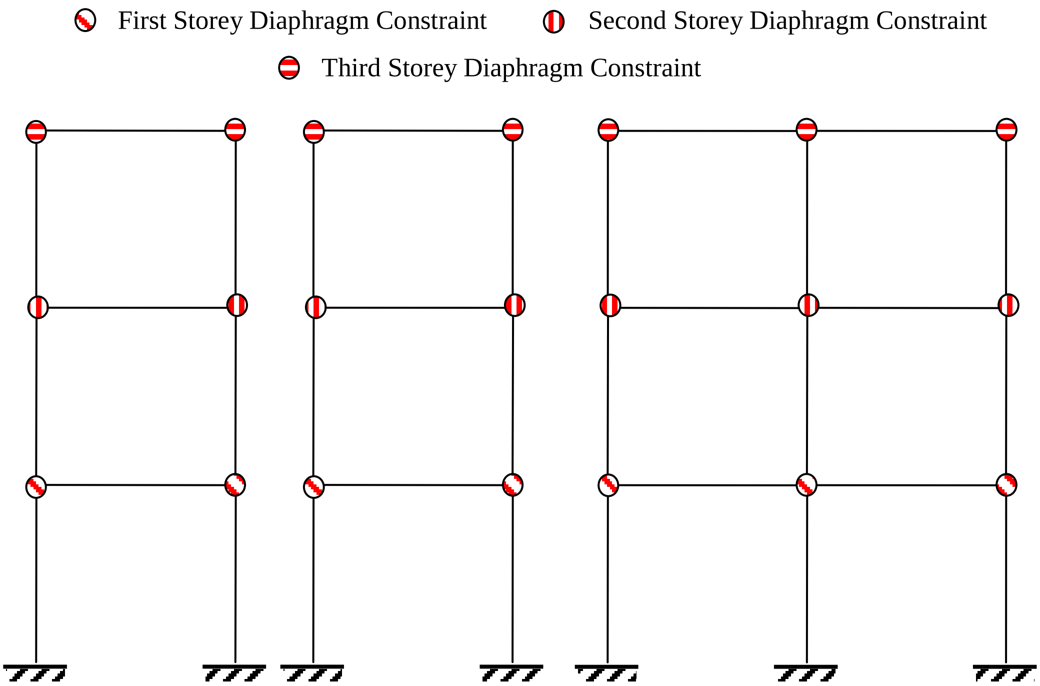

Figure 5.51. Diaphragm Constraints in X Direction

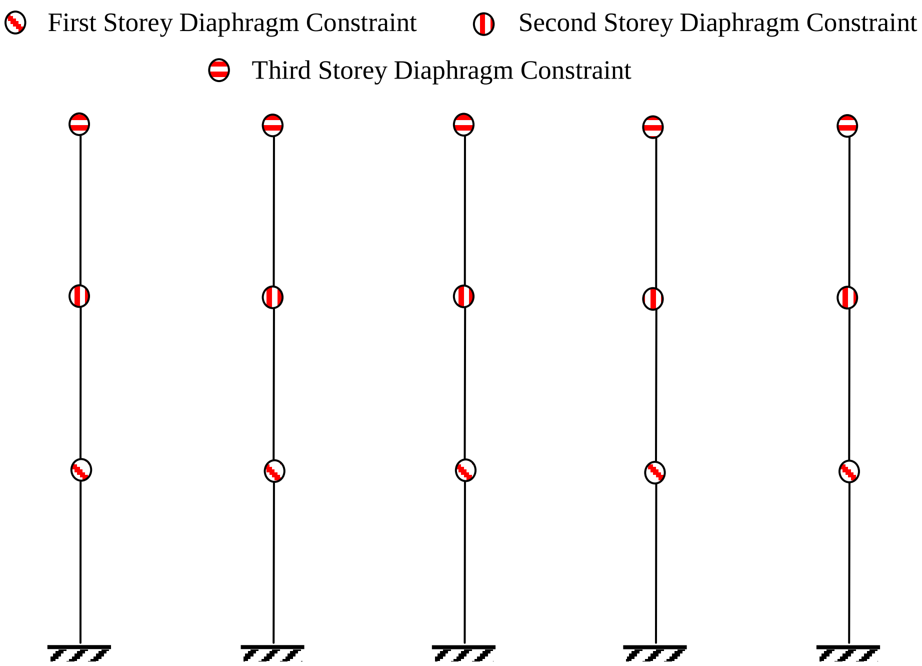

Figure 5.52. Diaphragm Constraints in Y Direction

Moreover, the effective heights of piers are obtained by using rigid end zones on both ends of piers (See Figures 5.53 and 5.54), for which the effective heights are calculated by utilizing Dolce Offset Method (Dolce, 1989).

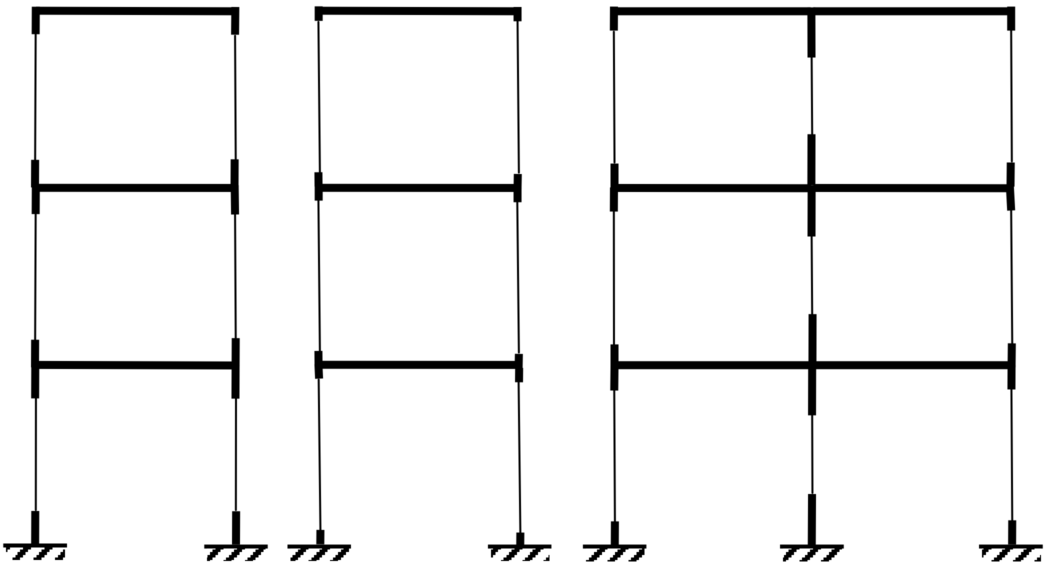

Figure 5.53. Rigid End Zones in X direction (Bold lines are rigid zones.)

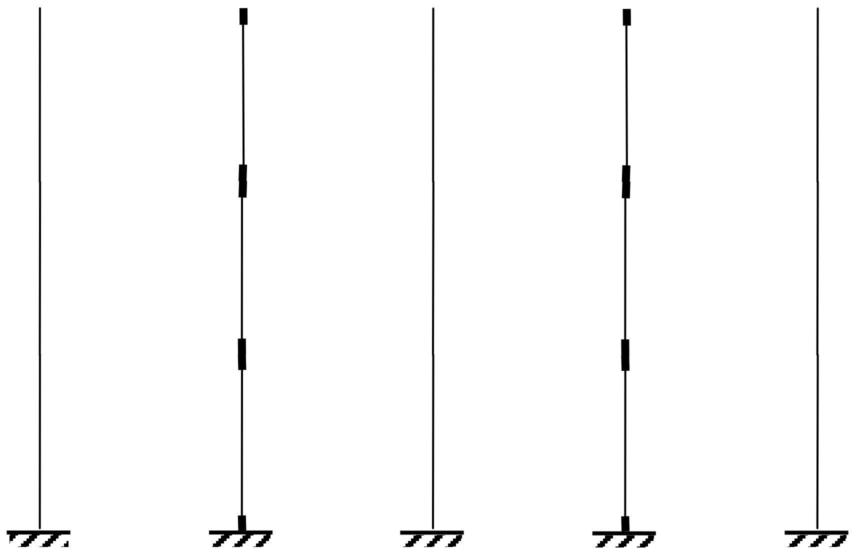

Figure 5.54. Rigid End Zones in Y direction (Bold lines are rigid zones.)

After that, every pier is assigned a shear hinge whose properties are acquired from both ANSYS analysis and simplified formulas generated throughout this study (See Figures 5.55 and 5.56). In this step, it is important to note that the shear hinge properties vary in every storey because of the different axial loads. Furthermore, the shear hinges are placed just above the rigid end zones, so the positions of shear hinges are different for every pier.

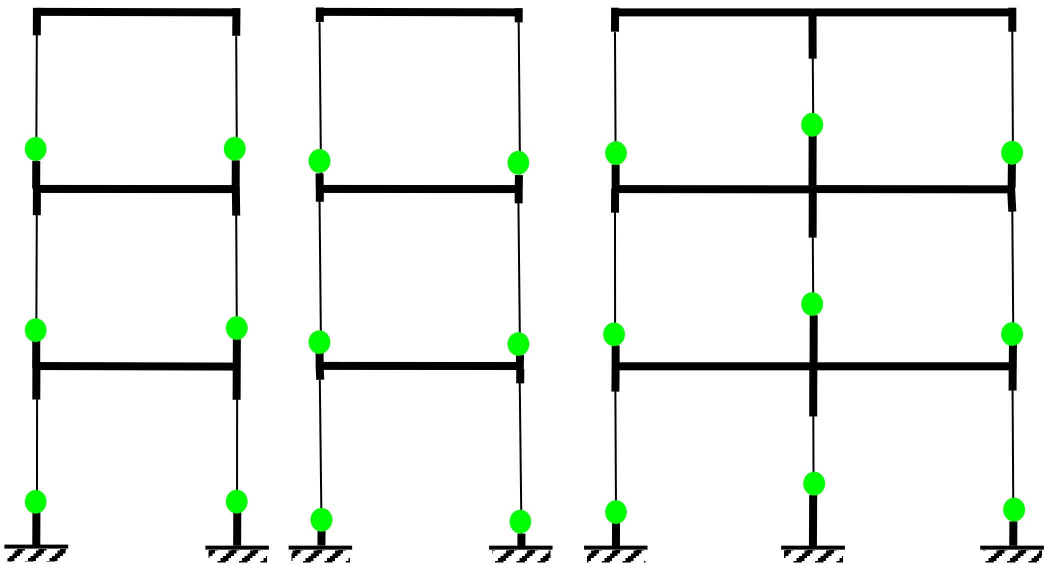

Figure 5.55. Shear Hinges in X direction

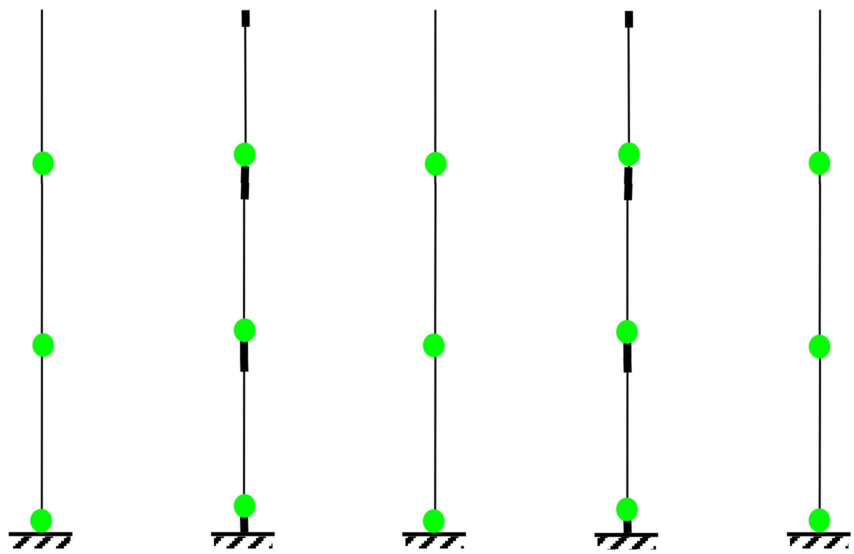

Figure 5.56. Shear Hinges in Y direction

Then, the modal analysis is carried out by assigning the floor masses given in Table 5.15 to every storey in a lumped fashion and its results are summarized in Table 5.16. Finally, the pushover curves of this structure along both X and Y directions are formed by utilizing a lateral loading pattern exactly equal to the dominant modal shape in the considered direction.

Table 5.15. Storey Masses

Storey	***Wall Mass (ton)***	***Floor Mass (ton)***	***Total Mass (ton)***
1	53.843	20.957	74.800
2	54.756	20.957	75.713
3	27.378	20.957	48.335

Table 5.16. The first two modal shapes and corresponding periods

Storey	**$T_{1,x}$ (s)**	**w_x (rad/s)**	**u_x**	**$T_{1,y}$ (s)**	**w_y (rad/s)**	**u_y**
1	0.22	28.417	0.025	0.14	45.225	0.027
2			0.069			0.069
3			0.111			0.110

The lateral capacity curves obtained from non-linear static analysis (first-mode lateral loading pattern is utilized.) for both X and Y directions are depicted in Figures 5.57 and 5.58, respectively.

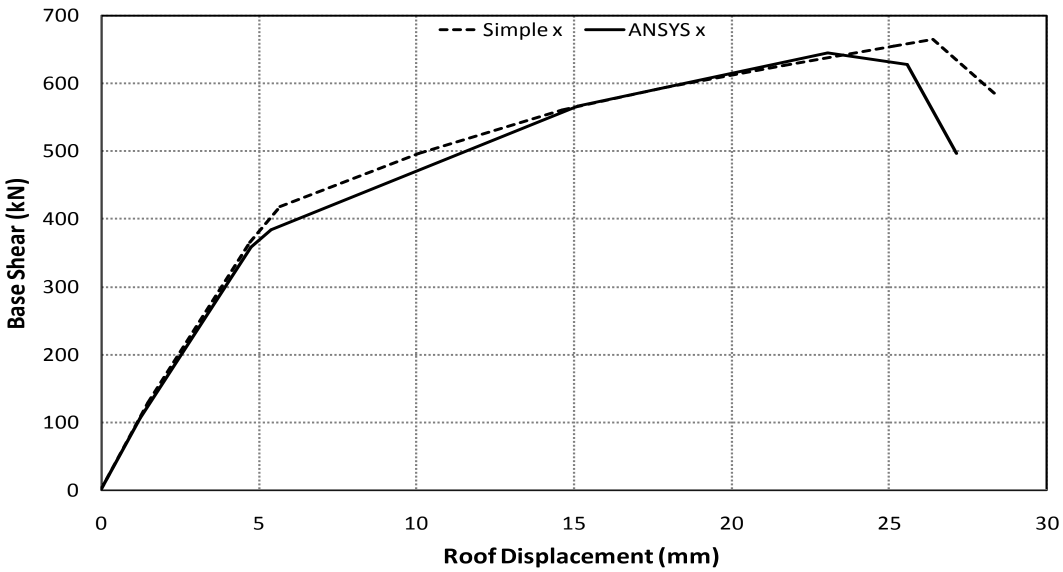

Figure 5.57. Lateral Capacity Curves for X direction

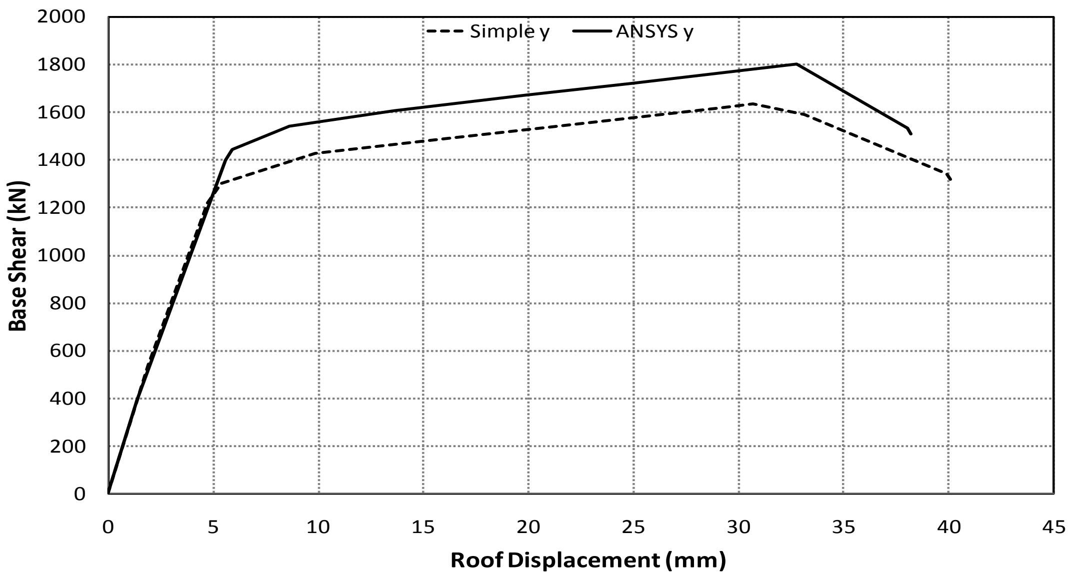

Figure 5.58. Lateral Capacity Curve for Y direction

Except for the ultimate load capacity in Y direction, the capacity curves obtained by both methods for two orthogonal directions are similar.

5.6.3. Demand Calculations

The earthquake demand from this inspected structure is calculated by utilizing the procedure given in TEC2007. The earthquake effect is taken into account by using the design spectrum in TEC2007. However, this design spectrum is not adequate for a masonry structure whose damping ratio is usually taken as 10% of the critical (Erberik, 2008 and Magenes & Calvi, 1997). Yet, there is no formula postulated in TEC2007 to transform the 5% design spectrum to a design spectrum with a different damping ratio. Therefore, it is adjusted by using Newmark-Hall (ATC40) formulas (See Equations 5.13 and 5.14).

$$\alpha_A = 3.21 - 0.68 \ln \xi \quad for\, T < T_B \tag{5.13}$$

$$\alpha_V = 2.31 - 0.41 \ln \xi \quad T > T_B \tag{5.14}$$

The new design spectrum (with 10% damping ratio) along with the TEC2007 design spectrum (with 5% damping ratio) for the first earthquake region (Istanbul) and Z3 class of soil is depicted in Figure 5.59.

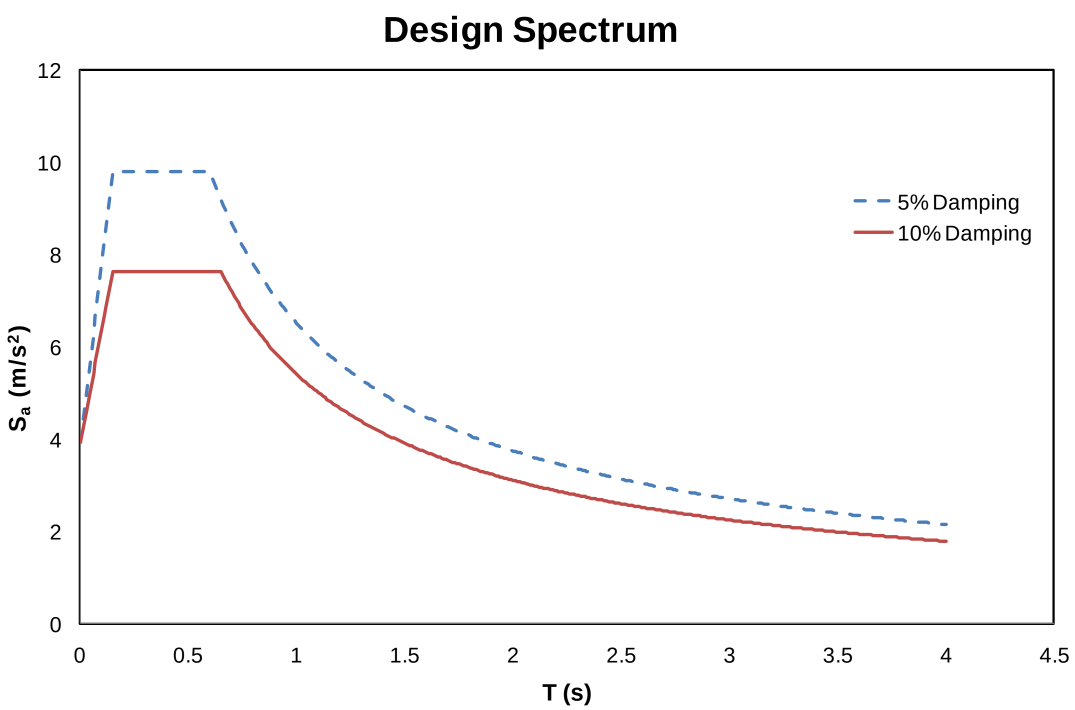

Figure 5.59. Design Spectrum for 1st Earthquake region and Z3 Class of Soil

The displacement demands found by utilizing TEC2007 procedure are summarized in Tables 5.17 and 5.18. These tables show that the damage is accumulated in the first storey as far as X direction is concerned whereas the storey displacement demands for Y direction are similar to the first mode shape. This is because; in X direction, the structure goes beyond its elastic limit, after which the modal analysis loses its validity. However, it stays nearly elastic in Y direction (See Figure 5.60).

Table 5.17. Displacement Demands in X Direction

	Displacement / Interstorey Drift Demands in X Direction (ANSYS)	**Displacement / Interstorey Drift Demands in X Direction (Simple)**
First Storey	9.95 mm / 0.343 %	10.13 mm / 0.349 %
Second Storey	18.07 mm / 0.271 %	19.2 mm / 0.302 %
Third Storey	27.548 mm / 0.316 %	28.355 mm / 0.305 %

Table 5.18. Displacement Demands in Y Direction

	Displacement / Interstorey Drift Demands in Y Direction (ANSYS)	**Displacement / Interstorey Drift Demands in Y Direction (Simple)**
First Storey	1.38 mm / 0.048 %	1.36 mm / 0.047 %
Second Storey	3.58 mm / 0.073 %	3.85 mm / 0.083 %
Third Storey	5.876 mm / 0.077 %	6.36 mm / 0.084 %

In addition, the roof demands are also marked on the capacity curves (See Figure 5.60) in order to evaluate the performance of the structure.

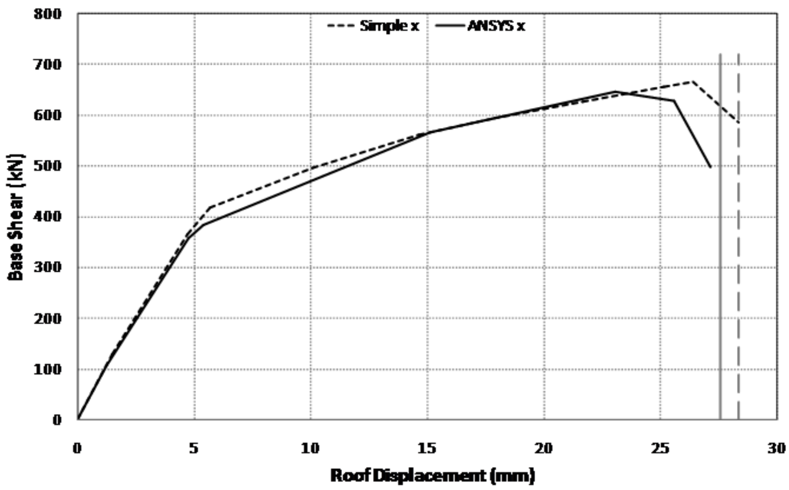

(a)

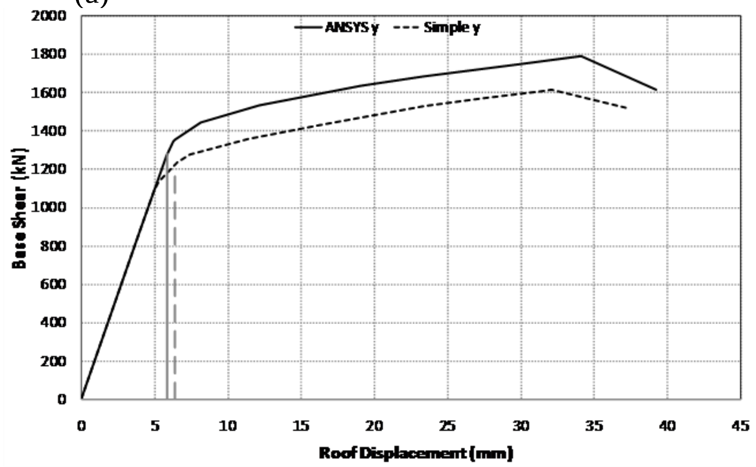

(b)

Figure 5.60. Lateral Capacity Curve and Roof Displacement Demand: (a) for X direction; (b) for Y direction

It is apparent from Figure 5.60 that the capacity curves from both ANSYS and regression formulas are consistent with each other except the direction Y. This is because; in that direction, the building depends on mainly three huge walls without openings over a length of 7.4 m (See Figure 5.40). Therefore, the capacity curve is underestimated because one of these walls' ultimate displacement is predicted less than its ANSYS counterpart. However, this situation is not a common one as there are, most of the time, window or door openings on all walls unlike this tested structure. As a result, this simple method is still dependable as it predicts the X direction very well, which has more realistic wall distribution (See Figure 5.39). Besides, it can easily be inferred that the structure does not meet the earthquake demand in the X direction whereas it has very little damage in the Y direction due to its large piers along this direction (See Figure 5.60).

CHAPTER 6

SUMMARY AND CONCLUSIONS

6.1. Summary

In the first part of this study, recommendations about unreinforced masonry design from different national and international codes or standards are investigated in detail. For this purpose, three versions of Turkish Earthquake Code (TEC1975, TEC1998 and TEC2007), Masonry Standards Joint Committee 2005 (MSJC2005), International Code Council 2006 (IBC2006) and European Committee for Standardization 2003a (Eurocode 6) and 2003b (Eurocode 8) are utilized. Although the design approaches from different standards show similarities, their recommendations are dissimilar in various cases, i.e. they interchangeably prefer suggesting more conservative designs for different situations. It should be stated that since the section regarding the design of masonry buildings in Turkish Earthquake Code is based on empirical rules (i.e. based on geometrical restrictions like maximum height, length, thickness, slenderness ratio, layout of walls, etc.), it is much more conservative when compared to other international codes under consideration.

After the comparison of various code criteria about unreinforced masonry structures, different design approaches namely ***force-based design*** and ***displacement-based design*** for any structural types along with the several analysis techniques utilized in these design techniques are mentioned.

Since this study is interested in the determination of seismic performance of unreinforced masonry structures, a brief review of recently developed performance state definitions advised by different researchers is introduced. Nearly all of these researchers suggest using three performance states and determine the performance state of any masonry structure in terms of the drift ratios in the critical storey.

In the last part of this study, it is intended to develop a simple method for determining the performance of unreinforced brick masonry walls or piers in an existing building. The method is more suitable for a population of buildings rather than a single building. In the first phase, the load-deformation curves of masonry walls are obtained. To achieve this; analytical models of masonry walls are created in ANSYS 11.

The choice of ANSYS 11 is due to several reasons:

- It has lots of different element types, some of which are capable of simulating damage under specific types of loading.
- Several material models can be combined in order to generate more enhanced failure criteria.
- It has improved numerical methods like line search and degree of freedom predictor (DOF predictor) to accelerate the convergence, which is really a big problem for, especially, nonlinear finite element solutions.
- Unlike its counterparts, it has force and displacement controls at the solution step, which makes more reliable results.

All of these models are generated by using 3D macro-modeling (Finite Element Analysis). Therefore, a plasticity capable of simulating the real behavior of unreinforced masonry walls is generated as there are no common fracture models for masonry. This is accomplished by combining two well-known material models: ***William-Warnke*** and ***Bilinear Plasticity***. This new failure criteria is tested by comparing the results obtained with the actual test results that were done in ETH Zurich (Lourenco, 1996). The comparison reveals that lateral capacity curves are close to each other with a good match. Although the crack patterns have not been estimated with the same accuracy, they are sufficiently good to be used.

After that, this analytical model is utilized to form the lateral capacity curves of masonry piers and to identify the effect of some geometrical and mechanical properties, like the compressive strength of masonry, applied vertical load and the aspect ratio, on the lateral load and displacement capacities. At this step, three categories for compressive strength of masonry, six categories for level of axial load and eight categories for aspect ratio are developed. 252 analytical models are formed from the combinations of the above categories and their lateral load capacity curves are obtained from the previously defined finite element models. These curves are, then, simplified to generate a database by finding their bilinear counterparts. This bilinearization procedure is done by using equal energy principle given in FEMA356.

Then, the database of the bilinearized force-deformation relationships of previously developed analytical models are utilized to obtain simple formulas for yield displacement, yield lateral load, ultimate lateral load and ultimate displacement capacities from nonlinear regression analyses. A single formula is recommended for each of these parameters after trying numerous regression models.

In the final stage, the proposed procedure is employed to an existing unreinforced masonry building in Istanbul. The results obtained by using detailed Finite Element Modeling are compared with the results obtained from simplified method. Seismic capacity and demand of the building is obtained and the seismic performance of the building is assessed.

6.2. Conclusions

This study is based on the simplified assessment of the seismic performance of unreinforced masonry buildings in Turkey. There exist many assumptions and simplifications in different stages of this study. Considering this fact, the following conclusions are drawn:

Comparison of code based rules regarding unreinforced masonry design in Turkey and other earthquake-prone countries reveal that the Turkish code is too simple and empirical. This means that it is based on many simplifications and assumptions; therefore, it is more conservative than the other codes. On the other hand, it is not flexible since it enforces some geometrical and architectural restrictions. Perhaps, the most important drawback of the masonry section of the Turkish Earthquake Code is that it does not encourage enhanced types of masonry construction, like reinforced masonry.

It is possible to model lateral capacity curves of masonry components by using finite element approach in ANSYS. However, the current database of ANSYS does not contain suitable analytical tools to model brick masonry walls. Therefore, different failure criteria were used together for a better simulation of the actual behavior. This was achieved to a certain extent in terms of force and displacement capacities, crack patterns and failure modes. But still, it was not possible to obtain the descending portion of the lateral capacity curves due to limitations of the program.

The novel contribution of this study is that it proposes an approach that enables quick and simple estimation of lateral capacity curves of masonry components in terms of basic structural parameters like compressive strength, axial load ratio and aspect ratio. By using this simplified approach, the capacity curves of masonry buildings can be constructed in a short period of time without the need to perform finite element analysis. The method has proven to be satisfactory after comparisons with actual finite element analysis of masonry components. However, it is best to use this approach to assess the seismic performance of a population of buildings rather than a single building since it involves some simplifications and approximations.

The simplified approach has been tested on an existing building in Istanbul and it has proven to be satisfactory for use in the case of a population of buildings which has to be assessed in a short period of time.

REFERENCES

1 Abrams, D.P. (2001), "Performance-based engineering concepts for unreinforced masonry building structures", Structural Engineering and Materials; 3: 48-56.

2 Alcocer, S.M., J.C. Arias and L.E. Flores (2004), "Some developments in performance-based design of confined masonry structures", Report PEER 2004/05, Pacific Earthquake Engineering Research Center

3 ANSYS Inc. (2007), “Basic Analysis Guide for ANSYS 11", SAS IP Inc.

4 ANSYS Inc. (2007), “Element Reference for ANSYS 11", SAS IP Inc.

5 ANSYS Inc. (2007), “Structural Analysis Guide for ANSYS 11", SAS IP Inc.

6 ANSYS Inc. (2007), “Theory Reference for ANSYS 11", SAS IP Inc.

7 Arya A.S., T. Boen, Y. Ishiyama, A.I. Martemianov, R. Meli, C. Scawthorn, V.Julio and Y. Yaoxian (1986), “Guidelines for Earthquake Resistant Non-Engineered Construction”, The International Association for Earthquake Engineering, Tokyo, Japan.

8 Atımtay, E. (2001), "Betonarme Sistemlerin Tasarımı: Temel Kavramlar ve Hesap Yöntemleri", 2nd Edition, Bizim Büro Basımevi, Ankara, Turkey (in Turkish).

9 Bayülke, N. (1992), "Yığma Yapılar", 2nd Edition, Bayındırlık ve İskan Bakanlığı, Afet İşleri Genel Müdürlüğü, Deprem Araştırma Dairesi, Ankara (in Turkish).

10 Belmouden, Y. and P. Lestuzzi (2009), "An equivalent frame model for seismic analysis of masonry and reinforced concrete buildings", Construction and Building Materials; 23: 40–53.

11 Benedetti, D. and Tomazevic, M. (1984), “Sulla verifica sismica di costruzioni in muratura”, Ingegneria Sismica; 1(0): 9-16 (in Italian).

12 Bertero, V.V. (1977), "Strength and Deformation Capacities of Buildings under Extreme Environments", Structural Engineering and Structural Mechanics, K. S. Pister, ed., Prentice Hall, Englewood Cliffs, NJ, 211–215.

13 Calvi, G.M. (1999), "A displacement-based approach for vulnerability evaluation of classes of buildings", Journal of Earthquake Engineering, Vol. 3, No. 3, 411-438.

14 Chen, W.F. (1982), "Plasticity in Reinforced Concrete", McGraw-Hill Inc., New York.

15 Chopra, A.K. (2001), "Dynamics of Structures: Theory and Applications to Earthquake Engineering", 2nd Edition, Prentice Hall, New Jersey, USA.

16 Chopra, A.K. and R.K. Goel (2002), "A Modal Pushover Analysis Procedure for Estimating Seismic Demands for Buildings", Earthquake Engineering and Structural Dynamics, 31:561-582.

17 Cook R.D., D.S. Malkus, M.E. Plesha and R.J. Witt (2002), "Concepts and Applications of Finite Element Analysis", 4th Edition, John Wiley and Sons Inc., New Jersey, USA.

18 Costa, A. (2007), "Experimental testing of lateral capacity of masonry piers - An application to seismic assessment of AAC masonry buildings", MS Thesis, Rose School, Pavia, Italy.

19 Dolce, M. (1989), “Schematizzazione e modellazione per azioni nel piano delle pareti (Models for in-plane loading of masonry walls)”, Corso sul consolidamento degli edifice in muratura in zona sismica, Ordine delgi Ingegneri, Potenza, Italy (in Italian).

20 Erbay, O. and D.P. Abrams (2001). “Seismic rehabilitation of unreinforced masonry shear walls”, Proceedings, 9th Canadian Masonry Symposium, University of New Brunswick, Canada.

21 Erberik, M.A. (2008). "Generation of Fragility Curves for Turkish Masonry Buildings considering in-plane Failure Modes", Earthquake Engineering and Structural Dynamics; 37: 387-405.

22 Erberik, M.A., A. Aldemir and B.O. Ay (2008). “A Critique on the Turkish Earthquake Code Regulations Regarding Masonry Construction”, 8th International Seminar on Structural Masonry, Istanbul, Turkey, paper 31.

23 European Committee for Standardization (CEN) 2003a, "Eurocode 6: Design of Masonry Structures", prEN 1996-1, Brussels, Belgium.

24 European Committee for Standardization (CEN) 2003b, “Eurocode 8: Design of structures for earthquake resistance”, Part 1, prEN 1998-1, Brussels, Belgium.

25 FEMA273, "NEHRP Guidelines for the Seismic Rehabilitation of Buildings", Washington,DC: Federal Emergency Management Agency. 1997.

26 FEMA356. "Prestandard and Commentary for the Seismic Rehabilitation of Buildings", Washington, DC: Federal Emergency Management Agency. 2000.

27 Gilmore, A.T., Cuevas O.Z. and Garcia J.R. (2009), “Displacement-Based Seismic Assessment of Low-Height Confined Masonry Buildings”, Earthquake Spectra; 25: 439-464.

28 Grünthal, G. (1998). “European Macroseismic Scale 1998”, In Cahiers du Centre Europeen de Geodynamique et de Seismologie Vol.15. European Seismological Commission, Luxembourg, Brussels.

29 International Code Council (2006), "International Building Code (IBC)", Whittier, California, USA.

30 Kaushik, H.B., D.C. Rai and S.K. Jain (2007), “Stress – strain chacracterisitcs of Clay Brick Masonry under Uniaxial Compression”, Journal of Materials in Civil Engineering, 9(728).

31 Lourenco, P.J.B.B. (1996), “Computational Strategies for Masonry Structures”, Thesis Delft University of Technology.

32 Magenes, G. and G.M. Calvi (1992). "Cyclic behavior of brick masonry walls", Proceedings, 10th European Conference on Earthquake Engineering, Madrid, 3517-3522.

33 Magenes, G. and G.M. Calvi (1997), "In-plane seismic response of brick masonry walls", Earthquake Engineering and Structural Dynamics Volume 26, 1091-1112.

34 Masonry Standards Joint Committee (MSJC) (2005), "Building Code Requirements for Masonry Structures and Specification for Masonry Structures and Commentaries", American Concrete Institute, American Society of Civil Engineers, The Masonry Society, Boulder, Colorado.

35 Penelis, Gr.G. (2006), "An efficient approach for pushover analysis of unreinforced masonry structures", Journal of Earthquake Engineering; Vol. 10 No: 3, 359-379.

36 Plowman, J.M. (1965), "The Modulus of Elasticity of Brickwork", Proceedings of Brick Ceramic Society, 4: 37-44.

37 Postacıoğlu, B. (1962), "Memleketimizde imal edilen tuğlaların özellikleri" Tuğla Kiremit Semineri 14-16 Haziran 1962, İmar ve İskan Bakanlığı Yayınları No:5-20 (in Turkish).

38 Priestley, M.J.N., G.M. Calvi and M.J. Kowalsky (2007), "Displacement-Based Seismic Design of Structures", IUSS Press, Pavia, Italy.

39 Sahlin, S. (1971), "Structural Masonry", Prentice Hall, Englewood Cliffs, New Jersey, USA.

40 Salonikios T., C. Karakostas, V. Lekidis and A. Anthoine (2003), “Comparative inelastic pushover analysis of masonry frames", Engineering Structures; 25: 1515–1523.

41 SAP2000 Ver. 14, CSI Analysis Reference Manual, Computers and Structures Inc., Berkeley, California, 2009.

42 Schubert, P. (1982), "Modulus of Elasticity of Masonry", Proceedings of the Fifth International Brick Masonry Conference, Washington: 139-144.

43 Senthivel, R. and H.C. Uzoegbo (2004), "Failure Criterion of Unreinforced Masonry under Biaxial Pseudo-Dynamic Loading", Journal of the South African Institution of Civil Engineering, 46(4) 2004, Pages 20–24, Paper 578.

44 Sinha, B.P. and R. Pedreschi (1983), "Compressive Strength and Some Elastic Properties of Brickwork", International Journal of Masonry Construction, 3(1).

45 SPSS Manual, SPSS Inc., SPSS Ver. 15.0, Chicago, IL, 2006.

46 Sucuoğlu, H. and M.A. Erberik (1997), "Performance Evaluation of a three-storey unreinforced masonry building during the 1992 Erzincan Earthquake", Earthquake Engineering and Structural Dynamics, Vol. 26, 319-336.

47 Taly, N. (2000), "Design of Reinforced Masonry Structures", McGraw Hill, New York, USA.

48 Tolunay, H. (1966), "Investigations on the characteristics of brick masonry walls", MS Thesis, METU, Ankara, Turkey.

49 Tomazevic, M. (1999), "Earthquake Resistant Design of Masonry Buildings", Series on Innovations in Structures and Construction, Vol.1, Imperial College Press, London, UK.

50 Tomazevic, M. (2007), "Damage as a measure for earthquake-resistant design of masonry structures: Slovenian experience", Canadian Journal of Civil Engineering; 34: 1403-1412.

51 Turkish Ministry of Public Works and Settlement (1975), "Specification for Structures to be Built in Disaster Areas", TEC1975, Ankara, Turkey.

52 Turkish Ministry of Public Works and Settlement (1998), "Specification for Structures to be Built in Disaster Areas", TEC1998, Ankara, Turkey.

53 Turkish Ministry of Public Works and Settlement (2007), "Specification for Structures to be Built in Disaster Areas", TEC2007, Ankara, Turkey.

54 Turkish Standards Institution (1977), "Design and Construction methods for Masonry ", TS2510, Ankara, Turkey.

55 Turkish Standards Institution (1985), "Solid Bricks and Vertically Perforated Bricks ", TS705, Ankara, Turkey.

56 Turkish Standards Institution (2004), "Specification for masonry units-Part 1: Clay masonry units", TS EN 771, Ankara, Turkey.

57 Turnsek, V. and F. Cacovic (1971). “Some experimental results on the strength of brick masonry walls”, Proceedings, 2nd International Brick Masonry Conference, Stoke-on-Trent, 149-156.

58 Vamvatsikos, D. (2002), "Seismic Performance, Capacity, and Reliability of Structures as Seen Through Incremental Dynamic Analysis", Ph.D. Dissertation, Department of Civil and Environmental Engineering Stanford University.

59 Willam, K.J., and E.D. Warnke (1975), "Constitutive Model for the Triaxial Behavior of Concrete", Proceedings, International Association for Bridge and Structural Engineering, Vol. 19, ISMES, Bergamo, Italy, p. 174.

Internet Source

1 Pacific Earthquake Engineering Research Center, PEER NGA Database, http://peer.berkeley.edu/nga, last visited on 15.01.2010.